INFORMATION TO USERS

This manuscript has been reproduced from the microfilm master. UMI films the text directly from the original or copy submitted. Thus, some thesis and dissertation copies are in typewriter face, while others may be from any type of computer printer.

The quality of this reproduction is dependent upon the quality of the copy submitted. Broken or indistinct print, colored or poor quality illustrations and photographs, print bleedthrough, substandard margins, and improper alignment can adversely affect reproduction.

In the unlikely event that the author did not send UMI a complete manuscript and there are missing pages, these will be noted. Also, if unauthorized copyright material had to be removed, a note will indicate the deletion.

Oversize materials (e.g., maps, drawings, charts) are reproduced by sectioning the original, beginning at the upper left-hand corner and continuing from left to right in equal sections with small overlaps. Each original is also photographed in one exposure and is included in reduced form at the back of the book.

Photographs included in the original manuscript have been reproduced xerographically in this copy. Higher quality 6" x 9" black and white photographic prints are available for any photographs or illustrations appearing in this copy for an additional charge. Contact UMI directly to order.

UMI

A Bell & Howell Information Company
300 North Zeeb Road, Ann Arbor MI 48106-1346 USA
313/761-4700 800/521-0600

Cloning, characterization and genetic analysis of the *Hmx* genes, a novel homeobox gene family required for sensory organ development and maternal reproduction

by

Weidong Wang

A dissertation submitted to the Graduate Faculty in Biomedical Science in partial fulfillment of the requirements for the degree of Doctor of Philosophy, The City University of New York

1998

UMI Number: 9820589

UMI
300 North Zeeb Road
Ann Arbor, MI 48103

This manuscript has been read and accepted for the Graduate Faculty in Biomedical Science in satisfaction of the dissertation requirement for the degree of Doctor of Philosophy.

1·9·1998
Date

Dr. Francesco Ramirez
Chair of Examining Committee

1/12/99
Date

Dr. Terry A. Krulwich
Executive Officer

Dr. Manfred Frasch

Dr. Thomas Lufkin

Dr. Joy Reidenberg

Dr. Thomas Van De Water
Supervisory Committee

THE CITY UNIVERSITY OF NEW YORK

Abstract

Cloning, characterization and genetic analysis of the *Hmx* genes, a novel homeobox gene family required for sensory organ development and maternal reproduction

by

Weidong Wang

Advisor: Dr. Thomas Lufkin

Three novel homeobox genes were isolated, one from *Drosophila melanogaster* (*Drosophila Hmx* gene) and two from mouse (murine *Hmx2* and *Hmx3*). The striking similarity between the homeodomains of these three genes and the previously identified genes, *TgHbox5*, *gH6*, human *H6* as well as recently cloned mouse *Hmx1* gene together with the low level identity to other homeobox genes indicate that the *Hmx* genes are a novel gene family.

Hmx1 is assigned to the proximal region of mouse Chromosome 5. *Hmx2* and *Hmx3* are closely linked on the distal region of mouse Chromosome 7. In addition to their similar expression in the central and peripheral nervous systems, *Hmx2* and *Hmx3* show identical expression patterns in sensory organ related structures. *Hmx3* is one of the earliest markers for vestibular inner ear development, and is also up-regulated in the myometrium of the uterus during pregnancy. Mice lacking *Hmx3* exhibit abnormal circling behavior owing to severe vestibular defects. Histological analysis indicates a depletion of sensory cells in the saccule and utricle, and a complete loss of the horizontal semicircular canal crista, as well as a fusion of the utricle and saccule endolymphatic spaces into a common utriculosaccular cavity of these *Hmx3* null mice. The majority of *Hmx3* null females are infertile, even though they show normal ovulation and fertilization. Embryos fail to implant successfully

in the *Hmx3* null uterus and subsequently die. Transfer of preimplantation embryos from *Hmx3* null uterine horns to wildtype pseudopregnant females results in successful pregnancy, indicating a failure of the *Hmx3* null uterus to support normal post-implantation development of the embryos. Molecular analysis reveals a perturbation in *Hmx*, *Wnt* and LIF gene expression in the *Hmx3* null uterus. Interestingly, expression of both *Hmx1* and *Hmx2* is down-regulated in the *Hmx3* null uterus, suggesting a regulatory hierarchy exists among the *Hmx* genes during pregnancy.

Mice carrying disrupted *Hmx2* and *Hmx3* genes display a more severe phenotype than *Hmx3* null mice. The double knockout results in perinatal lethality. The few surviving offspring show a complete loss of balance, severe developmental retardation and premature death.

Acknowledgments

I would like to thank Dr. Thomas Lufkin, my preceptor, not only for the opportunity he gave me to work on this project, but for his persistent guidance during the past four years.

Dr. Van De Water deserves my special gratitude. Without his collaboration, this work could not have been finished as quickly and completely as it was. My appreciation also goes to Dr. Francesco Ramirez. I have benefited greatly from his encouragement whenever I have had a hard time. My special thanks also go to Dr. Manfred Frasch and Dr. Joy Reidenberg for their involvement, comments and criticisms in relation to this work.

In addition, I want to thank Maria Nikolova for her excellent technical assistance and David Neustaedter for spending the time to read the thesis. I have been extremely fortunate to have worked with following nice and smart peers: Rafique Islam, Xue Li, Ullrich Treubert-Zimmermann and Carla Tribioli.

Finally, I would like to thank my wife, Shanshan Qian who contributed to this work through her support and understanding.

Contents

Lists of Tables and Figures

Introduction

The homeobox was originally described in *Drosophila melanogaster* as a highly conserved nucleotide sequence. The homeodomain encoded by the homeobox shows a typical helix-turn-helix DNA-binding motif and binds target DNA in a sequence-specific manner (Kissinger et al., 1990). Proteins containing homeodomains likely function as transcriptional regulators. Based on the conservation of the homeobox, a growing number of homeobox genes are being found. The functions of some of these genes have been extensively investigated.

In *Drosophila*, the well-documented *Antennapedia-Bithorax* genes (referred to as *HOM-C*) are involved in body plan patterning. Genes in *HOM-C* are clustered and the temporal and spatial expression of these genes is colinear with their position along chromosome 3. Generally, genes at the 3' end in the complex are expressed earlier and at more rostral regions than those at 5' end. For example, the most 3' gene in the complex, *labial*, is expressed most anteriorly with respect to other genes in the cluster (McGinnis and Krumlauf, 1992). Normal function of genes in *HOM-C* is required for the identity of regions from the abdomen to the posterior part of the head. Null mutations of most *HOM-C* genes cause the transformation of a segment to a more anterior phenotype. Interestingly, the affected regions in the null mutants of these genes correspond to the anterior-most domains of each gene's expression. The null *Antennapedia* mutation is lethal and embryos possessing this mutation show homeotic transformations. Ectopic expression of *Antennapedia* in the head can induce the development of legs next to the eyes in the place of antennae. Combined with the data obtained from other homeotic genes, these homeobox genes can provide positional information specifying the identity of *Drosophila* segments along the anteroposterior (A-P) axis. Additional evidence shows that homeobox-containing genes are also involved in the development of the head region and in specifying identity along the dorsoventral (D-V) axis.

Many homeobox genes have been isolated from higher animals. Homeobox genes can be classified into distinct gene families based on similarities in their homeodomains. In vertebrates, the best-studied examples of homeobox genes are the mouse *Hox* genes. The *Hox* genes are clustered on 4 different chromosomes (McGinnis and Krumlauf, 1992). The genomic organization of *Hox* genes within each cluster and the timing and pattern of an individual gene's expression are strikingly similar to those of the paralogues in *HOM-C* of *Drosophila*. As in the fly, the most 3' *Hox* gene in each cluster, such as *Hoxb-1* in the *Hox-B* complex, is expressed earliest and in the most anterior region, whereas the 5' most gene, such as *Hoxb-9*, is expressed latest and in the most posterior region. The anteriormost boundaries of *Hox* genes are located in the hindbrain. No expression of *Hox* genes has been detected beyond the mid-hindbrain boundary.

Like the *Antennapedia-Bithorax* genes in *Drosophila*, *Hox* genes are involved in body plan patterning along the A-P axis in the hindbrain and trunk regions. Patterning of the vertebrate hindbrain also involves segmentation. Rhombomeres set up different microenvironments to induce the cells to adopt different regional identities. Rhombomere segmentation has been demonstrated to play roles in developmental events including the migration patterns of sensory and motor neurons (Krumlauf, 1993). Besides its role in patterning the central nervous system, rhombomere segmentation is important for craniofacial development. For example, tissues in the branchial arches are derived from the hindbrain rhombomeres. In chick embryos, cranial neural crest migration was followed by using a vital dye (DiI) to trace positional fates of the neural crest, demonstrating that crest cells in branchial arches 1, 2 and 3 came from rhombomeres 2, 4, 6 respectively (Lumsden et al., 1991). Expression patterns of *Hox* genes show that the most rostral expression domain always stops at a boundary between rhombomeres. For example, the rostral boundary of *Hoxa-1* is located at the rhombomere 3/4 boundary. The functions of *Hox* genes in A-P axis body patterning have been investigated by either ectopic expression or by

disruption through homologous recombination in embryonic stem (ES) cells. As with *Drosophila HOM-C* genes, ectopic expression of some *Hox* genes can cause homeotic transformations. Expression of *Hoxd-4* under the control of the *Hoxa-1* promoter results in a homeotic transformation of the occipital bones into a more posterior structure (Lufkin et al., 1992). As in *Drosophila*, mice carrying null mutations in *Hox* genes show defects in their anterior regions of expression. Disruption of *Hoxa-1* in the mouse results in abnormalities in tissues derived from rhombomeres 4-7, including craniofacial structures such as the inner ears and certain cranial ganglia (Lufkin et al., 1991). Evidence thus far indicates that homeobox genes in *Drosophila* and vertebrates are highly conserved both structurally and functionally. Even their regulatory elements are evolutionally conserved to some extent. For instance, a murine rhombomere 2-specific enhancer can direct a *lacZ* reporter gene to be expressed in the corresponding region in *Drosophila* (Frasch et al., 1995). Studies on *Drosophila* homeobox genes may provide informative clues regarding the functions of their vertebrate homologues.

Homeobox-containing genes also play some roles in the dorsoventral patterning of the central nervous system (CNS) in vertebrates. Paired-box genes, *Pax3* , *Pax6* and *Pax7* each contain a paired box and a homeobox. These genes are all expressed in the central nervous system. Longitudinally, the expression domains of these genes cover the regions from the caudal diencephalon to the spinal cord. For the *Pax6* gene, transcripts can be detected even in the forebrain. Both *Pax3* and *Pax7* are expressed in the dorsal neural tube, with *Pax3* restricted to the roof plate. Normal function of *Pax3* is important for neural tube closure. In the developing spinal cord, *Pax6* is restricted to the ventral region of the neural tube. The dorsoventrally restricted expression pattern of these three *Pax* genes, established by diffusible factors from the notochord and floor plate, may be responsible for neural differentiation along the dorsoventral axis of the neural tube (Goulding et al., 1991 and

1993). Besides its expression in the CNS, *Pax6* also plays a critical role in eye development.

A great deal of information has accrued regarding the involvement of homeobox genes in midbrain and forebrain development. In *Drosophila*, *empty spiracle*, *orthodenticle* and *Distal-less* are expressed in specific regions rostral to the anterior-most *HOM-C* expression domains. The null mutant of *orthodenticle* displays severe deletions in the head region (Wieschaus et al., 1992). Mouse homologs of these genes, referred to as *Emx*, *Otx* and *Dlx* respectively, have already been cloned. The expression patterns of these genes strongly suggest that they may be involved in development of the rostral brain, since messengers corresponding to these genes can never be detected in the hindbrain and the trunk regions. *Otx1*, *Otx2*, *Emx1* and *Emx2* show nested expression patterns, in which *Otx2* is expressed earliest and with an expression domain completely encompassing those of the other three genes. *Otx2* is first detectable at E embryonic day 5.5 (E5.5) in the entire embryonic ectoderm. During gastrulation, its expression is restricted to the anterior region of the body. At later stages, *Otx2* is expressed in several regions of the telencephalon, diencephalon and mesencephalon, including the rostral cortex, optic stalk and noncortical basal ganglia (Simeone et al., 1992). Early and extensive expression of the *Otx2* gene suggests that it may play a more important role in brain development than *Otx1*, *Emx1* and *Emx2*. *Otx1* null mice survive even though abnormalities can be seen in the cortex, mesencephalon and cerebellum (Acampora et al., 1996). However, inactivation of the *Otx2* gene caused the absence of brain structures anterior to rhombomere 3 (Matsuo et al., 1995; Ang et al., 1996; Acampora et al., 1995). *Emx1* and *Emx2* are mainly expressed in the primordia of the cerebral cortex in the central nervous system (Simeone et al., 1992). Knockout experiments have shown the requirement of *Emx2* for normal dentate gyrus development and hippocampal formation (Pellegrini et al., 1996). Some genes in the *Dlx* family may

also be involved in forebrain development, but these genes are also detectable in limb ectoderm and the branchial arches (Price et al., 1991 and 1993; Qiu et al., 1995 and 1997).

Unlike the *Hox* genes in the hindbrain and trunk region, and *Emx* and *Otx* in the midbrain and forebrain, some other homeobox genes are not restricted to specific regions and show no obvious axial patterning activity. These genes may be required for the determination of cell fate in the regions where they are expressed. Certain members of the *Nkx* gene family have been shown to be required for heart and visceral mesoderm specification (Evans et al., 1995; Lints et al., 1993). Knockout of the *Nkx2.5* gene in mouse results in abnormal development of the heart. The *Drosophila sine oculis* homeobox gene is required for pattern formation of the eye disc and development of the optic lobes. However, its murine homologs, *Six1* and *Six2*, show expression only in connective tissue and muscle precursor cells (Oliver et al. 1995a), suggesting that some members of this gene family have acquired a new function during evolution. The other member of *Six/sine oculis* family, *Six3*, retains its original function in eye development (Oliver et al., 1995b).

The initial goal of my project was to isolate and characterize homeobox gene(s) involved in craniofacial and sensory organ development. Generating animal models for human inherited diseases has proven to be useful in investigating the molecular basis of these diseases. For example, the *Splotch* mouse which carries null mutations in *Pax3* has severe malformations of the CNS and is a good animal model for Waardenberg's syndrome in humans (Epstein et al., 1991 and 1993). Mice heterozygous for mutant *Pax6* (called the *Sey* mouse) have small eyes. The *Sey* mouse is considered homologous to aniridia (lack of iris) in humans (Hill et al., 1991). The deafness of *shaker-1* mice is caused by a mutation in the myosinVII gene which is located on mouse Chromosome 7. Interestingly, humans with Usher syndrome show similar phenotypes to *shaker-1* mice in neuroepithelial-type hearing impairment and vestibular dysfunction. Characterizing the human counterpart of the myosinVII gene in the patients confirmed that the same gene was responsible for this kind

of deafness in both mouse and humans (Weil et al., 1995). Accumulation of information obtained from these animal models will facilitate the process of identifying pathogenic genes for human inherited diseases. The expression of two other homeobox genes, *Msx1* and *Msx2*, suggests their involvement in brain and craniofacial development. Both genes are expressed in the developing skull bones, teeth, roof plate of the neural tube and eyes of developing embryos. *Msx1* knockout mice provide direct evidence of the involvement of *Msx1* in the proper differentiation of membranes and the alveolar bones of the head and face, and as well as in tooth and middle ear development (Sakokata and Mass, 1994). In humans, a missense mutation was determined to result in a familial tooth agenesis (Vastardis et al., 1996). *Msx2* is also detectable in neural crest-derived mesenchyme. Mutations in the human *MSX2* gene result in the craniosynostosis syndrome characterized by the premature fusion of calvarial sutures (Jabs et al., 1993).

Epilepsy is a visible marker of cerebral dysfunction. Inherited epilepsies, because of the likelihood of a genetic basis, are of particular interest to many investigators. By definition, the epilepsies are caused by a specific subset of cerebral dysrhythmias characterized by disorders of recurrent, spontaneous and aberrant synchronization in the neural networks (Noebels, 1996). Epileptic seizures normally initiate in the cerebral cortex, then spread to the hippocampus, from which they affect other brain regions. The neuronal hyperexcitability is always accompanied by abnormal levels of neurotransmitters, such as acetylcholine, glutamate, glutamine, and aspartate. Two widely accepted criteria to classify epilepsies are based either on their anatomic origin or on cause. Regarding cause, epilepsies are either "symptomatic" (caused by brain disorders or trauma) or "idiopathic" (normally genetic in origin). Considering origin, epilepsies are categorized into "partial" and "generalized", which can be distinguished by clinical and eletroencephalographic information. Partial epilepsies originate from a restricted region of the cerebral cortex, whereas generalized epilepsies involve a hyperexcitability of the entire cortex which is

thought to be mediated by the thalamus (Ryan, 1995). It has been taken for granted that idiophatic generalized epilepsies are genetic in origin. Recent studies have also confirmed that partial epilepsies can be inherited, even though most cases of partial epilepsies are associated with brain lesions (Ottman et al., 1995). Investigating the cellular and molecular mechanisms of epileptogenesis has the potential to lead to tremendous benefits in diagnosis and treatment, as well as genetic counseling. Unfortunately, so far, slow progress has been made to map epileptic loci and clone epileptogenic genes in humans. The major challenges confronted by researchers are small family size, heterogeneous phenotypes, variable expressivity, and complex inheritance (Frankel et al., 1994). In most cases, the distribution of epilepsy patients in the family does not follow Mendelian patterns of inheritance, suggesting most epilepsies are polygenic or multifactorial in origin. Complexity resulting from the involvement of multiple loci hampers the progress in identifying human epileptic genes. Until now, only a few epileptic loci have been mapped. For example, benign neonatal epilepsy (EBN1), the juvenile type of Ceroid lipofuscinosis, and Northern epilepsy syndrome (EPMR) are linked to genetic markers on Chromosome 20q, 16p, and 8p, respectively (Leppert et al., 1989; Ryan, 1995). A partial epilepsy, Nocturnal frontal lobe epilepsy, is mapped to Chromosome 20q. A novel inherited epilepsy associated with auditory symptoms is linked to genetic markers on chromosome 10q (Ottman et al., 1995). Coincidentally, the human *HMX2* gene is located close to that region (Stadler et al., 1995).

In the mouse, the introduction of transgenic techniques has resulted in a breakthrough in the identification of genes responsible for epilepsy. Much attention has been focused on ion channels, neurotransmitters and their receptors. Disruption of *mKv1.1*, a gene encoding a subunit of a delay rectifier K^+ channel, results in a lethal epilepsy phenotype (Smart et al., 1995, Soc. Neurosci., abstract). *mKv1.1* null mice fail to repolarize their presynaptic axon terminal, subsequently resulting in excess release of neurotransmitters. Tissue nonspecific alkaline phosphatase (TNAP) catalyzes the reaction of converting

pyridoxal phosphate (plp) to the nonphosphorylated form of vitamin B6 that can cross cell membranes. Disruption of the TNAP gene results in the elevated level of plp in the serum and dramatic reduction of plp level in the brain. Pyridoxal phosphate (plp) is a cofactor for glutamic acid decarboxylase, which synthesizes GABA. Reduction of GABA levels in the *TNAP* null mice results in lethal tonic-clonic seizure (Waymire et al., 1995). Serotonin (5-hydroxytrytryptamine, 5-HT) is a monoaminergic excitatory neurotransmitter which exerts its function in the mammalian nervous system via a large family of receptor subtypes. Targeted disruption of one of its receptors, 5-HC_{2c}, results in epileptic seizures in addition to abnormal eating behavior in mice, suggesting the inhibitory effect of 5-HC_{2c} in neuronal network excitability elicited by serotonin (Tecott et al., 1995). In the nervous system, normal levels of the excitatory neurotransmitter glutamate are maintained by the activity of its transporters. Nonfunctional transporters fail to remove glutamate from the extracellular space, resulting in increased levels of glutamate in the brain. Mice carrying null glutamate transporter *GLT-1* gene exhibit epilepsy and exacerbation of brain injury (Tanaka et al., 1997). Ample evidence indicates that epileptic activity stimulates alterations in neuronal gene (e.g. *BDNF* and *NT3* etc.) expression, which subsequently changes the levels of excitability and, hence, inducing further seizures. For example, patients with temporal lobe epilepsy show increased expression of glutamic acid decarboxylase in interneurons of the hippocampus (Schwarzer and Sperk, 1995). Overexpression of glutamic acid decarboxylase induces the increase in GABA synthesis, subsequently the increased GABA-ergic transmission. It is reasonable to predict that, by examining and cloning these epilepsy-induced genes, new candidate genes for epilepsy can be identified and promising targets for gene therapy can be obtained.

Products of homeobox genes are also important players in epileptogenesis. Since homeobox genes are primarily expressed at embryonic stages, their epileptogenic effects may not directly involve neurotransmitters or their receptors, but most likely are associated

with abnormalities in brain structures during early development. *Otx1* null mice display epileptic behavior with the characteristics of both partial and generalized seizures (Acampora et al., 1996). Anatomical and histological analyses revealed that *Otx1* knockout mice show size-reduced cortex, volume-increased mesencephalon and extra lobule(s) in the cerebellum (Acampora et al., 1996). Expression of murine *Emx2* in the developing neuroblasts of the cerebral cortex suggests a function in brain development (Simeone et al., 1992). *Schizencephaly* is a developmental disorder caused by a cell migration anomaly showing a full-thickness cleft within the cerebral hemispheres. Patients with severe *schizencephaly* exhibit seizures and severe neurological defects. *Schizencephaly* is linked to *EMX2* homeobox gene by the finding of mutations in the affected patients. Mutations at 3' splicing sites, as well as by frameshifting result in abnormal EMX2 products (Brunelli et al., 1996; Granata et al., 1997). Patients heterozygous for these mutations exhibit clinical signs. Correlation of *schizencephaly* with mutations in *EMX2* suggests *EMX2* is a good epileptic gene candidate. Epileptic behavior in our *Hmx3* null mice, combined with its expression in the hypothalamus and mapping to the syntenic region of human epileptic loci, makes *Hmx3* gene a novel homeobox gene involved in epileptogenesis.

Development of the mouse eye can be described as follows. At E9.0, two groups of neuroepithelium cells evaginate laterally from the ventrolateral wall of the diencephalon. The eye primordium is formed, containing the evaginating neural tube and underlying endoderm derived from the forebrain. This structure is called the optic vesicle. The optic vesicle is connected to the diencephalon by the optic stalk. When the eye primordium contacts the surface ectoderm, signals from the eye primordium induce the thickening of the surface ectoderm, which subsequently forms the lens placode. At E10.0, the lens placode rounds up into a lens vesicle and reciprocally forces the invagination of the optic vesicle to form a double-layered optic cup. At later stages (around E15.0), lens vesicles pinch off from the epidermis. The position of the lens relative to the optic cup is precisely

coordinated. Unlike the lens, which is comprised of fiber and epithelium, the retina has a complicated composition and structure. The outer layer of the optic cup differentiates into the pigmented retina, whereas the inner layer forms the neural retina. Detailed analyses show that the neural layer contains a variety of cell populations, including glia, ganglia neurons and photoreceptor neurons. Signals (light and color) received by photoreceptors are transmitted to the ganglia cells via the bipolar interneurons. Finally, signals are sent to the CNS by the optic nerves (Gilbert, 1994).

Several homeobox genes involved in the patterning of the eye have been found. The *Pax6* gene seems to be a master gene in the eye development. Null mutations of the *Drosophila Pax6* homologue, *eyeless*, result in loss of the eyes. In the mouse eye, *Pax6* is expressed in both the lens and retina (Walther and Gruss, 1991). Some human patients with aniridia show the mutations in *PAX6* (Jordan et al., 1992). Mice with a *Pax6* null mutation are not viable and do not develop eyes. *Pax2*, a paired box gene lacking a homeobox is also expressed in the ventral half of the optic cup, stalk and optic nerve (Nornes et al., 1990). Mutations in the *PAX2* gene have been reported in patients with optic nerve colobomas (Sanyanusin et al., 1996). The *Six3* homeobox gene is mainly expressed in neuronal structures, including the optic recess in the ventral forebrain (Oliver et al., 1995). The product of this gene may function as an transcriptional regulator of the inductive signaling molecules required for vertebrate eye development. Ectopically expressed murine *Six3* induced ectopic lens formation in the otic vesicle in fish embryos (Oliver et al., 1996). Unlike the *Pax6* gene, some other homeobox genes may not be directly involved in morphogenesis of the eyes, but are still required in cell-specific fate determination. Expression of the mouse homeobox gene *Chx10* is restricted in the anterior region of optic vesicle and the neuroblasts in the optic cup during early embryogenesis (Liu et al., 1994), suggesting its potential function in the determination of the neuroretina and inner nuclear layer. *Msx1* and *Msx2* are expressed in different regions of the inner layer of

the optic cup at different stages, suggesting that they may play some role in eye development (Monaghan et al., 1991). *Msx2* is expressed in the surface ectoderm and the optic vesicle at E 9.5. *Msx1* is restricted to the regions that form the ciliary body after formation of optic cup. But *Msx1* knock out mice do not show obvious defects in the eyes (Satokata and Maas, 1994). An explanation is that some other gene(s) may function redundantly. Recent results obtained from antisense attenuation contradict the above observation, since knock-outs of either *Msx1* or *Msx2* by antisense oligos result in eye anomalies. Furthermore, double knockouts of both genes did not show novel defects compared with the single knockouts, suggesting no functional redundancy existing between these two genes (Foerst-Potts et al., 1997).

Initiation of inner ear development in the mouse is induced by interactions between signals from the chordal mesoderm and otic epithelium. The otic placode, a thickening of surface ectoderm on the lateral hindbrain becomes competent to invaginate and pinchs off to form the otic vesicle. At this point, a subset of cells in the ventral part of the otic vesicle, which are *islet1*-positive, have committed themselves to develop into the neurogenic region and start delaminating from the otic vesicle, subsequently converging into the VIIIth ganglion. The invasion of neurites from the acoustic ganglion into the otic epithelium enables outside signals to be transmitted to the acoustic region in the rhombencephalon (Ekker et al, 1992; Gilbert, 1994). The remainder of the otic vesicle (nonneurogenic portion) undergoes elongation and distortion to form the three sensory systems of the inner ear. During this complex morphogenetic process, cells in the otic vesicle continue to proliferate and become specified to one of a variety of cell fates. Some cells (in the sensory regions) become determined to develop into sensory patches, whereas the nonsensory regions will give rise to the overall structures of the inner ear, like the semicircular ducts, cochlea, stria vascularis, and the endolymphatic duct and sac. The sensory patches contain the hair cells, whose function is to convert mechanical vibration into electrochemical signals

for hearing and balance (Corwin et al., 1993). The dorsal portion of the otic vesicle gives rise to the vestibular structure and the ventral part develops into the cochlear labyrinth. Six epithelia comprise the three sensory systems in the inner ear. The three cristae in the three semicircular canals are the sensory organs for detecting angular acceleration. The maculae in the saccule and the utricle are responsible for sensing linear acceleration (gravity). Sound pressure is received by organ of Corti in the cochlea (Fritzsch et al., 1997). Malformation of the inner ear structures can lead to abnormalities in hearing and balance and related behaviors. For example, *shaker-1* mutant mice exhibit circling, head tossing, deafness, and hyperactivity. Examination of the *shaker-1* mice revealed degeneration of the organ of Corti, the spiral ganglion, and the stria vascularis in the cochlea, and of the saccular macula and the vestibular ganglion in the vestibular labyrinth (Kikuchi et al., 1967).

Many gene products have been shown to be involved in otogenesis. Inductive signals from both the underlying rhombomeres and from the otocyst itself are required for the formation and function of the inner ear. *kreisler* mutants result from the chromosome inversion of *krml* gene on mouse Chromosome 2. The *krml* gene encodes a novel basic domain leucine zipper transcription factor. In wild type mice, the *krml* gene is only expressed in the neural tube adjacent to the otic vesicle, but not in the otocyst at the beginning of otogenesis (Deol, 1964; Cordes and Barsh, 1994). In *kreisler* mutant mice, abnormal segmentation and cell degeneration in the fourth rhombomere lead to the misplacement of the otic vesicle. Malformed vestibule and cochlea result in deafness and the typical shaker/waltzer phenotype of *kreisler* mice. In addition to the defects in the central nervous system, *Hoxa-1* null mice also exhibit severe morphogenetic malformation of their inner ears characterized by the absence of a cochlear labyrinth and semicircular canals (Lufkin et al., 1991; Chisaka et al., 1992). Since *Hoxa-1* itself is not expressed in the otic vesicle, these defects in the inner ear might be caused by secondary effects due to the absence of correct inductive signals from the underlying rhombomere. Malformation of

the external, middle or inner ears as a result of craniofacial malformations results in a kind of hearing impairment similar to Treacher Collins syndrome (Dixon et al., 1996 and 1997). *Otx1* is expressed in many regions in the forebrain, midbrain and developing inner ear. In addition to the defects in the brain, *Otx1* null mice show the absence of the lateral semicircular duct, which is responsible for their high speed turning behavior (Acampora et al., 1996). Some other genes encoding transcription factors, growth factors and growth hormone receptors also play important roles in otogenesis. They may not be directly involved in the overall morphogenesis of the inner ear, but are required in regional specification and correct cell-type induction. The gene encoding the POU-domain transcription factor Brn3.1 is primarily expressed in cochlear and vestibular hair cells. *Brn3.1* null mice display a shaker/waltzer behavioral phenotype of circling and hyperactivity and are also completely deaf (Erkman et al., 1996). Histological analysis of the inner ears of *Brn3.1* mice revealed apparently normal morphogenesis, but a complete failure of hair cell differentiation in both the organ of Corti and the vestibular labyrinth. As a result of the defects in hair cell development, many of the supporting cell populations were degenerated. Patients with congenital thyroid disorders accompanied by deafness show resistance to thyroid hormone. Complete deletion of the protein coding region of thyroid hormone receptor β gene is responsible for this syndrome (Takeda et al., 1992). Two thyroid hormone receptors, *Trα* and *Trβ*, are differentially expressed in the developing inner ear. The*Trα* gene can be detected throughout the cochlea and vestibular structures, whereas *Trβ* is strictly confined to the cochlea (Bradley et al., 1994). Mice lacking the *Trβ* gene exhibited a deficit in auditory function across a wide range of frequencies, although no overt morphological alternation can be observed (Forrest et al., 1996). Signals received by the sensory organs (hair cells in cristae, maculae and Corti's organ) of the inner ear are transmitted to the central nervous system via the somatic afferents from vestibular ganglion neurons and spiral ganglion neurons. Survival and

innervation patterns of these neurons depend on the activity of neurotrophic factors such as brain-derived neurotrophic factor (BDNF), and neurontrophin-3 (NT-3). *BDNF* mRNA is expressed in the sensory hair cells in both cochlear and vestibular sensory epithelia in the developing inner ear. Mice lacking *BDNF* or its receptor, *TrkB* show the complete loss of innervation to the semicircular canals and reduced innervation of the outer hair cells in the cochlea (Ernfors et al., 1995). Phenotypically, *BDNF* null mice display deficiency in balance and coordination of movement. The *Isk* gene which encodes a cofactor for K^+ channel subunits is also required for the normal function of the inner ear. No direct evidence suggests that *Isk* is involved in the early development of the inner ear. However, the integrity of the inner ear structures after birth requires the normal function of *Isk* . *Isk* null mice show a typical shaker/waltzer phenotype which is related to the collapse of both *Reissner's* membrane in the cochlea and the vestibular wall in the vestibular labyrinth. At the same time, hair cell death in both cochlea and vestibule can be observed (Vetter et al., 1996). Besides *Hoxa-1* and *Otx1*, many other homeobox genes may also be involved in the inner ear development in vertebrates based on their expression patterns. In addition to the expression in the brain, *Dlx2* and *Dlx3* can be detected at low levels in the otic vesicle and are subsequently restricted to the vestibular part of the vesicle. Expression of the *Dlx3* gene in the region under the first branchial arch suggests its potential role in external ear development (Robinson et al., 1994). Homeobox genes of the *Msx* family may play some roles in the development of auditory structures. Defects in the middle ear can be observed in *Msx1* knockout mice (Satokata and Mass, 1994). *Msx2* transcripts can be seen in the mesenchyme surrounding the otic vesicle and the endolymphatic ducts at embryonic stages (Mckenzie et al., 1992). No functional data have been available from the knockout experiments, but ectopic expression of *Msx2* leads to deafness and degeneration of the organ of Corti in mice (Hoffman et al., 1995; Rivolta, 1997). The *Msx3* gene may not be directly involved in ear development since its expression is restricted to the central nervous

system (Wang et al., 1996). Work presented in this thesis examines a novel homeobox gene family involved in sensory organ development, especially that of the inner ear.

Homeobox genes may also participate in the development of other sensory organs. In addition to the defects in the eyes and brain, the *Pax6* null embryos do not show structures of the nose. The mouse *goosecoid* gene is primarily expressed around the regions of the first branchial arch, which region may contribute to the formation of the lower jaw and the body of the tongue (Gaunt et al., 1993). Interestingly, besides its expression in the optic recess, *Six3* transcripts are also detectable in the nasal cavity and olfactory placode (Oliver et al., 1995b). When ectopically expressed in fish embryos, the *Six3* gene can induce an eye, but not a nose or a tongue. The underlying mechanisms remain to be elucidated.

Female reproduction in vertebrates is comprised of a series of events, including ovulation, fertilization, implantation and post-implantation development of the embryo(s). The egg develops in the ovary, which contains primordial follicles (meiotically arrested oocytes surrounded by granulosa cells). Periodically, as the follicle matures, the egg ruptures from the ovarian surface and enters the ovary ducts. Correct cell-cell signaling between the oocyte and granulosa cells plays a critical role in oogenesis and ovulation. The absence of the gap-junction molecule Connexin 37 in the knockout mice leads to a failure of follicle maturation and ovulation characterized by the arrest of oocyte development and accumulation of inappropriate corpora lutea derived from granulosa cells (Simon et al., 1997). In the oviduct, the egg is fertilized if it encounters sperm. The fertilized egg undergoes cell cleavage and finally develops into a morula in the oviduct. Then, the blastocyst hatches from the zona pellucida and starts the process of attachment to the uterine endometrial epithelium. In the mouse, implantation normally starts on day 3.5 after vaginal plugging. Proper implantation requires the uterus to become receptive to embryos. On E3.5, the uterus starts preparing for embryos by inducing closure of the uterus, which brings the trophectoderm and the luminal epithelium into close apposition. During this

period. LIF (leukemia inhibitory factor) produced by the glandular epithelium is upregulated, with a peak at E4.5. Functional LIF is essential for implantation since mice lacking LIF are infertile due to a failure in implantation (Stewart et al., 1992). At the same time, extracellular matrix (ECM) molecules and their receptors show altered expression patterns in both the uterus and the implanting embryos. A subset of integrins are upregulated in the trophectoderm and uterine wall on the implantation site(s). On the other hand, the *Muc-1* gene product, a glycoprotein, starts to be degraded in the uterine wall (Surveryor et al., 1995). These preparations allow the embryos and uterus to become attachment competent. Attachment of embryos (blastocysts) to the uterus induces the production of a heparin-binding protein encoded by *HB-EGF* in the uterine epithelium around the implantation sites (Raab et al., 1996). *HB-EGF* protein is thought to function as an adhesion molecule to anchor the embryos to the uterus. Right after the attachment of the embryos, the uterus shows increased vascular permeability at the implantation sites. Vascular endothelial growth factor (VEGF) and its receptors exhibit upregulated expression in the luminal epithelia and stromal cells. This increased expression persists in the mesometrial decidual bed. Altered expression of VEGF suggests its involvement in increased vascular permeability and angiogenesis during implantation (Chakraborty et al., 1995). Angiogenesis is critical for embryonic development in that it provides vascular connections linking the mother and fetus. Through these connections, the maternal endocrine system can maintain the hormonal environment required for the continuity of pregnancy, and nutrients can be transported to the developing fetus. Following the attachment of embryos to the uterine wall, the uterus undergoes decidualization of the stroma cells. At the same time, apoptosis of the luminal epithelium and degradation of collagen products take place in the decidualizing endometrium (Dziadek et al., 1995). Finally, the implantation stage finishes with the contact of the trophectoderm with maternal decidua. Cytokines are also deeply involved in peri-implantation development, consistent

with their differential expression during pregnancy. Their altered expression is required for the growth of the embryos in part by protecting them from infection and attenuating rejection from the maternal immune system. LIF deficient mice fail to initiate implantation and decidualization (Stewart et al., 1992 and 1994). The mononuclear phagocyte growth factor colony stimulating factor-1 (CSF-1) is needed during both pre- and post-implantation. Macrophages have been shown to produce immunosuppressive substances (Hunt et al., 1984 and 1985). Reasonably, involvement of CSF-1 in pregnancy is mediated by its immunoregulatory effect. Elevated expression of CSF-1 and its receptor is always associated with pregnancy. The fertility of the Osteropertrotic (op/op) mice is comprised by the absence of CSF-1 (Pollard et al., 1991).

Failure in implantation and placentation accounts for the majority of spontaneous abortions in humans (Cross et al., 1994). Using animal models, cloning and functional analysis of genes expressed at these stages will help us to gain insights into genes involved in this pathogenic outcome. Increasing evidence has shown or suggested that many developmentally important genes are also involved in maternal reproduction. The murine *Wnt* family is homologous to *Drosophila wingless*, and these molecules appear to be involved in cell-cell signaling (McMahon et al., 1992; Nusse and Varmus, 1992; Robertson et al., 1993). In addition to their early functions in embryonic development, these genes also display dynamic expression patterns in the adult uterus during pregnancy (see Results and Discussion), suggestive of their potential roles in maternal fertility. The absence of functional *Wnt2* in mice leads to insufficient vascularization, which causes failed placentation (Monkley et al., 1996). Two homeobox genes, *Hoxa-10* and *Hoxa-11*, have been shown to play a critical role in female reproduction. In *Hoxa-10* null mice, failed pregnancy results, in part, from an anterior homeotic transformation of the proximal region of the uterus into an oviduct-like structure (Benson et al., 1996; Satokata et al., 1995). The anterior transformation itself can not explain the female infertility since implantation of

wildtype embryos into the morphologically normal region of the *Hoxa-10* null uterus still resulted in a failed pregnancy, suggesting that other factors important for normal embryonic support are under the control of *Hoxa-10*. Surprisingly, the expression of LIF was unchanged in *Hoxa-10* null mice, suggesting that some mechanism other than the LIF-mediated pathway was being disturbed. The effect on maternal reproductive failure in *Hoxa-11* null mice was different from that in the *Hoxa-10* null mice. *Hoxa-11* null females showed deficiency in the development of stromal, decidual, and glandular cells at early gestational ages (Gendron et al., 1997; Small and Potter, 1993). Additionally, the *Hoxa-11* null uteri did not show responsiveness following pseudopregnancy to steroid-induced uterine stromal and glandular cell proliferation and to oil-induced stromal decidualization. Furthermore, the *Hoxa-11* null females failed to show a burst of LIF expression at the time of implantation.

A novel homeobox gene family, *Hmx*, has been isolated from different species by several groups. The first *Hmx* gene was characterized in sea urchin five years ago. Sequence analysis of sea urchin *Hmx* (previously *TgHbox5*) shows that its homeodomain shares only ~60% amino acid identity with homeodomains of any other previously characterized gene, suggesting that it belongs to a distinct gene family. Sea urchin *Hmx* is expressed in the embryo as two major developmentally regulated transcripts, which are predominantly expressed in the small and large intestine (Wang et al., 1990). The human *HMX1* gene (originally called *H6*) was isolated from a cDNA library constructed from human embryonic craniofacial tissues. Genetic mapping of *HMX1* showed that this gene is located at the 4p16.1 region of human Chromosome 4 (Stadler et al. 1992). The function of human *HMX1* during human embryogenesis is unknown. Existence of another member of the human *HMX* family, *HMX2* is now confirmed, with *HMX2* assigned to human Chromosome 10q25.2-26.3 (Stadler et al., 1995). By probing a stage 23 whole chick cDNA library with a PCR amplified portion of the human *HMX1* cDNA containing the

homeodomain, the chick *Hmx3* gene was identified (Stadler and Solursh, 1994). Temporally, chick *Hmx3* is strongly expressed between embryonic stages 23 and 26. High levels of chick *Hmx3* expression can be detected in stage 23 embryos, in discrete craniofacial regions including the second branchial arch, neural retina, optic nerve, otic vesicles. Chick *Hmx3* is also expressed in sensory spinal and craniofacial ganglia. These results suggest that chick *Hmx3* may participate in the development of a variety of structures, especially in the craniofacial regions and in the sensory organs (Stadler et al., 1994). The gene most closely related to the *Hmx* family based on amino acid similarity in the homeodomain is the *SoHo-1* homeobox gene from chick, the only described member of its gene family. Its transcripts can be detected in the retina, otic pit, dorsal root ganglia and other tissues at different stages, making it a promising candidate homeobox gene involved in sensory organ development (Deitch et al., 1994). Isolation of *Drosophila Hmx* in our laboratory adds extra evidence supporting the novelty of the *Hmx* gene family. The expression pattern of the *Drosophila Hmx* gene suggests a potential role in central nervous system development. Expression of the *Hmx* genes during vertebrate development has been examined in a number of species, and seems to be conserved among vertebrates (Bober et al., 1994; Rinkwitz-Brandt et al., 1995; Stadler et al., 1992; Stadler and Solursh, 1994; Yoshiura et al., 1997). Overlapping expression domains of the *Hmx* genes include the first and second branchial arches, central and peripheral nervous system, and the uterus. Their expression in the central nervous systems and internal organs (e.g., small and large intestine in sea urchin, duodenum in mice) may reflect the original function of the *Hmx* gene. In constrast, their expression in the sensory organs and uterus may represent recently evolved function of the *Hmx* genes. *Hmx2* and *Hmx3* are remarkable in that both are expressed in the developing inner ear. At E9.5, mouse *Hmx3* is strictly confined to the rostrodorsal portion of the otic vesicle. This differential expression becomes more pronounced at later stages. By E13.5, *Hmx3* expression is almost exclusively limited to the

vestibular portion of the inner ear. In adult mice, the *Hmx* genes are expressed in the medial portion of the stroma of the uterus in unpregnant females. During pregnancy, all three *Hmx* genes are significantly upregulated in the uterine myometrium. To reveal the unique developmental role of each *Hmx* gene, null mutations for each *Hmx* gene have been generated by gene targeting. Analysis of the resulting phenotype in *Hmx3* null mice indicates a critical role for *Hmx3* in inner ear vestibular development and pregnancy. Typical epileptic behavior exhibited by some *Hmx3* null mice suggests that *Hmx3* is a novel epileptic gene. Mice carrying null *Hmx2* and *Hmx3* alleles display a much more severe phenotype than *Hmx3* null mice, characterized by the complete loss of balance and perinatal lethality. Phenotypic comparison of each single knockout with double knockouts, or even triple knockouts, provide informative clues to the functional relationship among the three murine *Hmx* genes. In addition to *loss-of-function* analyses, *gain-of-function* studies will equally give us instructive insights into the function of *Hmx* genes. Continued investigation of the role of *Hmx* genes in other species (e.g., *Drosophila* and chicken) will enhance our understanding of the conserved developmental roles of this gene family.

More and more homeobox genes are being characterized. Most functional data regarding the function of these genes is derived by inactivating them. Relatively slow progress has been made in investigating their sufficiency for patterning, induction, regional specification and cell fate determination. The regulatory pathways through which homeobox genes act remain obscure. Finding out the cofactors, regulators and targets of homeobox genes is a big challenge for developmental researchers. Homeobox gene products *Pbx1* and *Pbx2* can function as cofactors of *Hox* gene products in vitro (van Dijk, et al., 1995). Finding the consensus binding sequence (5'CAAGTGCGTG3') for Hmx3 homeodomain may help us to identify genes downstream of *Hmx3* (Sutherland et al., 1997). Dissecting the regulatory elements of the *Hmx* genes will lead to the isolation of temporal or tissue-specific regulatory elements. Biochemical analyses of these elements

may give us hints as to the regulatory genes upstream of *Hmx*. By searching for the cofactors of the *Hmx* gene products or downstream genes of *Hmx*, the signaling pathway through which *Hmx* genes function will be outlined.

Materials and Methods

1. Isolation and identification of *Hmx* genes in both mouse and *Drosophila*.

a) Genomic library screening for mouse *Hmx* genes.

The homeobox of human *HMX1* (originally called human *H6* gene. Stadler et al., 1992) was PCR amplified using primers TL5 and TL6. The resulting 172-bp fragment was cut from a 1% agarose gel, electroeluted and then extracted with phenol/chloroform. DNA in the aqueous phase was precipitated with 2 volume of 95% ethanol and dissolved in 1xTE. The amplified *HMX1* homeobox was ^{32}P-dCTP labeled by random priming method (Sambrook et al. 1989). Specificity activity of the probe should be above 10^8 cpm/μg.

A mouse 129 genomic library constructed into phage lambda dashII vector was kindly provided by Dr. F. Ramirez's laboratory. More than $2x10^6$ plaques were screened. Plaques on each plate were transferred to duplicate nitrocellulose filters (Millipore, Cat# HAHY13750). After denaturation and neutralization, these filters were baked at 80°C for two hours and then hybridized with the *HMX1* homeobox probe overnight in 6xSSC, 5xDenharts', 0.5%SDS and 100μg/ml yeast RNA at 55°C. Filters were washed in 2xSSC, 0.1%SDS at different temperatures from 50°C to 65°C. The final wash was performed at 68°C in 0.1xSSC, 0.1%SDS. Plaques with positive signals on duplicate filters were purified by the method as described (Khan et al., 1994) with minor modifications. After the third round screening, pure positive plaques were picked into 1ml lambda diluent (10mMTris.HCl pH7.5, 10mM $MgSO_4$) and resuspended overnight at 4°C. Then, 100μl phage solution was incubated with 100μl 2x concentrated overnight culture of host bacteria (i.e., Y1090) for 20 minutes at 37°C. 15ml NZCYM medium was added and the culture was incubated overnight at 37°C with shaking. 500μl chloroform was added to the liquid lysate to kill host bacteria. The supernatant was transferred to a new 50ml tube and spun 5000rpm for 10 minutes to remove bacterial debris. To the clear liquid lysate, DNaseI and RNaseA were added to a final concentration of 20μg/ml, followed by a 45-min. incubation

at room temperature. Then, equal volumes of 2x phage precipitation solution (20% PEG8000, 2M NaCl, 10mM Tris.HCl pH7.5 and 10mM $MgSO_4$) was added and mixed well. The phage particles were precipitated by incubation on ice for 1 hour to overnight, followed by centrifugation for 20 minutes at 8000rpm at 4°C. The phage pellet was dissolved with 300ul 10mM Tris.HCl pH8.0 and then transferred to a 1.5 ml tube. To release phage DNA, 50ul 10% Triton X-100 was added to the dissolved phage particles and the suspension was heated at 85°C for 15 min. Then, 10mM NH_4OAc was added to a final concentration of 500mM. Finally, phage DNA was extracted and precipitated as described above. By this method, 5-10 μg of DNA can be obtained.

Purified phage DNA was digested with various restriction enzymes appearing on the polylinkers of the phage arms, and then subjected to Southern Blot analysis using the same probe for library screening. Both the smallest and biggest positive fragments on the Southern Blots were subcloned into pTZ18R or Bluescript KS^+. The cloned smallest fragment was used for sequencing to confirm the gene's identity. The cloned biggest fragment was used for analyzing the genomic organization of the genes and making transgenic or targeting constructs. To figure out the identity of these cloned phages, degenerated primers, derived from the highly conserved KIWFQN sequence in the third helix of the homeobox genes, were designed. These degenerated oligos are TL104 (5' RTTYTGRAACCADATYTT 3') and TL105 (5' AARATHTGGTTYCA RAAN 3'), where R is A or G, Y is C or T, D is G, A or T, N is A, C, G or T, and H is A, C or T. An experiment done by our laboratory showed that these degenerated oligos can be successfully used as internal primers to sequence many homeobox genes. Sequence analysis was carried out by the dideoxy chain termination method (Sanger et al., 1977) as recommended by USB except that 200ng of degenerated oligo was used for each sequence reaction. Use of degenerated oligos in our work facilitated the identification of new homeobox genes.

b) cDNA library screening for mouse *Hmx2* and *Hmx3* genes.

Using primers TL119 (5'AGAAGGCGAGGCGGTGCC3') and TL120 (5'GGCACGGACGAGACCACC3'), a 472bp genomic fragment of *Hmx3* spanning the homeo-box was PCR-amplified. This fragment was used to screen an E11.5 mouse cDNA library purchased from Clonetech (Cat# ML3003b). The same PCR-amplified fragment was also subcloned and used to make antisense probe for the RNase protection assay (see below). Hybridization was performed at high stringency. Phage DNA from the positive clones was purified as described above. The insert in each clone was released by EcoRI digestion and was then subcloned into the vector pTZ18R. The identity of these clones was verified by sequencing using degenerated primers TL104 and TL105.

In order to get the most 5' sequences of both genes, 5' RACE PCR was carried out essentially as described (Ausubel et al., 1994). The premade library of adaptor-ligated ds cDNA, Marathon-Ready cDNAs was ordered from Clontech (Cat# PR64097). This template was constructed by reverse transcription of poly A^+ RNA extracted from E11.5 mouse embryos. Then the same adaptors were ligated to both ends of the double-stranded cDNA. The first round PCR was performed using primer AP1 (5' CCCATCCTAATACGACTCACTATAGGGC 3') located in the adaptors and TL505 (5'CTCCGAGCTGCTCAGGTAGCGTTC3') specific for both *Hmx2* and *Hmx3*. Expand Long Template PCR System (Boehringer Mannheim, Cat# 1681834) was used. PCR reaction was performed at following conditions:

Marathon-Ready cDNA	5 ul
AP1 primer (10uM)	1.5 ul
TL505 (10uM)	1.5 ul
dNTPs(10uM)	10 ul
10X PCR buffer3	5 ul
$MgCl_2$ (25mM)	1.5 ul
Expand Long Template enzyme mixture	0.75 ul
H_2O	24.75 ul
	50 ul

Cycling Program 1:

1 X	92^0C	2 min
10 X	92^0C	10 sec
	65^0C	30 sec
	68^0C	4 min
20 X	92^0C	10 sec
	65^0C	30 sec
	68^0C	4 min+20 sec/additional cycle
1 X	68^0C	7 min; 4^0C.

After the first round PCR, 5' ends of both *Hmx2* and *Hmx3* cDNAs would be amplified. Aliquot of the reaction was run on a 1% agarose gel and blotted. Positive bands were tested by Southern and partially purified. The "purified" mixtures were diluted 100-folds for second round PCR. Nested primers were used in the following reactions. Nested adaptor primer AP2 (5'ACTCACTATAGGGCTCGAGCGGC3') and TL507 (5'GGCTCTTGGAGTCCAGCTCCTTGTG3') were used to amplify the 5' end of *Hmx3* cDNA Meanwhile, AP2 and TL508 (5'GGAAAGGGATGGGG GTATGGTGCTTAG 3') were used for *Hmx2* cDNA amplification. PCR conditions used is shown as follow:

Diluted 1st round PCR product	1 ul
AP2 (10um)	1.5 ul
TL507 or TL508 (10uM)	1.5 ul
dNTPs (10uM)	10 ul
10 X PCR buffer 3	5 ul
$MgCl_2$ (25uM)	1.5 ul
Expand Long Template enzyme mixture	0.75 ul
H_2O	28.8 ul
	50 ul

Cycling Program 2

1 X	92°C	2 min
10 X	92°C	10 sec
	65°C	30 sec
	68°C	4 min
10 X	92°C	10 sec
	65°C	30 sec
	68°C	4 min + 20 sec/additional cycle
1 X	68°C	7 min; 4°C.

After the second round PCR, the major PCR products were gel-purified and subcloned into vector pTZ18R by TA cloning. The identities of these bands were verified by sequencing using primers in the polylinkers of the vector.

In the above RACE experiment, amplification of *G3PDH* gene, using AP1 and *G3PDH*-specific primers, was performed as a positive control. An 1.3 kb fragment was observed on the 1% agarose gel stained with ethidium bromide (data not shown).

c) Genomic library screening for the *Drosophila Hmx* gene

A *Drosophila* EMBL4 genomic library was screened for *Hmx* genes. Purification of phage DNA and identification of the positive clones were performed essentially as described above.

d) cDNA library screening for the full length *Drosophila Hmx* gene

A *Drosophila* cDNA library of stage 4-8 hr was screened. The template used to make radioactive probe was a 700bp genomic fragment of *Drosophila Hmx* containing the 3' portion of the homeobox. Hybridization and washing conditions are as described above.

2. Chromosomal Mapping

By chromosomal mapping, we can learn the location of the *Hmx* genes on the mouse chromosomes and find pre-existing mutants on the corresponding region. Moreover, it may also help us to identify the human defects mapped to the syntenic chromosome.

The method we used is based on the restriction fragment length polymorphism (RFLP) analysis of DNA from mice having different genetic backgrounds. The first step is to find a DNA fragment (genomic fragment or cDNA sequence) that can distinguish the parental mice C57BL/6J and *M. spretus* when their genomic DNAs are digested with appropriate enzyme. DNA from interspecific backcross progeny generated by mating (C57BL/6J X *M. spretus*) F1 X *M.spretus* was extracted and digested with appropriate enzyme. Normally, 94 backcross progeny are required. Then Southern blot analysis was performed using *Hmx*-specific fragments as probes. The presence or absence of the C57BL/6J-specific fragment(s) in *Hmx* loci was followed in the backcross progeny. At the same time, other known genetic markers on each chromosome was used to detect the recombination frequency between the known genetic marker and *Hmx* loci during mitosis. Therefore, the genetic distance of *Hmx* loci relative to other genetic markers on various

chromosomes can be determined. Generally, a three-point analysis (three genetic markers on the same chromosome) can determine in which chromosome the gene of interest is located. However, to precisely map position of the gene of interest on specific chromosome, multipoint analysis will be required (Danielson et al., 1994).

94 DNAs from N2 animals of a ((C57BL/6J x SPRET/Ei)F1 females x SPRET/Ei males) backcross were obtained from the Jackson Laboratory Backcross DNA Panel Service, Bar Harbor, Maine (Rowe et al. 1994).

To map the chromosomal localization of *Hmx1*, a 0.8 kb EcoRI-XbaI genomic fragment (probe 8 shown in Figure 29) lying 5' to the homeobox of *Hmx1* was used to detect alleles between C57BL/6J and SPRET/Ei. This fragment hybridized to HindIII fragments of approximately 3.0kb in C57BL/6J DNA and 2.9kb in SPRET/Ei DNA.

Chromosomal mapping of *Hmx2* and *Hmx3* was performed by using a 0.6kb HindIII-BglII genomic fragment (probe 1-1 shown in Figure 5) located 1.5kb 3' to the *Hmx3* coding sequence as a probe. This probe detected a 1.5kb specific SPRET/Ei band and a 3.2 specific C57BL/6J on the Jackson Laboratory BSS2 panel digested with HindIII.

Raw data from The Jackson Laboratory BSS backcross were obtained from the World Wide Web address http://www/jax/org/resources/documents/cmdata/.

3. Temporal and spatial expression of *Hmx* genes

a) Northern blot analysis and RNase protection assay

Total RNA from embryos of different stages and from different tissues of adult mice was extracted according to Chomczynski and Sacchi (Chomczynski and Sacchi, 1987). 20μg of total RNA were run on a 1% agarose-formaldehyde gel and transferred to Hybond-N membrane (Amersham). After being baked for two hours at 80°C, the blot was hybridized with a *Hmx3*-specific probe in hybridization solution (50% formamide, 6xSSC,

5xDenharts', 0.02% Sodium Pyrophosphate, 0.1%SDS and 50µg/ul Salmon Sperm DNA) at 42°C. The blot was washed at 55°C in 2xSSC, 0.1%SDS. The film was exposed for a week at -80°C. The probe used in this experiment is a 500bp KpnI fragment purified from the most 5' end of the *Hmx3* cDNA clone (Figure 4). This probe has been tested to unique for the *Hmx3* gene by Southern analysis (data not shown).

More sensitive RNase protection assays were also performed essentially as described (Lufkin et al., 1993). Total RNA from various adult organs of wildtype mice, as well as from wild type, *Hmx3* heterozygote and *Hmx3* null embryos of E11.5 was extracted by a single-step isolation method using guanidinium thiocyanate (Chomczynski and Sacchi, 1987). 100µg total RNA from each sample was used for RNAse protection analysis. A 472bp PCR-amplified fragment (Figure 4 and 19) containing the *Hmx3* homeobox region was used to make ^{32}P-labeled antisense riboprobe. This probe protects a 472bp wildtype RNA fragment as well as two 308bp and 164bp RNA fragments in *Hmx3* mutant embryos. The internal control probe was derived from a 271bp cDNA fragment from the mouse *β-actin* gene. This fragment covers the region from 827 to 1098 bp of the mouse *β-actin* cDNA (Alonso et al., 1986) Hybridization was performed at 55°C. The samples were then digested with 40µg/ml RNaseA and 2µg/ml RNaseT1. After precipitation, the samples were run on an 8% acrylamide gel and exposed to X-OMAT film for 10 days.

b) In situ hybridization on paraffin sections and whole mount embryos

The *in situ* probe for *Hmx1* is derived from the 3' UTR of the *Hmx1* cDNA (Yoshiura et al., 1997). The 256bp XhoI-BamHI fragment was subcloned into the vector pT7T3a (Phamacia), resulting in plasmid pT7T3a-19. The antisense probe was transcribed from the XhoI-linearied pT7T3a-19 with T7 RNA polymerase. The sense probe was generated by transcription of BamHI-linearized pT7T3a-19 with T3 RNA polymerase.

The *Hmx2* in situ probe was produced from plasmid pW187. An 1.2 kb XhoI genomic fragment containing 3' portion of *Hmx2* gene was subcloned into pBluescript

KS$^+$, generating pW51a. pW187 was derived from pW51a by deleting the 340bp XhoI-HindIII fragment which contains the 3' portion of *Hmx2* homeobox. The resulting pW187 contains the entire *Hmx2* 3'UTR. Antisense probe for *Hmx2* was generated by the transcription of HindIII-linearized pW187 with T3 RNA polymerase. The sense probe was transcribed from XhoI-linearized pW187 with T7 RNA polymerase.

pW186 was generated by subcloning a 604bp BglII genomic fragment of the *Hmx3* gene into vector pBluescript KS$^+$. This genomic fragment contains the second exon of *Hmx3* gene. The antisense probe was made by the transcription of the EcoRI-linearized pW186 with T7 RNA polymerase. The sense probe was transcribed from the XhoI-linearized pW186 with T3 RNA polymerase.

Probe for *Wnt7A* is derived from plasmid p567 (from Dr. Andrew McMahon's Lab). This plasmid contains a 400bp insert which spans the position of 1189-1589bp of the *Wnt7A* cDNA.

The *Wnt4* probe was transcribed from plasmid p405 (from Dr. A. McMahon's Lab). The insert covers the region from 851bp to 1275bp of *Wnt4* cDNA.

The *Wnt5A* in situ probe was transcribed from plasmid p59 (from Dr. A. McMahon's Lab). The insert is a 400 bp PCR-amplified fragment of *Wnt5A* gene, which encodes the region from 260 to 391 amino acid of Wnt5A protein (Gavin et al., 1990).

A 387bp fragment of mouse smooth muscle myosin heavy chain cDNA, which contains exon I (75 nucleotide of the untranslated sequence) and most of exon II (remaining 5' UTR plus about 295bp of coding region), was used as a template to make the in situ probe (Miano et al., 1994).

A 421bp SmaI fragment (from position 290 bp to 711bp) of *GATA-3* cDNA (Ko et al., 1991) was subcloned into plasmid pTZ18R, resulting in plasmid pW191a. The antisense probe was transcribed from BamHI linearized pW191a with T7 RNA polymerase.

The in situ probe for mouse LIF was transcribed from a cDNA fragment spanning from position 3279 bp to 3721bp of the LIF gene (Stahl et al., 1990).

The following experiments on in situ hybridization were performed by Maria Nikolova in our laboratory. Briefly, transcription reactions were carried out as described below. 600ng of linearized DNA was mixed with 3µl ^{35}S-CTP (8000Ci/mmol), 12µM cold CTP, 500 µM ATP, GTP, UTP, RNASIN, 25 mM DTT and 20 units of appropriate RNA polymerase (T3 or T7 RNA polymerase). After incubation at room temperature for 1-2 hours, DNA templates were digested with DNAseI for 20 minutes. Then, the radioactive labeled RNA probes were extracted with phenol/chloroform, chloroform and precipitated with ethanol. Finally, the probes were purified by eluting through Sephadex G-50 column.

Embryos of different stages from E8.5 to E13.5 or uteri from pregnant or unpregnant mice (on mixed genetic background) were dissected in 1xPBS and then fixed in 4% paraformaldehyde overnight at 4°C. The fixed embryos were rinsed with 1xPBS and dehydrated in 70%, 95% and 100% ethanol for 30 minutes successively, followed by being treated with Americlear (Baxter, Scientific Products) for 30 minutes. Then the embryos were embedded in paraffin. Orientation of the embryos was adjusted in blocks. Serial sections were prepared and loaded on slides. Sections were deparaffinized and rehydrated in decreased concentration of EtOH from 100% to 30%, followed by being fixed in 4% paraformaldehyde and washed with depc-H_2O. After digestion with Proteinase K for 30 minutes at 37°C, sections were washed and ready for hybridization. Hybridization was performed at 70°C overnight in hybridization mix (300mM NaCl, 20mM NaOAc, 1mM EDTA, 0.1M DTT, 10xDenharts', 250µg/µl tRNA , 10% Dextran Sulfate, 50% formamide and 20,000cpm/µl RNA probe). Slides were washed with 5xSSC, 10mM DTT for 1 hour and then with 2xSSC, 50% formamide, 10mM DTT twice for 30 minutes. Unhybridized RNA was digested with RNaseA and RNaseT at the

concentration of 20ug/ul in NTE. The activity of RNAse was inactivated with 10mM ß-mercaptoethanol in 2xSSC. After washed in 0.1xSSC for 15 minutes at room temperature, the slides were dehydrated followed by being dipped in emulsion (NT2, Kodak) and dried for 2 hours. The slides were kept in the dark for 3-4 days and then developed with Developer D-19 (Kodak) followed by fixed in fixer (Kodak) for 4 minutes. The slides were washed with ddH_2O, stained with hematoxylin for 10 seconds, dehydrated and finally mounted with polymount acrylic mounting media (40%).

Alternatively, early stage expression patterns of the *Hmx* genes were also examined by whole mount in situ hybridization essentially as described (Henrique et al., 1995). This technique uses non-radioactive probes and avoids sectioning early stage embryos, so this method is fast and safe. Using this technique, even a single cell expressing gene of interest can be visualized. This method has the disadvantage in detecting gene expression in late-stage embryos due to the poor penetration ability of RNA probe. Probe for the gene of interest is prepared in the presence of digoxigenin-UTP followed by DNaseI digestion to remove the DNA template. When digoxigenin-labeled probe is incubated with pre-treated mouse embryos, it will hydridize with target RNA expressed by mouse embryos. Unhybridized RNA will be digested with RNaseA. After incubation of the embryos with anti-digoxigenin antibody conjugated to alkaline phosphatase, the embryos will be treated with the substrate of alkaline phosphatase, 5-bromo-4-cholro-3-indolyl phosphate (BCIP) that is mixed with nitro blue tetrazolium (NBT). Because NBT can detect precipitated digoxigenin-antibody-alkaline phosphatase-BCIP, the expression of the gene of interest can be discerned (Sambrook et al., 1989).

The expression of *Drosophila Hmx* gene in 4-hour *Drosophila* embryos was also examined in collaboration with Dr. Manfred Frasch's laboratory. The in situ probe used was derived from a 700 bp HindIII-EcoRI genomic fragment of the *Drosophila Hmx* gene, which contains the 3' portion of the gene.

4. Identification of regulatory elements in the *Hmx* loci.

In the following transgenic mouse assays, we are trying to analyze the structure of *Hmx* genes, especially the promoter or enhancer regions that result in tissue specific expression of *Hmx* genes. The experimental strategy is to make transgenic mice which express a fusion gene consisting of reporter gene *lacZ* under the control of the putative regulatory region(s) of the gene of interest. The functions of these regulatory elements can be precisely discerned by the pattern of β-galactosidase staining in the transgenic embryos.

Actually, the reporter gene used in our experiment is modified *lacZ*, called *ires.lacZ*. The internal ribosome entry site (ires) was originally discovered in the *Picornavirus* 5'NTRs. The complicated secondary structure of the *ires* can initiate cap-independent translation in eukaryotic cells. So, this *ires* element can be used to generate multi-cistronic transcripts in which the translation of each gene is independent from each other (Jang et al. 1988, 1989 and 1990). When the *ires.lacZ* is integrated into transcriptionally active genes, the expression patterns of these genes can be visualized by staining for β-galactosidase activity. This approach avoids the technical difficulty in fusing *lacZ* gene in frame to its upstream gene.

The original plasmid containing *ires.lacZ* gene is pWH7A. p1076 is derived from pWH7A by converting the unique SpeI site into a XhoI site with oligo TL151(5'CTAGCTCGAG3'). The unique SalI site of p1076 was blunted out by Klenow, resulting in plasmid p1085. The fragment containing *ires.lacZ* gene can be released by cutting p1076 with enzyme XhoI. Because we did not know the position of the polyadenylation site of *Hmx2* in the 31kb genomic fragment, construct containing *ires.lacZ.SV40.polyA+* had to be produced. Construct p1039 was generated by blunting out unique SalI site of pWH7A in the polylinker of the vector with Klenow. Using primers TL213 (5'TTTACTAGTAAAGCAAACTTGTTTATTG3') and TL214

(5'TTTACTAGTCTCGAGTCAGTGAGCGAGGAAG3'), a 256bp DNA fragment containing SV40 poly-adenylation site was PCR amplified. A SpeI site was introduced into the 5' end of this amplified fragment and a SpeI site and a XhoI site were introduced into the 3' end. Then, the polyA$^+$ signal was inserted into the unique SpeI site of p1039, resulting in plasmid p1101. The plasmid p1102 was derived from p1101 by blunting out the SalI site with Klenow. Thus, a DNA fragment containing *ires.lacZ.SV40.polyA*$^+$ can be purified from p1102 by XhoI digestion.

First, we tried to find out what regulatory elements exist in the isolated 31kb *Hmx* loci. A 20 kb SalI fragment containing the *Hmx3* homeobox was isolated from mouse phage 4 (Figure 5). This fragment was subcloned into the SalI site of pTZ18R by the "shot-gun" method. The resulting plasmid is named pW8. A restriction map of this 20kb fragment shows that there are two XhoI sites which are 4kb apart, with one located in the homeobox of *Hmx3* and another one 5' to the homeobox. In order to insert *ires.lacZ* into the XhoI site in the homeobox of *Hmx3*, the other XhoI site must be disrupted. ClaI and HpaI are two unique sites in pW8. The ClaI-HpaI genomic fragment containing the other XhoI site was subcloned into the ClaI and SmaI sites of vector pV2 that is derived from pBluescript KS$^+$ by blunting out the XhoI site with Klenow. The resulting plasmid is pW47. pW48 was derived from pW47 by blunting out the XhoI site in the insert with Klenow. Then, pW43 was linearized with BamHI and the resulting free ends were blunted with Klenow. The insert of pW48 was released by cutting the linearized pW48 with ClaI. Purified insert was put back into ClaI and HpaI sites of pW8, leaving the XhoI site in the homeobox unique and resulting in plasmid pW57. A 3.5 kb DNA fragment containing *ires.lacZ* was purified from p1085 and inserted into this unique XhoI site. Sequence analysis confirmed that, in the resulting plasmid pW65a, *ires.lacZ* and *Hmx3* have the same transcription orientation. The chimeric gene consisting of a 20kb *Hmx3* genomic fragment and 3.5 kb *ires.lacZ* was released by cutting pW65a with SalI. Then, this 24kb

fusion gene, *Hmx3.ires.lacZ* transgene (shown in Figure 16) was gel purified and dialyzed for two days in 1/4 x TE buffer.

The transgene construct for *Hmx2* was generated as follows. First, a modified pBluescript KS^+, pV4 was produced by inserting oligo pair 5' TCGATGGCGG CCGCCA 3' and 3' ACCGCCGGCGGTAGCT 5' into the XhoI site to destroy this XhoI site and introduce another NotI site in the polylinker. An 11kb EcoRI genomic fragment spanning the *Hmx2* homeobox was subcloned into pV4. In the resulting plasmid pW74a, there are two XhoI sites as shown in Figure 16. One XhoI site is located in the middle of the *Hmx2* homeobox. The other XhoI site is positioned 1.2kb 3' to the homeobox. To leave the XhoI site in the homeobox unique, pW74a was double digested with SalI and XhoI. A 700 bp SalI-XhoI fragment, designated probe 7 in Figure 28, was deleted. Then the 1.2kb XhoI fragment was inserted back into the XhoI and SalI sites of pW74a. The resulting plasmid pW75a contains a unique XhoI site in the *Hmx2* homeobox. pW79b is derived from pW75a by inserting *ires.lacZ.SV40 polyA*$^+$ into its unique XhoI site. Orientation of *ires.lacZ.polyA*$^+$ is determined by sequencing. The *Hmx2.ires.lacZ .polyA+* construct (shown in Figure 16) was released from the vector by cutting pW79b with NotI.

Injection of the *Hmx* transgene constructs into one-cell embryos and implantation into the oviducts of pseudopregnant females were performed by the transgenic core of Brookdale Center for Developmental and Molecular Biology, Mount Sinai Medical Center.

Based on in situ hybridization results, embryos were first removed at E10.5. Genomic Southern blotting was performed to determined whether these recovered postimplantation embryos are transgenic. Yolk sac DNAs were extracted as described (Lufkin et al. 1991) and digested with *BamH*I in this experiment Using ^{32}P-dCTP labeled *ires.lacZ* as probe, 3.2kb positive bands should be detectable in transgenic embryos. In some cases, transgenic animals may not express the transgenes if the transgene is integrated into a silent locus in the mouse genome. Expression of the transgenes can be visualized by staining for β-

galactosidase activity (Sanes et al., 1986). Dissected embryos were first fixed in 1ml fix solution (2% formaldehyde, 0.2% glutaraldehyde, 0.02% NP-40 and 0.01% sodium deoxycholate in 1xPBS) for 20 minutes on ice. Embryos were washed with 1xPBS 3-4 times rapidly and then stained with X-gal in staining solution (5mM $K_3Fe(CN)_6$, 5mM $K_4Fe(CN)_6$, 2mM $MgCl_2$ and 1.0mg/ml X-Gal in 1XPBS) overnight at 37°C. Stained embryos can be stored in 4% paraformaldehyde in 1xPBS or 70% ethanol. In this experiment, stained embryos were photographed on a dissecting microscope followed by sectioning these embryos to discern the cell types expressing *Hmx.ires.lacZ* transgenes.

To obtain permanent transgenic lines for the *Hmx* genes, tailtip DNAs from 2-week old offspring were extracted and subjected to genomic southern blotting. Transgenic mice were raised till they were ready to mate. Germline transmission of these transgenes was examined. These transgenic mice mated to wildtype females to produce transgenic embryos. Transmission and expression of these transgenes were determined by Southern Blot analysis and β-galactosidase staining, respectively. Embryos removed at different stages (i.e., in this experiment from E9.5-E14.5) were used to examine the temporal and spatial expression patterns of these transgenes. By this approach, regulatory elements responsible for temporal and spatial-specific expression of *Hmx* genes in the isolated 31kb genomic fragment of *Hmx* loci can be determined.

In the near future, we are going to make a series of constructs consisting of a fusion of subfragments from the isolated 31kb *Hmx* genomic fragment to the *TATA-lacZ* coding region to identify the minimal elements responsible for the spatiotemporal-specific expression of the *Hmx* genes (Frasch et al., 1995). By analyzing the minimal regulatory elements at the molecular level, we can get clues as to the regulatory factors binding to these elements. To generate the regulatory hierarchy involved in the *Hmx* genes in early mouse development, oligo competition and gel-shift assay are useful techniques. Furthermore, regulatory element conservation during evolution will be investigated by

testing whether these regulatory elements can direct *lacZ* expression in a similar spatiotemporal manner in other species such as *Drosophila.*

5. Targeted disruption of the *Hmx* genes by homologous recombination.

a) *Hmx3* targeting constructs.

An 11.5 kb *Xba*I genomic fragment spanning the homeobox of *Hmx3* gene (shown in Figure 19A) was subcloned into vector pTZ18R, generating plasmid pW7f. A copy of an 1.7kb XhoI fragment from plasmid p662 containing *neo*^{r} gene, was inserted into the unique XhoI site located in the homeobox of *Hmx3* in pW7f. The resulting plasmid was designated pW22a. The targeting construct is SalI-linearized pW22a (the targeting construct shown in Figure 19A).

This classic targeting strategy was refined by using *ires.lacZ.neo* instead of the *neo* gene only. The *ires.lacZ.neo* fusion gene was generated as follows. First, the 1.7 kb neomycin-resistance gene was purified by cutting p556 with KpnI and NotI. Then, both ends of the purified fragment were blunted out with T4 DNA polymerase. pWH7A was linearized with SpeI followed by blunting out its free SpeI ends with T4 DNA polymerase. Finally, the *neo* coding sequence was fused to *ires.lacZ* by blunt-end ligation with T4 DNA ligase, resulting in plasmid p1089. p1099 was produced from p1089 by blunting out its unique SalI site. *ires.lacZ.neo* used in the following experiment is derived from p1099 by XhoI digestion. pW93a (targeting construct shown in Figure 9A) is produced by inserting *ires.lacZ.neo* into pW7f. Using this approach, targeted integration of *ires.lacZ.neo* allows the *ires.lacZ* gene to be put under the control of the endogenous promoters of the *Hmx* genes. High resolution of *Hmx* gene expression can be monitored by β-galactosidase staining in heterozygous mice (embryos). So, the endogenous expression pattern and targeted disruption of *Hmx3* gene can be accomplished by making one construct. Both the

neo and *ires.lacZ.neo* are used to make targeting constructs for each *Hmx* gene. These targeting constructs can be linearized by SalI digestion (Figure 9A and Figure 19A).

b) *Hmx2* targeting construct.

pW64b was generated by inserting an 11kb EcoRI genomic fragment spanning the *Hmx2* homeobox into vector pTZ18R. As shown in Figure 27A, in this EcoRI fragment, there are two XhoI sites. One is located in the homeobox and the other is 1.2 kb 3' to the homeobox. pW64b was double digested with SalI and XhoI. By the "shot-gun" method, the 1.2 kb XhoI fragment was inserted into SalI and XhoI sites of pW64, leaving the XhoI site in the homeobox of *Hmx2* unique. Then, *ires.lacZ.neo* purified from p1099 was inserted into the *Hmx2* homeobox, resulting in plasmid pW78a (targeting construct shown in Figure 27A). The transcriptional orientation of *ires.lacZ.neo* was tested by sequencing. The targeting construct for *Hmx2* gene can be linearized by EcoRI digestion.

c). Targeting constructs for the double knock-out of *Hmx2* and *Hmx3*.

To avoid the phenomena that can be observed due to the functional redundancy of *Hmx2* and *Hmx3*, a construct for disruption of both *Hmx2* and *Hmx3* was produced by deleting an 11kb genomic fragment between *Hmx2* and *Hmx3* homeoboxes. pW67 is derived from pW57 by deleting a 5.5kb BamHI fragment at the most 5' end of the cloned 31kb *Hmx* loci. A 7kb genomic fragment 3' to the *Hmx3* homeobox was deleted by cutting pW67 with XhoI and SalI. The 1.2kb *Xho*I fragment of *Hmx2* gene was inserted into these XhoI and SalI sites, resulting in an 11kB deletion between *Hmx2* and *Hmx3*. The resulting plasmid is called pW70a which contains a unique XhoI site in the chimeric homeobox. The purified *neo* gene from p662 was inserted into the XhoI site of pW70a, generating plasmids pW71b. pW71b can be linearized by EcoRI digestion, resulting in the targeting construct for the double knock-out as shown in Figure 28A.

d) Generation of ES cell clones containing disrupted alleles of the *Hmx* genes.

ES cell transfections are essentially as previously described (Lufkin et al. 1991; Lufkin et al., 1993). Both R1 and D3 cells (Gossler et al., 1986; Nagy et al., 1990; Nagy and Rossant, 1993) were used for electroporation with equivalent success. 10μg of linearized targeting constructs was transfected into ES cells by electroporation. 200μg/ml G418 was used for positive clone selection.

To verify that the targeting construct had been faithfully integrated into the *Hmx3* locus by homologous recombination, DNAs extracted from the G418-resistant clones were digested with BamHI, electrophoresed in 1.0% agarose gels in 1xTAE without ethidium bromide, and transferred to Hybond-N+ membrane after denaturation in 0.5N NaOH. External probes, probe 1 and probe 2 shown in Figure 9A and 19A, were used for Southern Blot analysis. Probe 1 is a 1.5 kb XbaI-NotI fragment lying 3' outside the targeting construct. This probe should be able to detect a 17.8kb wildtype BamHI band and a 9.1kb mutant BamHI band. The 5' probe used in this genomic blotting is a 400bp fragment designated probe 2 (as shown in Figure 9A and 19A). Probe 2 can hybridize to a 17.8kb wildtype BamHI band and a 8.9kb mutant band. Southern genomic blots were also hybridized with ^{32}P-dCTP labeled *neo* gene to make sure that these positive clones contain only single copy of the *neo* gene.

To screen for ES clones containing the disrupted *Hmx2* gene, DNAs from G418-resistant clones transfected with pW78a (targeting construct shown in Figure 27A) were digested with either XbaI or ClaI and NotI. External probes for Southern screening are probe 4 for XbaI digestion and probe 3 for ClaI and NotI double digestion. Probe 4 can detect a 6.7kb wildtype and a 5.7kb mutant bands in the positive clones. Whereas, probe 3 will hybridize to a 21kb wildtype and 17kb mutant bands. Internal probes were also used to confirm that no multiple integration or chromosomal rearrangement occurred.

The targeting strategy for inactivating both *Hmx2* and *Hmx3* is shown in Figure 28A. Homologous recombination of the targeting construct into the *Hmx* locus results in the

deletion of the 11kb genomic fragment between the *Hmx2* and *Hmx3* homeoboxes. In the positive ES clones, the external probe 5 can hybridize to a 17.5kb wildtype EcoRI fragment and a 21kb mutant EcoRI band. Whereas, probe 7 is capable of detecting a 6.8kb wildtype XbaI fragment and a 5.7kb mutant XbaI fragment.

e) Transgenic mouse production.

Positive ES clones were grown in 6 cm culture dishes in ES medium (15% FCS, 0.1mM BME, 4mM L-glutamine, 40μg/ml gentamicin sulphate, 1000 U/ml LIF and 1mM sodium pyruvate in DMEM). Individual ES cells were obtained by trypsinizing these 6 cm dishes for 2 min. and pipetting to break up clumps. Then, 5ml ES medium was added into each dish and ES cells were transferred to 15ml centrifuge tubes and spun down at 1000 rpm for 5 minutes. Finally, ES cells were resuspended in ES medium. Embryos (blastocysts) were obtained as described (Lufkin et al., 1991). Approximately 10-20 ES cells were microinjected into each embryo. Injection of ES cells and reimplantation of injected embryos were performed by Dr. Lufkin.

Male chimeras were backcrossed to either C57BL/6J females for a mixed genetic background, or to 129/Sv females for an isogenic background.

The tetraploid↔ES cell aggregation technique (Nagy et al., 1990; Nagy and Rossant, 1993) using CD-1 mice, was performed to generate $Hmx3^{lacZ}$ heterozygotes (targeting strategy shown in Figure 9A). This technique allows us to produce embryos derived solely from the ES cells carrying one wildtype allele and a mutant allele in which reporter gene *ires.lacZ* has been inserted. By examining β-galactosidase activity, the expression pattern of the endogenous *Hmx* genes can be precisely monitored. Blastomere fusion was carried out using a BLS CF-150 Cell-fusion apparatus and a GPT-250 electrode chamber in 0.3M mannitol (Sigma). Fused embryos were transferred to a microdrop of KSOM (Specialty Medium) and incubated overnight to the 2-cell or 4-cell stage. The zona pellucida was subsequently removed with Tyrode's solution and aggregates were set up with 2-4

tetraploid embryos per ES cell clump in a microdepression in KSOM under oil at 37^0C and 5% CO_2. 24-48 hours later, resulting expanded chimeric embryos were reimplanted into E2.5 Swiss-Webster pseudopregnant females. Embryo collection and β-galactosidase staining of embryos was performed as previously described (Frasch et al., 1995).

f) Histology and scanning electron microscopy.

To analyze the defects in the inner ear of *Hmx3* knockout mice, mice were cardiac perfused with 4% paraformaldehyde for tissue sections or 2.5% glutaraldehyde in cacodylate buffer for SEM. Inner ears were rapidly dissected out in fixative at room temperature (RT). Once the bony labyrinths had been removed, they were fixed with shaking for 4 hours at RT and then at 4^0C overnight. The tissue was then decalcified in 10% EDTA at 4^0C for five days then dehydrated in ethanols followed by histoclear (for sections) and paraffin embedding. 7 μm sections were cut and stained with toluidine blue and coverslipped in Permount. For SEM, during dissection, the stapedial footplate, round window, and the apex of the cochlea were opened to allow fixative penetration. Following washing in PBS, the tissue was osmicated in 1% osmium tetroxide, followed by microdissection in 70% ethanol to remove the utricle, saccule, and the utriculosaccular complex, critical point drying and sputter coating essentially as described (Lufkin et al., 1991). The area of macula sensory epithelium fro the utricles and saccules of *Hmx3* wildtype +/+, heterozygotic +/-, and homozygotic -/- inner ears was determined by measuring the linear extent of each macula sensory epithelium on every 7 μm section of serial sectioned temporal bones. An eyepiece grid reticule in a Zeiss Axiphot microscope was used to count the number of grid boxes filled with macula sensory epithelium at 62.5x magnification and then the grid box count was converted into an area measurement of sensory epithelium in mm^2 by the following formula:

$$\frac{n \text{ x grid box length x section thickness}}{1000 \text{ x magnification}} = \text{macula sensory area in mm}^2$$

where n = number of grid boxes, grid box length = 160 µm, section thickness = 7 µm, magnification = 62.5.

Results

1) The *Hmx* genes belong to a novel gene family of ancient origin.

Table 1 Summary of library screening for *Hmx* genes

Drosophila				Mouse			
genomic		cDNA		genomic		cDNA	
phage#	gene	phage#	gene	phage#	gene	phage#	gene
1	***Hmx***	1	***Hmx***	1	*Msx3*	1	*Otp*
4	***Hmx***	2	***Hmx***	4	***Hmx3***	2	***Hmx3***
others	*Labial etc.*	3	***Hmx***	5	***Hmx3***	3	*Otp*
		4	***Hmx***	8	*Msx3*	6	*Otp*
				10	***Hmx3***	7	*Otp*
				12	*Msx3*	15	*Otp*
				13	***Hmx2&3***	18	*Otp*
				32	*Otp*	AA144	***Hmx3***
				others	*Hoxa-1 etc.*	096EST	

Using the ^{32}P-labeled homeobox of human *HMX1* as a probe, eight positive plaques were obtained from *Drosophila* EMBL4 genomic library. Two were determined to contain the same *Drosophila* homolog of *Hmx* gene by sequencing with primers TL104 and TL105 (Table 1). From a *Drosophila* cDNA library of stage 4-8hr, four positive clones (Table 1) were tested to be the *Hmx* gene. Figure 1 shows the full-length cDNA sequence of *Drosophila Hmx* gene derived from the longest cDNA clone. This gene has a 5' untranslated region longer than 1kb. The first in-frame ATG of the longest open reading frame is located at position 1200. This ATG codon is in the sequence context

Figure 1. Full length cDNA sequence of *Drosophila Hmx* gene. *Drosophila Hmx* gene has a long 5' untranslated region followed by the translation initiation codon (ATG) at position 1200. *Drosophila Hmx* encodes a 364 amino acid polypeptide with a predicted molecular mass of 39 kDa. The amino acid sequence of the homeodomain is in bold. The underlined amino acid sequence, AAELEALNMA is highly conserved among the members of *Hmx* gene family.

Drosophila Hmx cDNA sequence

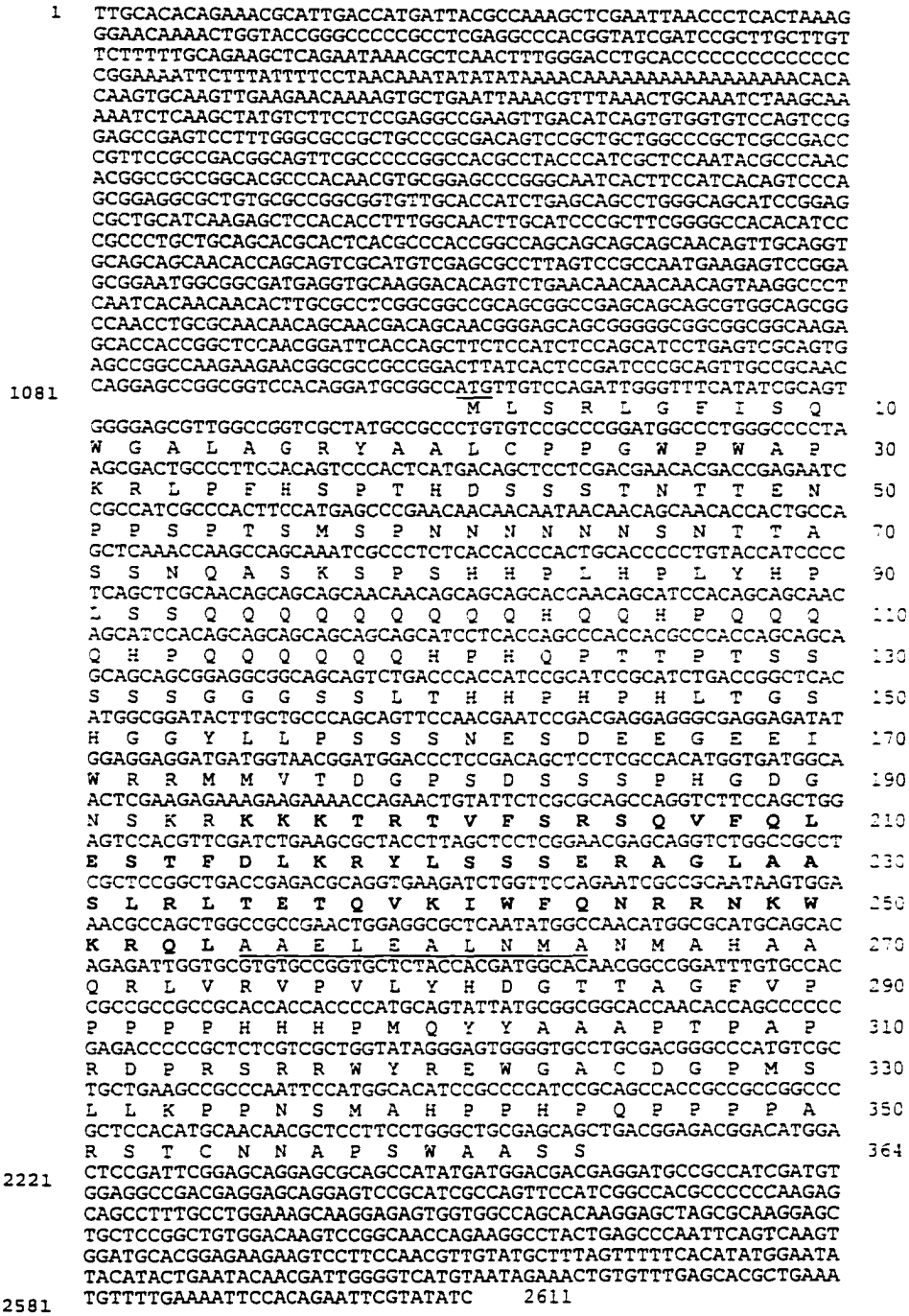

Figure 1

Figure 2. Full length cDNA sequence of mouse *Hmx1* gene. This gene encodes a protein of 350 amino acids. The bold region shows the homeodomain of the Hmx1 protein. The underlined amino acid sequence is the conserved region in the *Hmx* gene family. The nucleotide sequences of the two XhoI sites are also underlined. In the knock out experiment (Figure 29), this XhoI fragment was replaced by *ires.lacZ.neo* cassette. The two doubly underlined nucleic acids (also in bold and italic) show the position of the intron.

Mouse *Hmx1* cDNA sequence

```
   1  AGCCGAGGCCCCGCCTTCTCCCACTCCCTGGCGCGGGTACCGGGGTGGGGGGCGCCGGAA
      GCATCTCGCGGGGTCGTACCCCCAGGACCACCGGGTCTCCTGCCCTGGGCCCTGCCACCA
      CCTGCGCGCAGAGTCCGGCCGGGCAGCATCTCCGGCAATGGCTTCTCTCCGGGCTGCAGC
      GGGTCGTTGGGGCTGAGCCTACGAAACTCGCGCCGCCCCGCCCCCGGCACCGCCCCCTCC
      CCCTCCCGTGAGGCCAGCCGGGGCGGCGACCTGAACCGCTCGGAGAAACGCGAGGGAGGC
      TGCTGCGGGAACGGCCGTCCGCGCGCACCCGCTCCCGCTCCCGCCCAGCCCAGCCCGGCA
      CAGAAGCCGACGCCCGCCTCGTGGAGCCCGACGCCCTCACTCCGGGCAGCGGCTCTCCAG
      GGCCAGGCCGCGCGTGCGCCAGGCGGCCGTTCGCCACTATCCAAACGGGGCCGGGAAGAG
      CAGCTGCGCCCCAGGCAACCAGGGACCCCCAGGATCCCAGCCTTGCCCGACGGGCCCGCG
 541  GCCGCCATGCCGGATGAGCTGACCGAGCCCGGGCGCGCCACACCAGCTCGCGCCTCCTCC
           M  P  D  E  L  T  E  P  G  R  A  T  P  A  R  A  S  S   18
      TTCCTCATCGAGAACCTGCTAGCAGCCGAGGCCAAGGGCGCGGGGCGCTCAACCCAGGGC
       F  L  I  E  N  L  L  A  A  E  A  K  G  A  G  R  S  T  Q  G   38
      GATGGCGTCCGCGAGGAAGAGGAAGAGGACGACGACGACCCCGAGGACGAGGATCCGGAG
       D  G  V  R  E  E  E  E  E  D  D  D  D  P  E  D  E  D  P  E   58
      CAGGCGCGACGACGACTACAGCGGCGGCGACAGCAGCGCGCGGGCAGCGGGCCGGGCGGG
       Q  A  R  R  R  L  Q  R  R  R  Q  Q  R  A  G  S  G  P  G  G   78
      GAGGCGAGGGCCCGGGCACTGGGCCTAGGGCCCCGGCCGCCTCCTGGGCCCGGCCCGCCC
       E  A  R  A  R  A  L  G  L  G  P  R  P  P  P  G  P  G  P  P   98
      TTCGCGAGGGCCCGGGCACTGGGCCTAGGGCCCCGGCCGCCTCCTGGGCCCGGCCCGCCC
       F  A  R  A  R  A  L  G  L  G  P  R  P  P  P  G  P  G  P  P  118
      TTCGCGCTCGGCTGCGGAGGTACAACGCGGTGGTACCCACGGGTGCACGGCGGCTACGGA
       F  A  L  G  C  G  G  T  T  R  W  Y  P  R  V  H  G  G  Y  G  138
      GGTGGTCTAAGTCCTGACACAAGCGACCGGGACTCTCCGGAGACCGGCGAGGAGATGGGC
       G  G  L  S  P  D  T  S  D  R  D  S  P  E  T  G  E  E  M  G  158
      CGCGCAGAGAGCGCCTGGCCGCGGTGCCCCGGGCCGGGAACCGTTCCGCGGGAGGTGACG
       R  A  E  S  A  W  P  R  C  P  G  P  G  T  V  P  R  E  V  T  178
      ACGCAGGGCCCGGCGACCGGCGGGGAGGAGGCGGCGGAGTTGGCCGAGGCTCCAGCGGTG
       T  Q  G  P  A  T  G  G  E  E  A  A  E  L  A  E  A  P  A  V  198
      GCGGCGGCGGCGACAGGGGAGGCGCGCGGTGGCCGCAGGAAGAAGACGCGCACGGTCTTC
       A  A  A  A  T  G  E  A  R  G  G  R  R  K  K  T  R  T  V  F  218
      TCGCGCAGCCAGGTCTTCCAGCTCGAGTCCACTTTCGATCTGAAGCGCTACCTGAGCAGC
       S  R  S  Q  V  F  Q  L  E  S  T  F  D  L  K  R  Y  L  S  S  238
      GCAGAGCGCGCGGGCCTCGCCGCCTCGCTGCAGCTCACGGAGACGCAGGTCAAGATCTGG
       A  E  R  A  G  L  A  A  S  L  Q  L  T  E  T  Q  V  K  I  W  258
      TTTCAGAACCGCCGCAACAAGTGGAAGCGGCAGCTGGCAGCGGAGCTGGAGGCGGCCAGC
       F  Q  N  R  R  N  K  W  K  R  Q  L  A  A  E  L  E  A  A  S  278
      CTGTCCCCGCCGGGTGCGCAGCGCCTGGTCCGCGTGCCGGTGCTCTACCACGAGAGTCCC
       L  S  P  P  G  A  Q  R  L  V  R  V  P  V  L  Y  H  E  S  P  298
      CCGGCCGCCGCGGGGCCCGCGCTGCCTTTCCCGCTGGCGCCGCCCGCACCGCCGCCGCCG
       P  A  A  A  G  P  A  L  P  F  P  L  A  P  P  A  P  P  P  P  318
      CTGCTTGGTTTCTCGGGCGCGCTTGCTTACCCGCTTGCCGCCTTCCCTGCCGCCGCCTCG
       L  L  G  F  S  G  A  L  A  Y  P  L  A  A  F  P  A  A  A  S  338
      GTGCCCTTCCTTCGCGCGCAGATGCCGGGGCTAGTGTGAGCCGGCGCCCTCCATGTAGGA
       V  P  F  L  R  A  Q  M  P  G  L  V                          350
 1621  GGCGGTTGGGGGAAGGCGCCGCGCACCTCGCAGTCCCTCGAGCGGCCGTCTCCGTGGGCA
      GCTGCTCTACAGTGTACCGGACAGCGGCGGCAGCCGGGACTCGCAGCCAGCTGCAGGACT
      GGAGACCCGTTCCGATGGAAAGCCGCGGCGATGCGCTAGCTCTCGCCGGACGGAGTGCTG
      AGCAGATGCCGGCTCCGAGTCAGCAAACGGACACTTGGAATGGGCTGGCCGAGGAACGGT
      ATGGCGACTGTCCCGAGGCATCCTGGCCCTAATTCACATTGTCCTTTTCTCGGGAGGGAT
 1921  CTTGCAGGAACCCAGACATCAGGGGCCCCTCCAAGGGACAGTACAGAGTGCTGCGGGCC
```

Figure 2

(GGCCATGTTG) most closely matching the Kozak consensus sequence (Kozak, 1987). From this ATG, the deduced single open reading frame encodes a 364 amino acid polypeptide with a predicted mass of 39kDa. The homeodomain is situated between residues 194 and 254 (Figure 1). The amino acid sequence AAELALNMA immediately 3' to the homeodomain is highly conserved within the *Hmx* gene family. Analysis of the genomic organization of the *Drosophila Hmx* gene is in progress.

Using the ^{32}P-dCTP labeled human *HMX1* (previously *H6*) homeobox as a probe, a mouse lambda dashII genomic library was screened for murine *Hmx* genes. The results are summarized in Table 1. More than 32 positive plaques were obtained. Clones which were still positive after high stringency washing were subcloned and characterized. Four of them contain murine *Hmx* genes. Phages 4, 5 and 10 correspond to murine *Hmx3* genes. Phage 13 contains the homeoboxes of both *Hmx2* and *Hmx3*, indicating that *Hmx2* and *Hmx3* are closely linked on the same chromosome. The corresponding regions of these phage inserts are shown in Figure 5. An approximately 31 kb genomic *Hmx* -containing fragment was obtained. Based on restriction analysis (Figure 28A) and sequence results obtained from various subcloned fragments (data not shown), the homeobox of *Hmx3* is about 18 kb from the 5' end of this 31 kb genomic fragment. The *Hmx2* homeobox is 11.0 kb 3' to that of *Hmx3*.

An E11.5 cDNA library was screened for *Hmx2* cDNAs. We failed to clone an *Hmx2* cDNA, possibly because of a low expression level. By 5' RACE PCR, a 5' portion of the *Hmx2* gene about 300bp long was cloned (Figure 3). The rest of the sequence was adapted from published work (Bober et al., 1996). No in-frame ATG having a favorable context for initiation can be found in this partial cDNA sequence. Comparison of cDNA sequence and genomic DNA sequence showed an approximately 1.5 kb intron located in the coding region of the *Hmx2* gene (Figure 2 and 5).

Figure 3. Partial cDNA sequence of the mouse *Hmx2* gene. The homeodomain is shown in bold and the conserved region among *Hmx* genes is underlined. In the *Hmx2* knock out experiment (Figure 27), the *ires.lacZ.neo* cassette was inserted into the underlined XhoI site in the homeobox. The position of the intron is shown by the two doubly underlined (also in bold and italic) nucleotides.

Mouse *Hmx2* cDNA sequence

```
   1 CTTGGACGTTCTTGGTTTCCTCCGATTTCTTATGAACCCAGGATGGCAGCAAGGAAGATG
     L  G  R  S  W  F  P  P  I  S  Y  E  P  R  M  A  A  R  K  M  20
     TGGGGAAGGGATGTCCGGCGGCCGGTGGCGTCTCCAGCTTCACCATCCAGTCCATCCTGG
     W  G  R  D  V  R  R  P  V  A  S  P  A  S  P  S  S  P  S  W  40
     GCGGGGGCCCTCCGAGGCACCGCGGGAGCCCGCCGGGTGGCCAGCCAGGAAACGCAGCCT
     A  G  A  L  R  G  T  A  G  A  R  R  V  A  S  Q  E  T  Q  P  60
     GTCTGTGTCCTCGGAGGAGGAGGAGCCGGAGAAGGTTGGAAGGCTCCGGCTTGCTTCTGC
     V  C  V  L  G  G  G  G  A  G  E  G  W  K  A  P  A  C  F  C  80
     CCAGATCCGCACGGCCCCAAGGAGCCAAGCCCTAAGCACCATACCCCCATCCCTTTCCCT
     P  D  P  H  G  P  K  E  P  S  P  K  H  H  T  P  I  P  F  P  100
     TGCCTGGGTACCCCCAAGGGCAGCGGAGGCGCAGGGCCTGCGGCCTCGGAGCGCACGCCA
     C  L  G  T  P  K  G  S  G  G  A  G  P  A  A  S  E  R  T  P  120
     TTCCTTTCTCCTTCTCACCCGGACTTTAAGGAAGAGAAGGAGAGGCTTTTGCCGGCGGGC
     F  L  S  P  S  H  P  D  F  K  E  E  K  E  R  L  L  P  A  G  140
     TCGCCTTCTCCGGGCCCGGAGCGGCCACGGGACGGCGGTGCGGAGCGCCAAACCGGAGCG
     S  P  S  P  G  P  E  R  P  R  D  G  G  A  E  R  Q  T  G  A  160
     GCCAAGAAGAAGACGCGCACCGTCTTCTCCCGCAGCCAAGTGTACCAGCTCGAGTCTACC
     A  K  K  K  T  R  T  V  F  S  R  S  Q  V  Y  Q  L  E  S  T  180
     TTCGACATGAAACGCTACCTGAGCAGCTCGGAGCGCGCTTGCCTCGCCTCCAGCCTGCAG
     F  D  M  K  R  Y  L  S  S  S  E  R  A  C  L  A  S  S  L  Q  200
 601 CTCACCGAGACCCAGGTTAAGACTTGGTTCCAGAATCGCCGCAACAAGTGGAAGCGGCAG
     L  T  E  T  Q  V  K  T  W  F  Q  N  R  R  N  K  W  K  R  Q  220
     CTCTCAGCCGAGCTTGAGGCAGCCAACATGGCACACGCGTCGGCGCAGACTCTCGTGGGC
     L  S  A  E  L  E  A  A  N  M  A  H  A  S  A  Q  T  L  V  G  240
     ATGCCGCTCGTGTTTCGGGACAGTTCGCTGCTGCGAGTGCCGGTGCCGCGCTCTCTGGCC
     M  P  L  V  F  R  D  S  S  L  L  R  V  P  V  P  R  S  L  A  260
     TTCCCGGCTCCGCTTTATTACCCGAGCAGCAATCTCTCGGCCTTACCGCTCTACAACCTG
     F  P  A  P  L  Y  Y  P  S  S  N  L  S  A  L  P  L  Y  N  L  280
     TACAACAAGCTTGACTACTGACATGCTCGCCCGCCGGCTCCCGGGACGCCCCTGGTCGCC
     Y  N  K  L  D  Y                                              286
 901 TGCAGCTGCCTGCATAGCCCGGCGCGGTCGGGATCCTTCGCAGAGCTCCGGAGCAGACGC
     GCGCGTGTCCAGAAATATTAAGAAATACACCATGTGTATTCGTTATGTCTTATTTATGGC
     CTCTTTCCTACCTTTTGTTTTGTTTTGTTTTATTTTGTTTTGTTTTGTTTTGAGTATTTA
     TCTGCATTCCTCACGCCAGAGCACCTGCTTTCTACACAAAACCAAACAACTCGCGTTTGA
     AACTATTTTGGAAGGGGAGGCTCTCGGGTGGTGGTGGGAAGTGGGGTTTTGATTAGGTCG
     GTTTTGACCAGTAGCAAGAAAAAAAAAAAAAACATCAGAAAAACCACCAACAGAACCAGG
     CAGTCTTTCTCCCATATATACACCTGTATATAGAAAATGTGGTAGGACACAAGCTCAGCC
     GAGCCGAACCAACTAGGGCTTTGGTCGTTGAACTAATCACTTCTCTTTATTCCCTTCATC
     TTGAGGATGGGTAGGGGCAAAACGAGGAGAGTACAGATCTGTAAATATTTTTAAAGAGAA
1441 AAAAATAAAACGTTTTAAACATGGTTGCTAAAAAAAAAAAAAA  1483
```

Figure 3

Figure 4. Full length cDNA sequence of the mouse *Hmx3* gene. *Hmx3* contains three exons. The positions of the introns are shown by the doubly underlined (also in bold and italic) nucleotides. The homeodomain of *Hmx3* is in bold and the conserved amino acid sequence 3' to the homeodomain is underlined. At the 5' portion of *Hmx3*, the bold nucleic acid sequences are the putative translation initiation codons. The arrows show the positions of primers used for PCR amplification. This PCR-amplified fragment was used as a template to make antisense ribo-probe for RNase protection (Figure 19). To disrupt the *Hmx3*, the *ires.lacZ.neo* or *neo* cassette was inserted into the underlined XhoI site in the homeobox of *Hmx3* (Figure 19).

Mouse *Hmx3* cDNA sequence

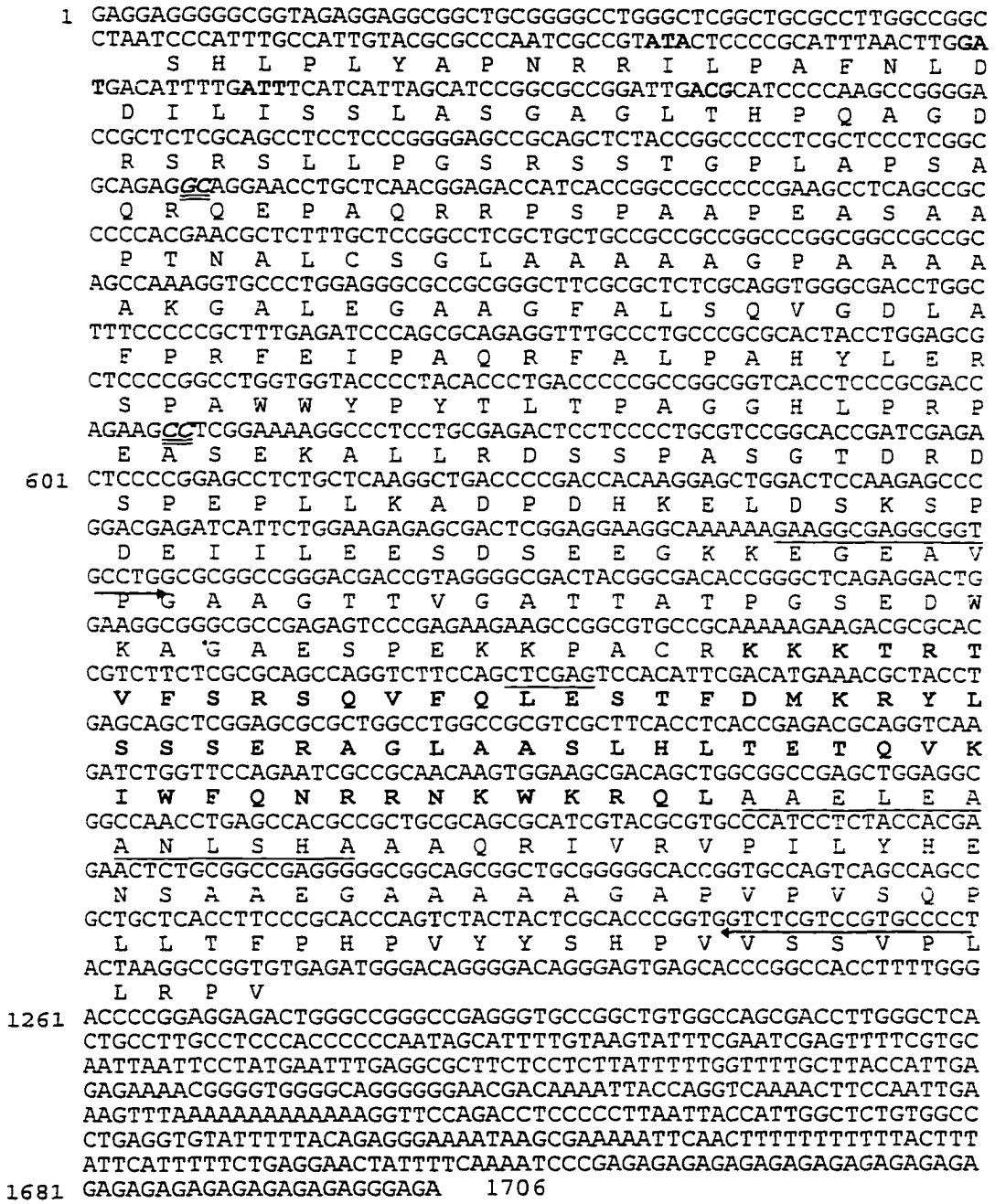

Figure 4

From an E11.5 mouse cDNA library, one positive clone (phage 2 shown in Table 1) was proven to be the *Hmx3* gene (Figure 4). The *Hmx3* cDNA is about 1.7kb in length. The longest open reading frame encodes a 383 amino acid polypeptide. However in this open reading frame, there is no optimal ATG codon capable of functioning as a translation initiation codon at the 5' end of *Hmx3* gene. To confirm the accuracy of the *Hmx3* cDNA sequence, one EST clone shown in Table 1 (Genebank ID# AA144096) was bought from Genome Systems, Inc. This EST clone was obtained from a cDNA library constructed from adult mouse thymus. Two other independent clones were obtained from the 5' RACE PCR products. One clone contains the same insert as does phage 2. The other clone contains a 600bp 5' portion of the *Hmx3* gene. All four independent clones show the same sequence at the 5' end of the *Hmx3* gene. For this reason, we are confident that translational initiation of *Hmx3* does not start with an AUG. Based on the results from other genes (Becerra et al., 1985; Hann et al., 1988; Mehdi et al., 1990), codons other than AUG can be recognized by eukaryotic ribosomes to initiate protein synthesis, although at a low efficiency. In the case of *Hmx3*, ATA, GAT, ATT or ACG may function as the translation initiation codon. In addition to its usage of a non-ATG initiation codon, the *Hmx3* gene is unusual in its genomic organization. Alignment of cDNA and genomic DNA sequences identified that there are three exons in *Hmx3* (shown in Figure 5), whereas most other homeobox genes have two exons. The homeodomain resides in the third exon. The conserved AAELEAAN sequence following the homeodomain is present in the Hmx3 protein.

The homeodomains of these three genes are about 90% similar to each other. Comparison of the homeodomains of these three genes with previously identified genes revealed that they also share striking similarity to *TgHbox5* (Wang et al., 1990), *SpHmx* (Martinez and Davidson, 1997), *gH6* (Stalder et al., 1994), *H6* (human *HMX1*, Stadler et

Figure 5. Genomic organization of the *Hmx2* and *Hmx3* genes. The regions covered by the four overlapping phage clones are shown on the top. Open boxes show the exons of *Hmx2* and *Hmx3*. The position of the homeoboxes is indicated by the closed boxes. The arrows show the transcriptional orientation of both genes. Probe 1-1 is a genomic fragment used for chromosomal mapping.

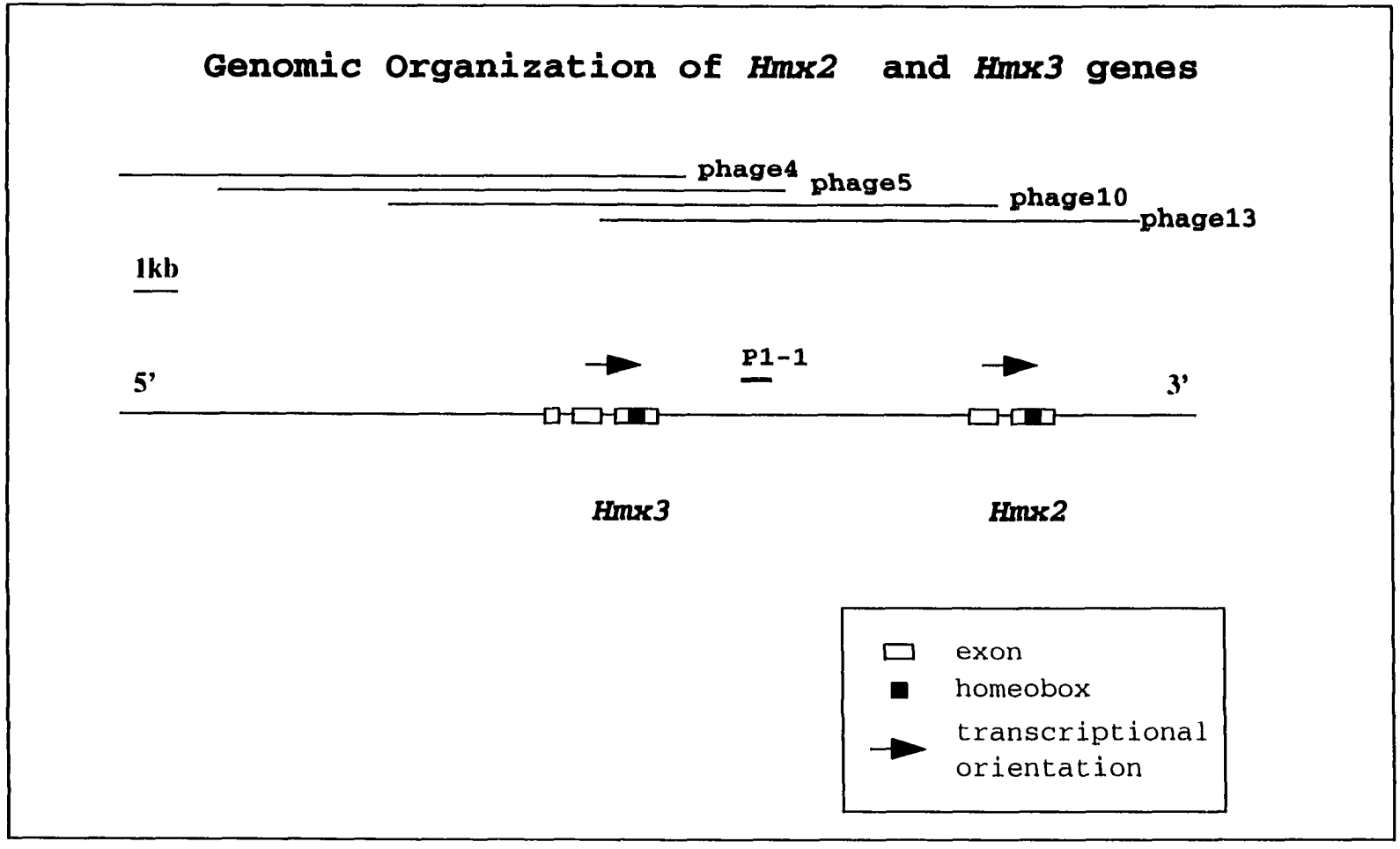

Figure 5

al., 1992) and murine *Hmx1* (Yoshiura et al., 1997), but low level identity to any other homeobox genes except *SoHo-1* (Deitcher et al., 1994). For example, as shown in Table 2, *Hmx* genes are only about 63% similar to the *NK3* gene and less than 60% to the other members in the *NK* gene family. *Hmx* genes do not belong to the *NK* gene family. Moreover, the homeodomain similarities between *Hmx* genes and other homeobox genes, such as *Dlx* and *Hox* genes, are less than 55%. Thus, *Hmx* genes do not fit into any existing classes of homeobox genes. Isolation of the *Drosophila* paralog of *Hmx* further convinces us that *Drosophila Hmx*, murine *Hmx2* and *Hmx3*, together with *TgHbox5*, *SpHmx*, *gH6*, *H6* and murine *Hmx1*, comprise a distinct homeobox gene family, which evolved from the same primordial gene. In addition, the amino acid sequences 3' of these genes' homeodomains are also highly conserved within the *Hmx* gene family. This AAELEAAN sequence can be considered to be characteristic of the *Hmx* genes. For that reason, the *SoHo-1* gene is not classified as a member of the *Hmx* gene family, although its homeodomain is very similar to those of *Hmx* genes. However, *SoHo-1* in chick is closely related to the *Hmx* genes.

Using radioactively labeled *Hmx3* homeobox as a probe, "Zoo" Southern blotting was performed (data not shown). *Hmx* genes exist in a wide variety of species in the animal kingdom, such as cricket, *Drosophila*, Sea Urchin, Zebra fish, mouse and human. No *Hmx* homologs were detectable in yeast, *trypanosome* and hydra. These results indicate that *Hmx* genes have diverged from other homeobox genes and established their own identities conserved in the distant evolutionary past. Existence of *Hmx* gene homologs in horse, sheep and lamprey were confirmed by PCR amplification of the homeobox regions (Stadler et al., 1995). The above results indicate that the *Hmx* genes belong to a novel gene family which exists in a wide variety of species. The function of these genes remains to be investigated further.

Table 2 Homeodomain sequence comparison of *Hmx* genes and other homeobox genes

Drosophila Hmx	DGNSKR**KKKTRTVFSRSQVFQLESTFDLKRYLSSSERAGLAASLRLTETQVKIWFQNRRNKWKRQL**AAELEAANMAHAAQ	**100% (1)**
T.gratilla *Hmx*	SPQK-K----------**EV**----------**N-H**----------**M**--------L-----	**92% (2)**
G.gallus *Hmx3*	QRAAG----------**V**----------**H**----------**HV**--D-----LS----	**93% (3)**
Murine *Hmx1*	EARGG-R----------**A**---------**Q**----------SLSPPGA	**95% (6)**
Murine *Hmx2*	RQTGAA----------**M**----------**C**--**S**--**Q**-------**T**----------**S**----------SA	**92% (1,4)**
Murine *Hmx3*	KKPACR----------**M**----------**H**----------LS---A	**96% (1,4)**
Human *HMX1*	GVGAG----------**Q**----------**HV**-------SLSPPGA	**95% (5)**
SoHo	CSAAGG------**I**--**K**----------**V**------**A**-------**A-H**----------**L**----**S**--P-GPGQ-EPPG	**88% (7)**
NK1(S59)	**PRRA**--**A-TYE-LVS**--**NK-KTT**----**VC**--**LN**--**L**--**S**----------**T**---**K-N**	**58%**
NK2	**--RK-VL-TKA-TYE**--**RR-RQQ**----**AP**--**EH**--**SLI**---**P**---------**H-Y-T**--**AQ**	**53%**
NK3	**--RS-AA**--**HA**---**E**--**RR-AQQ**----**GP**--**SEM-K**----------**Y-T**--**KQ**	**63%**
Nkx2.2	**-R-R-VL**--**KA-TYE**--**RR-RQQ**----**AP**--**EH**--**SLI**---**P**---------**H-Y-M**--**AR**	**55%**
Sax2	**PRRA**--**A-TYE-LVA**--**NK-KAT**----**VC**--**LN-GL**--**S**----------**T**---**K-N**	**57%**
Msx1	**NR-P**--**P-TTA-LLA**--**RK-RQ-Q**---**IA**---**EFSS**--**S**-------**T**------**A-A-L-Q**	**55%**
Emx1	**P-RI**--**A**--**P**--**LLR**--**RA-EKNH-VVGA**--**KQ**--**G**--**S-S**-----**VN**-----**T-Y**---**K**	**53%**
Otx1	**Q-RE**--**T-T**---**LDV**--**AL-AKT**--**PDIFM-EAVELKIN-P-SR-QV**--**K**---**A-CRQ-Q**	**38%**
Dlx2	**VR-P**--**IY-SF-LAA-QRR-QKTQ**--**ALP**---**E**----**G**--**Q**----------**S-F-KMW**	**53%**
Pax3	**QRSS**--**T-TAE-LEE**--**RA-ERTH-PDIYT-EE**--**QRAK**---**AR-QV**--**S**---**AR-RK-A**	**38%**
Evx1	**MRRY**--**A-T-E-IAR**--**KE-YREN-V-RPR-CE**---**ANCP-T**--**I-V**------**M-D-R-R**	**45%**
En-1	**D-RP**--**A-TAE-LQR-KAE-QAN**--**ITEQR-QT**--**QE-S-N-S-I**------**K-A-I-KAS**	**42%**
Hoxa-1	**PNAV**--**N-TTK-LTE**--**KE-HFNK**--**TRAR-VEI**----**Q-N**----------**M-Q-KRE**	**48%**
Ubx	**RRRG-QTYT-Y-TLE**--**KE-HTNH**--**TRAR-IEM-HA-C**---**R-I**--------**M-L-KE-**	**43%**
Antp	**R-RG-QTYT-Y-TLE**--**KE-HFN**---**TRRR-IEI-HA-C**---**R-I**--------**M**---**KEN**	**47%**

(1) this work; (2) Wang et al., 1990; (3) Stadler et al., 1994 (4) Bober et al., 1994; (5) Stadler et al., 1992 (6) Yoshiura et al., 1997; (7) Deitcher et al., 1994; Other homeodomain sequences were from Kappen et al., 1993 The homeodomains of various genes are shown in bold. Identical amino acids are indicated by dashes.

2) The murine *Hmx2* and *Hmx3* homeobox genes are closely linked on the distal region of mouse Chromosome 7, whereas *Hmx1* is assigned to the proximal region of mouse Chromosome 5.

Using a 0.8 kb EcoRI-XbaI genomic fragment (probe 8 in Figure 29) lying 5' to the homeobox of *Hmx1* gene as a probe, we were able to detect a HindIII restriction fragment length polymorphism (RFLP) between C57BL/6J and *Mus spretus* genomic DNA. This probe hybridized to HindIII fragments of 3.0 kb in C57BL/6J DNA and 2.9 kb in SPRET/Ei DNA. The 3 kb HindIII band can be used to follow the segregation of the *Hmx1* allele in 94 N2 progeny of a (C57BL/6J x SPRET/Ei) F1 females x SPRET/Ei males backcross (Rowe et al., 1994). By analyzing the backcross panel, *Hmx1* is mapped to the proximal region of Chromosome 5 (Figure 6). This location is homologous with the 4p16.1 region of Chromosome 4 on which human *HMX1* is located (Stadler et al., 1992). Genetic markers flanking *Hmx1* are shown in Figure 6. Two other homeobox genes, *Sax2* (Chen and Lufkin, 1997), and *Bapx1* (Tribioli et al., 1997), are also mapped to this region.

Chromosomal mapping of the *Drosophila Hmx* (*dHmx*) gene is still in progress. If it is the case that *dHmx is* linked to *S59* (*Drosophila* homologue of *Sax2*) and *bagpipe* (*Drosophila* homologue of *Bapx1*), then, *Hmx1*, *Sax2* and *Bapx1* will constitute an homeobox gene cluster highly conserved during evolution, similar to the *Hox* gene clusters. Moreover, these three genes are also linked to the mouse homologue of *Deosophila msh*, *Msx1*.

A 0.6 kb HindIII-BglII genomic fragment (probe 1-1 in Figure 5) isolated from the *Hmx2* and *Hmx3*-containing genomic phage was used to detect the RFLP between C57BL/6J and *Mus spretus* genomic DNA. This probe is located 1.5 kb 3' to the *Hmx3* coding sequence and 4 kb 5' to the *Hmx2* coding sequence. This probe detects a 1.5 kb SPRET/Ei-specific band and a 3.2 kb C57BL/6J-specific band. Analysis of the backcross panel results reveals that *Hmx2* and *Hmx3* are located on the distal region of mouse

Figure 6. Chromosomal location of *Hmx1* in the mouse genome. (A) Partial linkage map showing the location of *Hmx1* in relation to other flanking loci on the proximal region of Chromosome 5. The centromere (open circle) is shown on the top. Genetic markers and genes linked to *Hmx1* are shown on the right of the chromosome map. Loci mapping to the same position are listed in arbitrary order. Syntenic region of mouse *Hmx1* in human is indicated on the left of the map. A 5-CM scale bar is also shown to the right of the figure. Raw data for the cross are accessible through the Jackson Laboratory World Wide Web site: http://www.jax.org /resources/documents/ cmdata. (B) A haplotype figure for *Hmx1* and adjacent genetic markers on Chromosome 5. Loci are listed in order with the most proximal on top. The solid boxes represent the presence of a C57BL/6J allele and white boxes represent the presence of the SPRET/Ei allele. Numbers of offspring inheriting each haplotype are listed at the bottom of the each column of boxes. To the right of the figure, the percent recombination (R) is given with the standard error (SE) for each R.

Hmx1 maps to the proximal region of mouse Chromosome 5

A

Jackson BSS Chromsosome 5

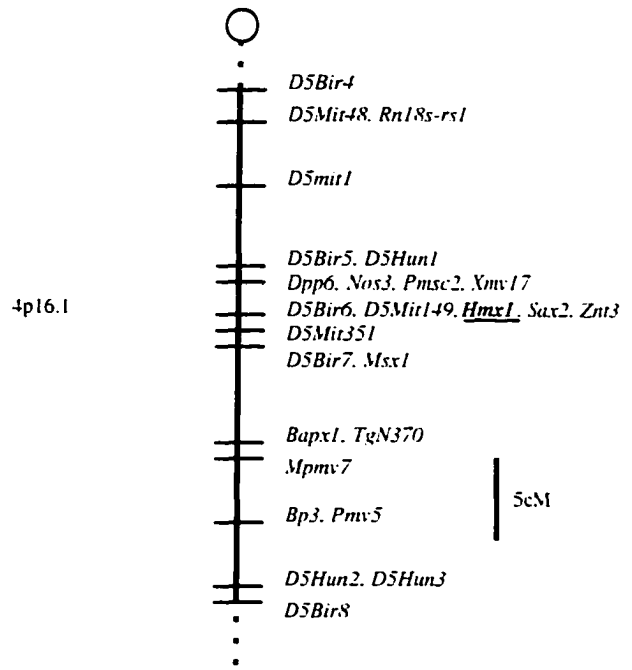

B

Chromosome 5

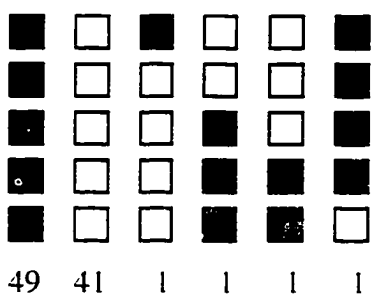

	R	SE
D5Bir5	1.06	1.06
DPP6	1.06	1.06
*D5Mit149, **Hmx1***	1.06	1.06
D5Mit351	1.06	1.06
D5Bir7		
	49 41 1 1 1 1	

Figure 6

Figure 7. Chromosomal mapping of mouse *Hmx2* and *Hmx3*. (A) Genetic linkage map from The Jackson Laboratory BSS backcross showing the distal region of mouse Chromosome 7, with genetic markers linked to *Hmx2* and *Hmx3* genes. The circle on the top is the centromere. Markers linked to the *Hmx2* and *Hmx3*, as well as a 5-cM scale bar are shown to the right of the map. Loci mapping to the same position are listed in arbitrary order. The homologous positions of loci in human chromosomes, identified by flanking genetic markers, are shown to the right. (B) A haplotype figure from the Jackson Laboratory BSS backcross showing loci linked to *Hmx2* and *Hmx3* on the distal region of Chromosome 7. Loci are listed in order with the most proximal on top. The solid boxes represent the C57BL/6J allele and the white boxes represent the SPRET/Ei allele. Numbers of mice carrying each haplotype are listed at the bottom of each column of the boxes. The recombination frequencies (in term of percentage R) between adjacent markers is presented to the right of the figure, with the standard error (SE) for each R. Raw data from the Jackson Laboratory BSS backcross can be obtained from the World Wide Web address http://www/jax.org/resources/documents/cmdata.

Hmx2 & *Hmx3* map to the distal region of mouse Chromosome 7

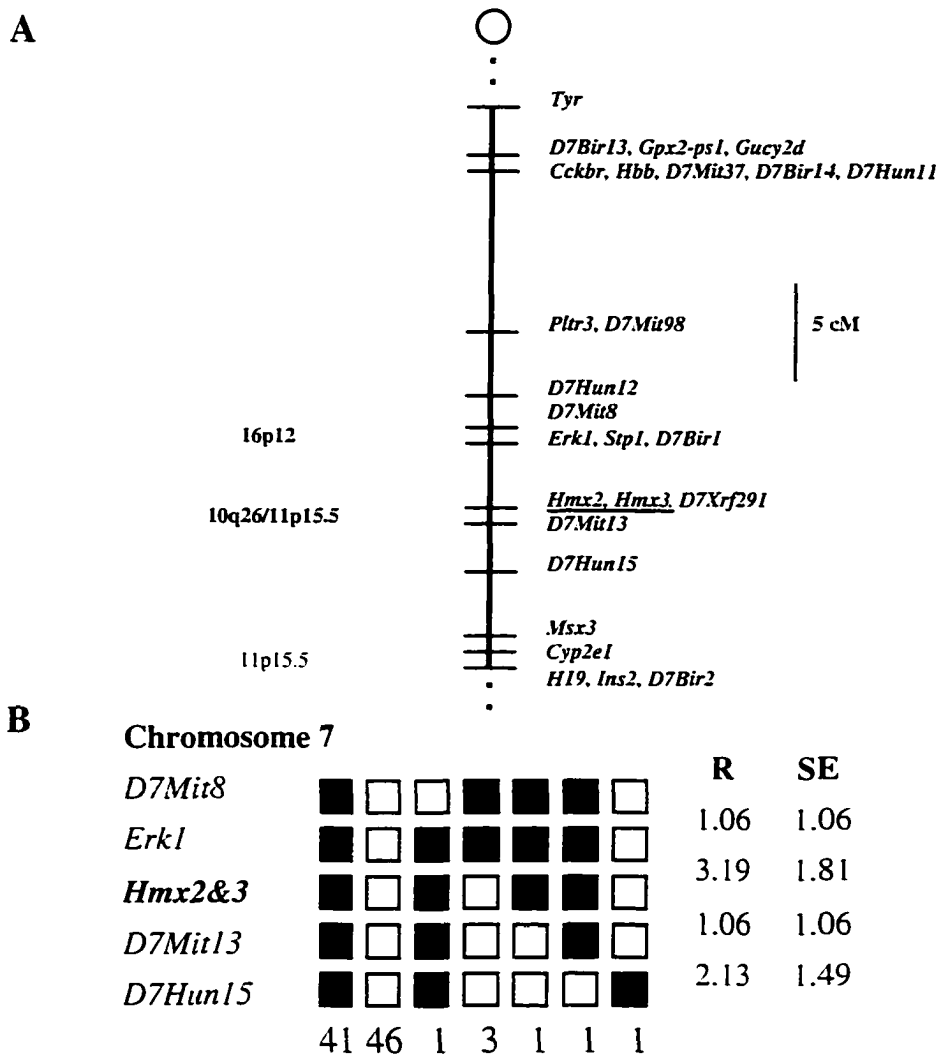

Figure 7

Chromosome 7, to which more than 160 different markers have been mapped. The *Hmx2* and *Hmx3* loci are flanked by markers whose homologues map to the 10q26 region of human Chromosome 10, where human *HMX2* resides (precisely, *HMX2* maps to the 10q25.2-q26.3 region of human Chromosome 10; Stadler et al., 1995). Interestingly, another homeobox gene, *Msx3*, is about 5 map units away from *Hmx2* and *Hmx3*. Furthermore, *Hmx2* and *Hmx3* are also linked to the imprinted genes *H19* and *Igf2*.

The above mapping data from the Jackson Laboratory BSS backcross can be obtained from the World Wide Web address http:www.jax.org/resources/documents /cmdata/.

3) At embryonic stages, *Hmx* genes are expressed in a variety of structures, including the developing central and peripheral nervous systems, the cleft between the first and second branchial arches, the developing sensory organs and the developing duodenum.

In adult mice, *Hmx* genes show a dynamic expression pattern in the uterus during pregnancy.

Whole mount in situ hybridization shows that at the blastoderm stage (~3 hr) *Drosophila Hmx* is expressed in bilateral patches in the dorsal ectoderm of the head (Figure 8). These regions will give rise to brain neuroblasts. No other regions were determined to be positive for *Hmx* gene expression. Its expression in the developing central nervous system may reflect the ancestral function of *Hmx* genes.

In situ hybridization on whole mount mouse embryos with digoxigenin-labeled probes or using radioactive-labeled probes on sections was performed to investigate the expression pattern of *Hmx2* and *Hmx3* genes. Examination of the expression pattern was refined by a knock-in of an *ires.lacZ* reporter gene into *Hmx2* or *Hmx3* (see Material and Methods). In this way, the reporter gene is put under the control of the endogenous *Hmx* gene promoter/enhancer. By staining for β-galactosidase activity, the endogenous *Hmx2* or *Hmx3* expression pattern can be precisely discerned in the heterozygous embryos. The

Figure 8. Expression pattern of *Drosophila Hmx* examined by whole mount in situ hybridization. At blastoderm stage (~3hr), *Drosophila Hmx* is expressed in bilateral patches in the dorsal ectoderm of head (arrows). These regions will give rise to brain neuroblasts.

Expression pattern of *Drosophila Hmx*

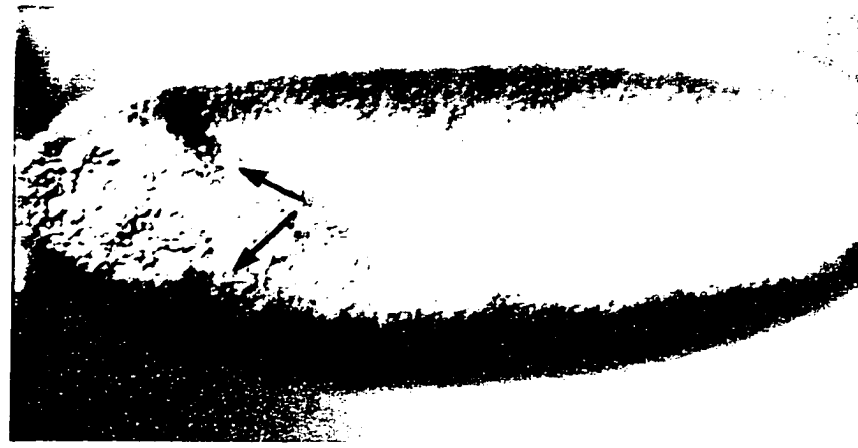

Figure 8

Figure 9. Targeting strategy for knock-in of *ires.lacZ.neo* reporter gene into *Hmx3* locus and ES cell screening for correctly targeted clones. (A) *Hmx3* wildtype locus, targeting construct and *Hmx3* mutant allele. The targeting construct contains the *ires.lacZ* reporter gene followed by the neomycin-resistance gene (*neo*) which was inserted into the unique XhoI site in the homeobox of *Hmx3* gene. The mutant allele will produce β-galactosidase enzyme and a nonfunctional truncated Hmx3 protein. The positions of the *Hmx3* exons are indicated with black rectangles. The external probes for ES cell screening, probe 1 and probe 2 are indicated. (B) Southern blot analysis of ES cell DNAs. Insertion of *ires.lacZ.neo* into the *Hmx3* homeobox yields a new 9.1 kb BamHI fragment detected by probe 1 and a new 9.3 kb BamHI band detected by probe 2 in addition to the 17.8 kb wildtype fragment. Genomic DNA from wildtype ES cells was also included as control (Figure 9B).

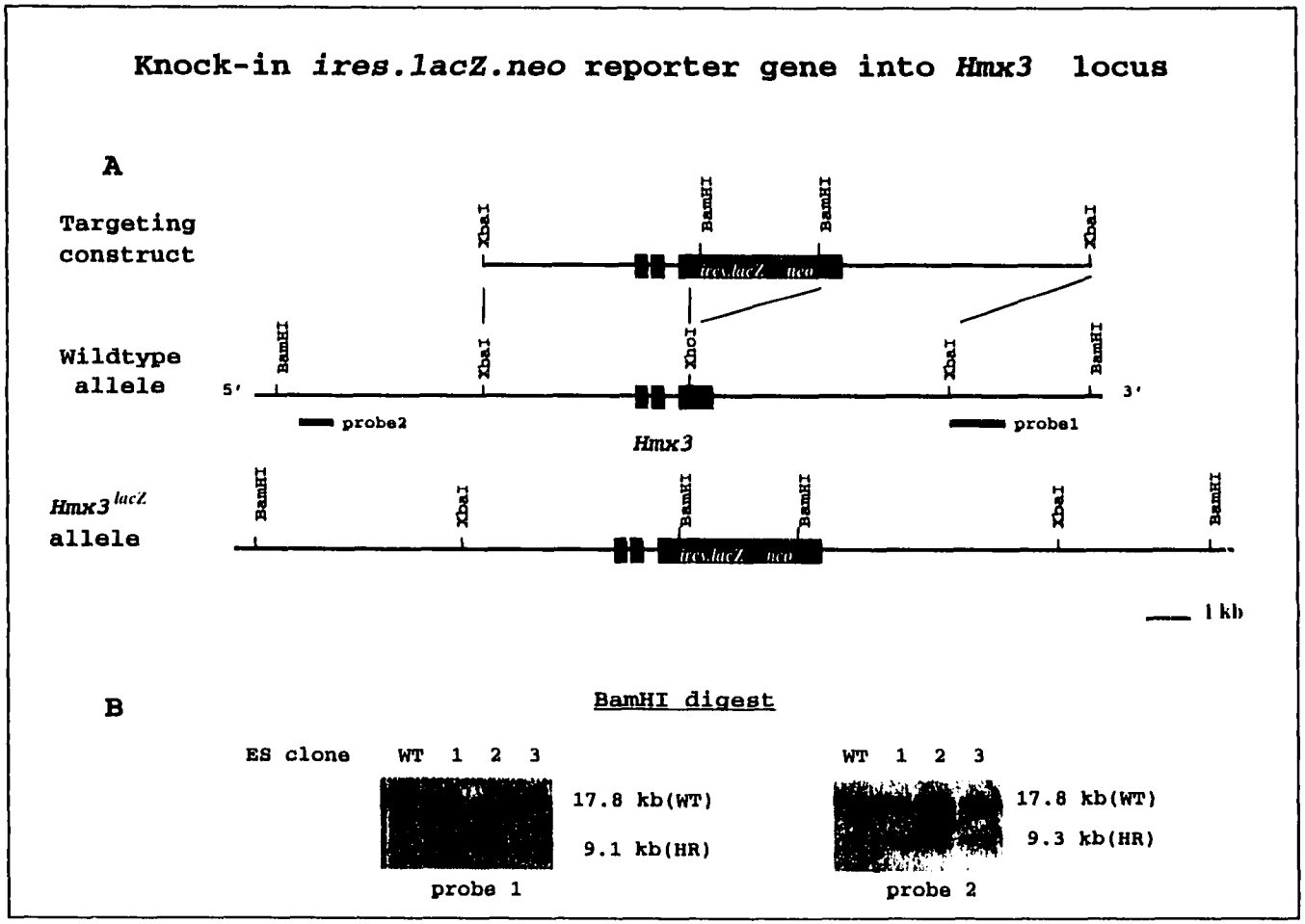

Figure 9

expression pattern of *Hmx2* and *Hmx3* displayed by β-galactosidase staining is identical to the results obtained by RNA in situ hybridization using both radioactive and non-radioactive methods (data not shown). The high resolution of β-galactosidase staining allows us to detect *Hmx* genes expression even at the single cell level.

Expression patterns of *Hmx2* and *Hmx3* are similar in their temporal and spatial distribution (Figure 15). *Hmx3* was first detected at E8.5 in the otic placode and the first branchial arch region (Figure 10A). At the stage of E9.5, expression of *Hmx3* continues to increase in the otic vesicle and the cleft between the first and second branchial arches (Figure 10B-10F). In the otic vesicle, stronger expression can be seen in the rostrodorsal half of the otic vesicle (Figure 11A), which will form the precursor of the vestibular structures (Li et al., 1978; Li et al., 1976). At E10.5, the expression in the central and peripheral nervous systems is turned on (Figure 10G). The expression in the developing inner ear persists throughout gestation. Sectioning of E13.5 $Hmx3^{lacZ}$ embryos revealed strong expression in the epithelium of the developing vestibular ducts and no expression in the adjacent cochlear epithelium.

Interestingly, besides its expression in the developing inner ear, *Hmx3* expression can be detected in almost all sensory organ-related structures (Figure 12). In E10.5 embryos, *Hmx3* signal can be found in the neuroepithelium, which may form the future retina and lens (data not shown). At a later embryonic stage (E13.5), *Hmx3* expression in the eye can be seen strongly in the optic stalk, but weakly in the neural retina and the lens (Figure 12A). Strong signal of *Hmx3* can also be detectable in the ciliary ganglia (Figure 12C). In the regions around the developing tongue, significant *Hmx3* expression can be seen in the regions around the lingual vessels and submandibular duct (Figure 12B). *Hmx3* can also be found in two discrete regions which are the olfactory neuroepithelia of the nasal cavity (Figure 12C).

Figure 10. Beta-galactosidase expression in *Hmx3*^{lacZ} heterozygotes during embryogenesis. *Hmx3*^{lacZ} heterozygote embryos from stages E8.5-13.5 were stained for β-galactosidase activity as wholemounts (A-H) and then serial sectioned (I-P). The expression of *Hmx3* gene is first detectable at E8.5 embryos (A) in the otic placode (arrow) and the developing branchial arch (arrow head). At the stages of E9.0 (B) and E9.5 (C-F), its expression in the otic vesicle (arrow) and in the cleft between the first and second branchial arches (arrow head in C) persists. In E9.5 and later stage embryos, *Hmx3* gene shows stronger expression in the rostral half of the otic vesicle, which is the tissue subsequently giving rise to the vestibule. At later stages (E10.5, G and E12.5, H), *Hmx3* expression extends to the central and peripheral nervous systems significantly. Sagittal (I-L) or transverse (M-P) sections of E13.5 embryos show the strongest expression in the epithelial portion of the developing vestibule. Abbreviations: AD, anterior semicircular duct; ED, endolymphatic duct; HD, horizontal semicircular duct; PD, posterior semicircular duct.

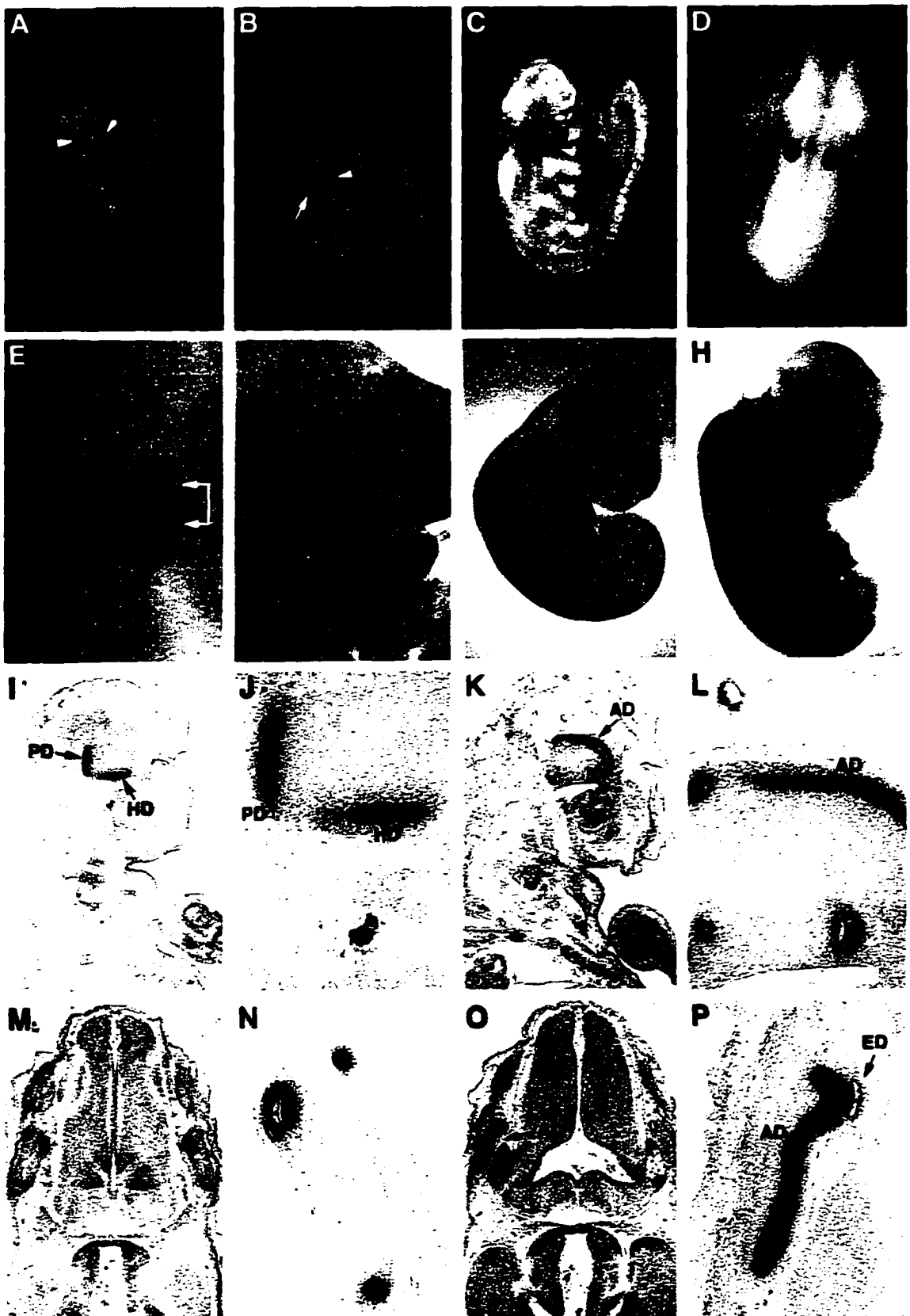

Figure 10

Figure 11. High power view of *Hmx3* expression in the developing inner ear. In E10.5 embryos, *Hmx3* gene is strongly expressed in the rostral half of the otic vesicle. At later stage (E13.5), *Hmx3* signals can be detected exclusively in the epithelium of all three semicircular ducts in the developing inner ear.

Hmx3 expression in the developing sensory organ

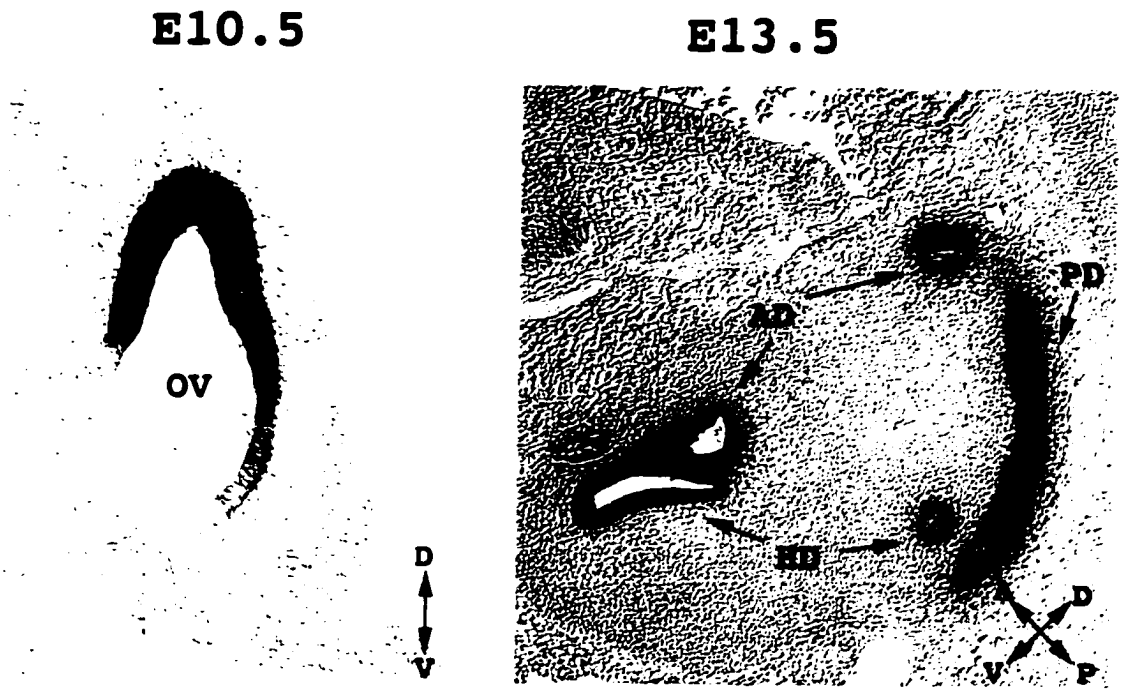

Inner ear

Figure 11

Figure 12. Expression of *Hmx3* in other sensory organs. *Hmx3* expression can be seen in almost all sensory organ-related structures. (A) A transverse section shows *Hmx3* signals present in the optic stalk at E13.5. (B) In the regions around the developing tongue, *Hmx3* expression is restricted to certain regions around the lingual vessel and submandibular duct. (C) In the nasal cavity, *Hmx3* gene is defined to two discrete regions, possibly part of the olfactory neuroepithelium. Ciliary ganglia are also positive for *Hmx3*. Abbreviations: OS, optic stalk; SMD, submandibular duct; LV, lingual vessel; CG, ciliary ganglia; OE, olfactory epithelium.

Hmx3 expression in the sensory organs

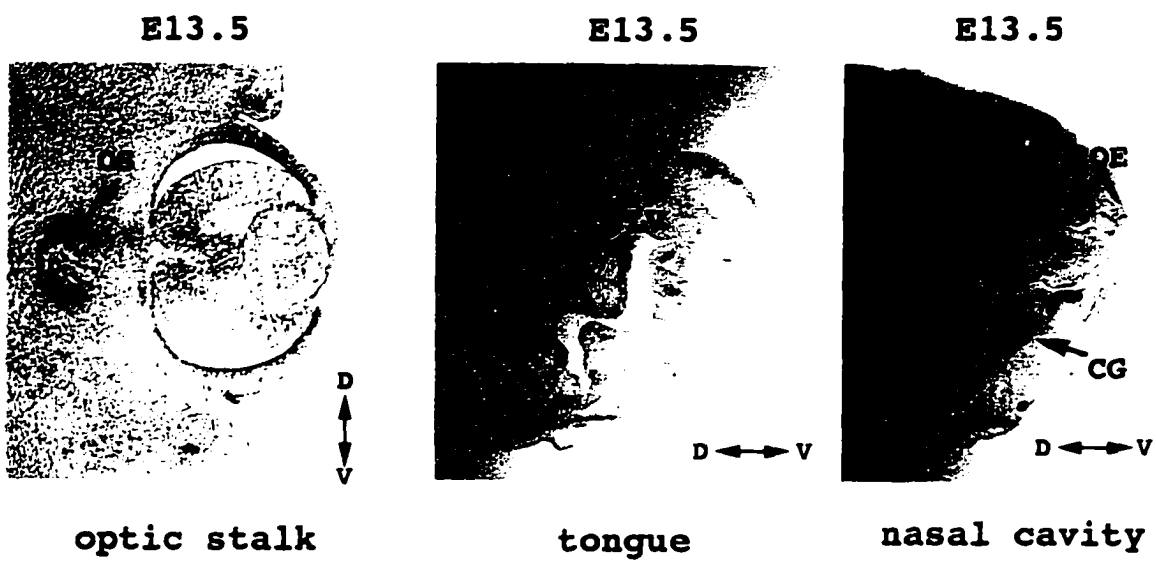

Figure 12

Figure 13. *Hmx3* expression in the nervous system. In the developing brain, *Hmx3* is expressed in discrete regions, including the hypothalamus in mesencephalon, pons, ganglionic eminence, medulla oblongata, choroid invagination as well as the choroid plexus in the myelencephalon (A, B). In neural tube, *Hmx3* is restricted to the edge of neural tube along the longitudinal axis. Strong signals can be seen in a column of cells which lies immediately dorsal to the developing motor column. Relatively weak signals can be detected in floor plate (C). In the peripheral nervous system, cells in the sympathetic chain are also positive for *Hmx3* gene (C). Abbreviations: GE, ganglionic eminence; HT, hypothalamus; MO, medulla oblongata; HB, hindbrain; CI, choroid invagination; Ps, pons; CP, choroid plexus; NT, neural tube; NC, notochord; SC, sympathetic chain.

Hmx3 expression in the CNS and PNS

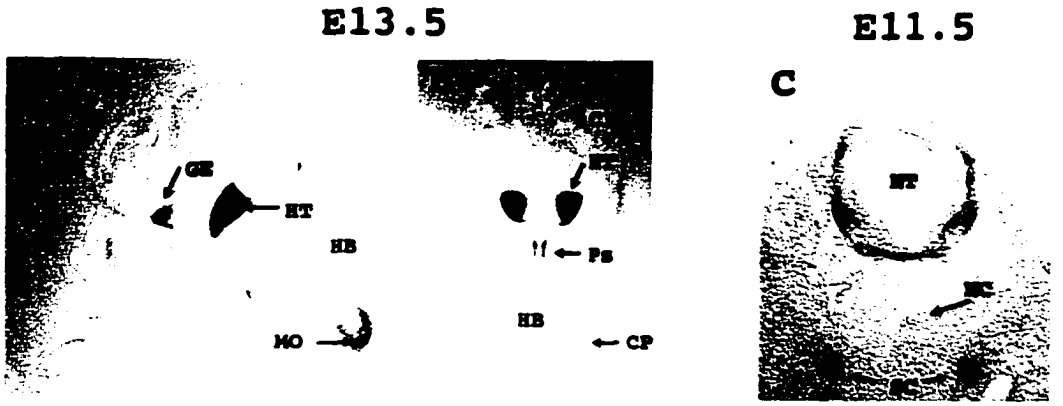

Figure 13

In the central nervous system, *Hmx3* transcripts were restricted to the edge of the neural tube along the longitudinal axis (Figure 10G). The expressing cells are likely postmitotic cells surrounding the mitotically active inner cell layer in the neural tube (Bober et al., 1994). Strong signals can be seen in a column of cells which lies immediately dorsal to the developing motor column. The identity of the cells in this region is uncertain, but may correspond to future interneurons (Rinkwitz-Brandt et al., 1995). Relatively weak signals can be detected in a certain region in the floor plate, possibly the neuronal fibers crossing the floor plate (Figure 13C). In the developing brain, *Hmx3* gene expression extends to discrete regions, including the hypothalamus in the mesencephalon, pons, ganglionic eminence, medulla oblongata, choroid invagination, as well as the choroid plexus in the myelencephalon (Figure 13A and B). In the peripheral nervous system, cells in the sympathetic chain are also positive for *Hmx3* (Figure 13C). Clear signal of *Hmx3* gene expression in the duodenum can be discerned in the muscle layer (Figure 14). The identity of these expressing cells is not known yet. They may be peripheral neurons innervating the muscle layer of the duodenum.

Hmx1 is first detectable in the trigeminal (V) ganglion at E9.5. At E10.5, signal can be seen in the eye, second branchial arch, and the dorsal root ganglion (Yoshiura et al., 1997). In E12.5 embryos, *Hmx1* is expressed in the eye, sympathetic ganglion, and dorsolateral mesenchyme near the developing ear (Figure 15). At later stages, the vagal nerve (X) ganglia becomes positive for *Hmx1* (Yoshiura et al., 1997).

Northern Blot analysis failed to show *Hmx3* expression in mouse embryonic and adult stages due to strong cross hybridization of the *Hmx3* probe to ribosomal RNAs.

At adult stages, *Hmx3* may be expressed at low levels in the thymus, since the EST clone, AA144096, was cloned from a cDNA library of 4-week old mouse thymus. RNase protection failed to detect any signal in heart, lung, liver, spleen, kidney, and skeletal muscle (data not shown). However, *Hmx3* does show expression in the uterus of

Figure 14. Expression of *Hmx3* in the internal organ. *Hmx3* is expressed in the muscle layer of the duodenum. The identity of cells expressing *Hmx3* remains to be investigated further.

Hmx3 expression in the internal organ

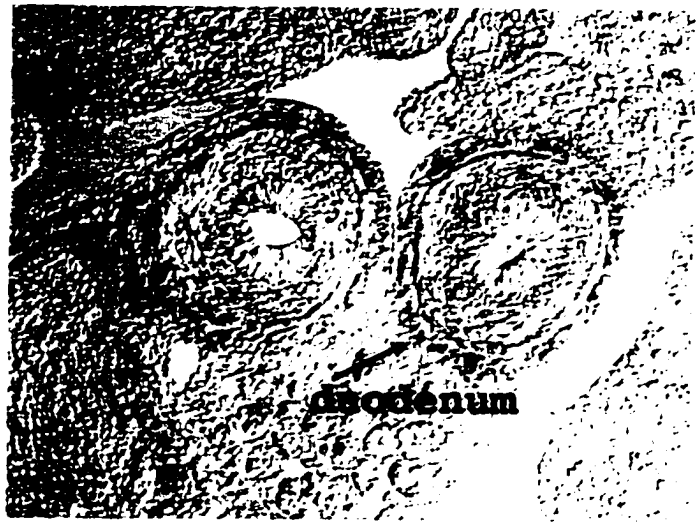

Figure 14

Figure 15. Expression pattern comparison of murine *Hmx* genes. whole mount in situ hybridization shows the expression of *Hmx1* gene in the eye, dorsal root ganglion, sympathetic ganglion, dorsal-lateral mesenchyme near the developing ear. $Hmx2^{lacZ}$ and $Hmx3^{lacZ}$ heterozygote embryos stained for β-galactosidase activity show identical expression pattern of *Hmx2* and *Hmx3* genes in the inner ear and nervous systems.

Expression pattern comparison of murine *Hmx* genes

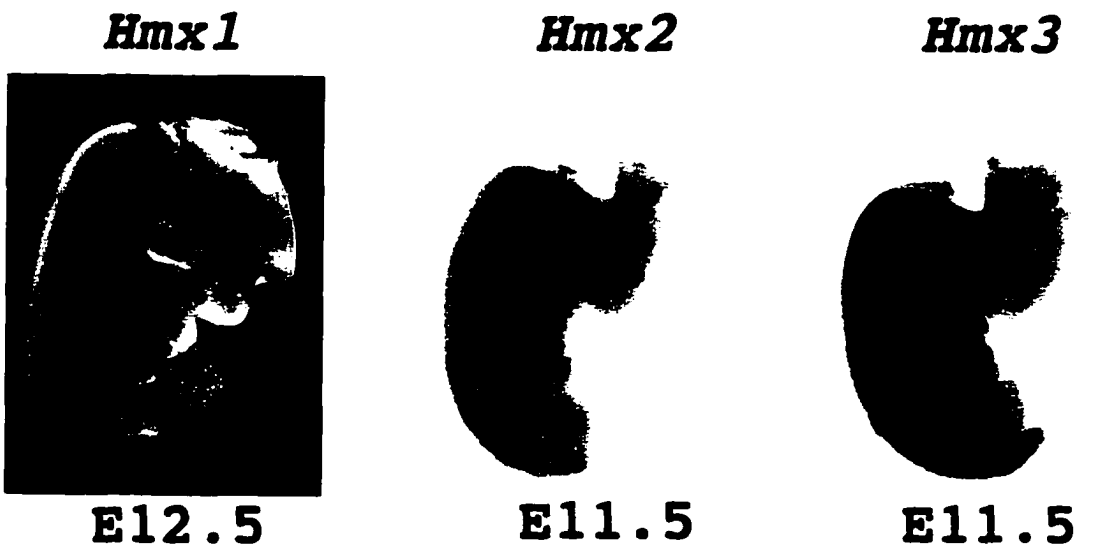

Figure 15

nonpregnant and pregnant females (Figure 25). In situ hybridization using ^{32}P-labeled *Hmx3* was performed in order to closely investigate the expression pattern in the uterus. In nonpregnant uteri, *Hmx3* transcripts show a gradient expression pattern in the uterine stroma, with the strongest expression in cells closest to the luminal epithelium and decreasing levels of expression with the increasing distance from the uterine lumen (Figure 25). During pregnancy, *Hmx3* gene expression alters dramatically. Its expression in the uterine stroma decreases to background levels, whereas a marked increase in the myometrial layer can be discerned (Figure 25). *Hmx1* and *Hmx2* are expressed in a manner almost identical to *Hmx3*, except that *Hmx1* shows weaker expression in the nonpregnant uterus than *Hmx2* or *Hmx3* (Figure 25).

The expression patterns of *Hmx* genes give us informative clues as to the tissue or organs in which *Hmx* genes may function. Expression of all three murine *Hmx* genes in the CNS and PNS, together with the CNS expression of *Drosophila Hmx* gene, may reflect the original functions of the ancestral *Hmx* gene. During evolution, each *Hmx* gene also acquired unique function as shown by their distinct expression domains in the developing sensory organs and adult uterus. Investigation of the function of this gene family is quite interesting and challenging because members of this gene family may function redundantly or synergistically, based upon their expression patterns.

4) The 31kb isolated *Hmx* locus contains regulatory elements which can drive *Hmx* genes to be expressed in the neural retina, lens, tongue, nasal cavity, dorsal root ganglia, as well as the dorsolateral region of the neural tube.

To determine what regulatory elements are located in the 31kb genomic fragment, the fragment was divided into two pieces. Each of them contains the homeobox of *Hmx2* or *Hmx3*. A reporter gene, *ires.lacZ* or *ires.lacZ.poly(A)* was inserted into the homeoboxes. The transgene constructs (Figure 16) were injected into one-cell embryos. Then embryos

Figure 16. Identification of regulatory elements of *Hmx* genes by transgenic analyses. A 20 kb EcoRI genomic fragment containing *Hmx3* gene was subcloned into vector pTZ18R. Reporter gene *ires.lacZ* was inserted into the unique XhoI site in the homeobox. *Hmx3.ires.lacZ* transgene were released from the vector by SalI digest and purified for pronuclei injection. Similarly, an 11 kb EcoRI genomic fragment spanning *Hmx2* homeobox was subcloned into vector pV4. In the resulting plasmid, the XhoI site positioned 1.2 kb 3' to the homeobox was deleted, leaving the XhoI site in the homeobox unique. Then, the *ires.lacZ* reporter gene was inserted into this XhoI site and the *Hmx2.ires.lacZ* transgene was released from the vector by NotI digest.

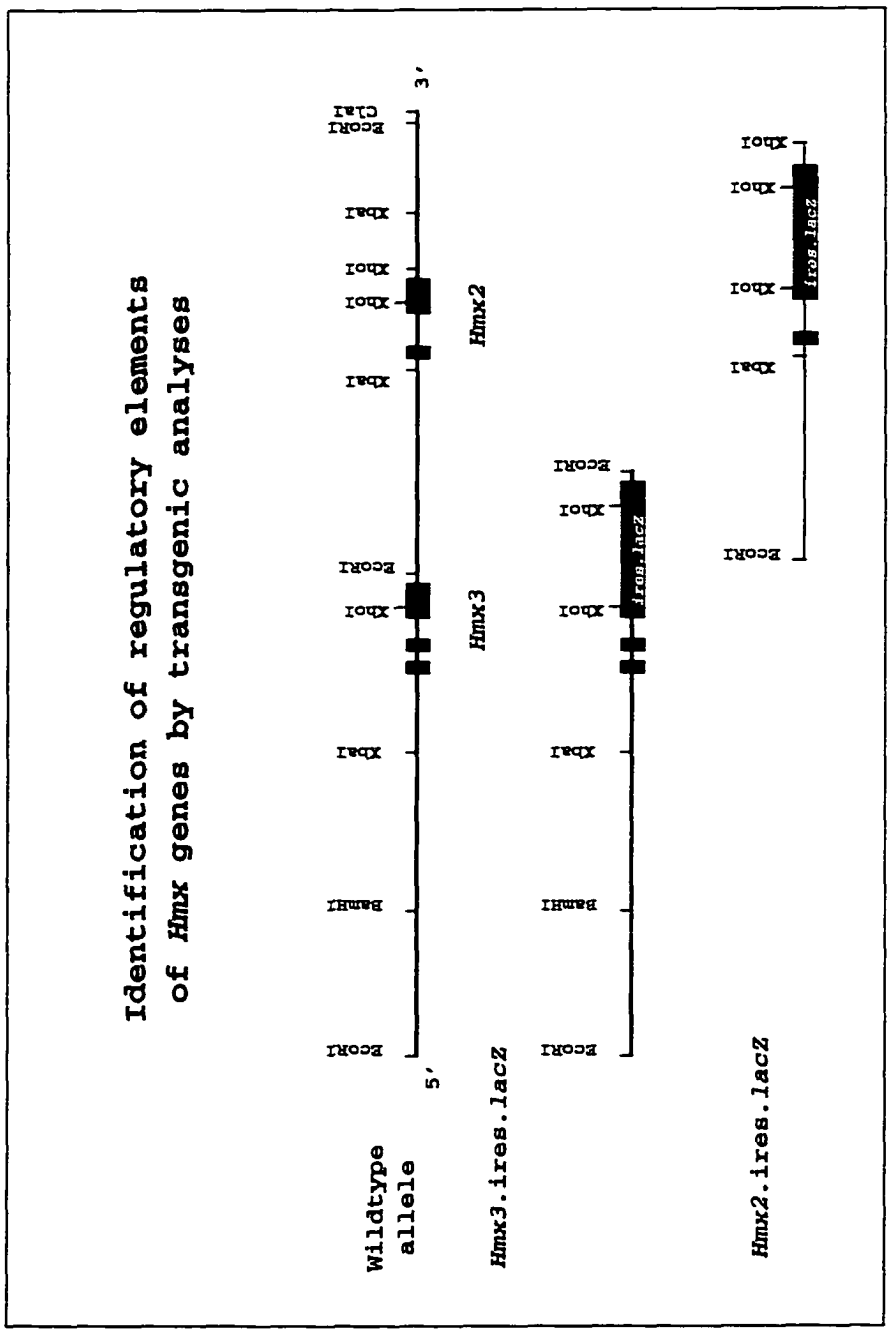

Figure 16

were removed at stage E10.5 and the expression of the transgenes were examined by β-galactosidase staining.

Two transgenic embryos containing *Hmx2.ires.lacZ* (Figure 17) were obtained out of 7 embryos removed at day 10.5 p.c. High expression could be seen in the dorsal edge of neural tube posterior to the otic vesicle (Figure 17A and B). Longitudinally, β-galactosidase positive cells were scattered in the neural tube from the posterior region of the myelencephalon to the prespinal cord in the hindbrain. Two independent permanent lines were generated. Both lines show similar expression patterns in the CNS and PNS, with minor differences. At E11.5-12.5, the transgene extended to the dorsal root ganglia, the cranioganglia, lens, sympathetic chain, tongue and nasal cavity (Figure 17C-G). At E13.5, strong signal can be observed in the craniofacial region.

Out of 20 embryos removed, two were determined to contain the *Hmx3.ires.lacZ* transgene by both Southern analysis and β-galactosidase staining. These two positives showed the same β-galactosidase staining pattern in the eyes. Figure 18A shows an X-gal stained embryo containing the *Hmx3.ires.lacZ* transgene. The eye-specific expression of *lacZ* indicates that the 20kb fragment corresponding to the 5' portion of the cloned *Hmx* loci contains a regulatory element which can direct *Hmx* genes to be expressed specifically in the eye. Sections of this embryo give us the details of the transgene expression. Figure 18B and 18C show that this regulatory element is capable of directing the *Hmx3.ires.lacZ* gene to be expressed in the anterior region of the neural retina in a gradient fashion with the highest level in the anterior region and the lowest in the mid-lateral region. Almost no expression can be seen in the pigmented layer of the optic cup. Within the neural retina, its expression is clearly restricted to the outer layer (neuroepithelium) in which the rods and cones of photoreceptors reside. Two other permanent lines containing the *Hmx3.ires.lacZ* transgene were obtained and determined to be capable of germline transmission. Embryos removed at E10.5 showed the same expression pattern in the eye. In the central and

Figure 17. Expression profile of *Hmx2.ires.lacZ* transgene. (A) A E10.5 embryo carrying the *Hmx2.ires.lacZ* transgene shows expression in the neural tube around the otic vesicle. (B) A coronal section of the embryo shown in (A) reveals the expression in the edge of the neural tube. (C, D) Lateral and dorsal view of an E11.5 embryo carrying the *Hmx2.ires.lacZ* transgene. The transgene can be seen in the dorsal root ganglion (C, D and E), lens (F), as well as certain cranionfacial regions (G). (H) Strong expression in the craniofacial region at E13.5 stage.

***Hmx2.ires.lacZ* transgene**

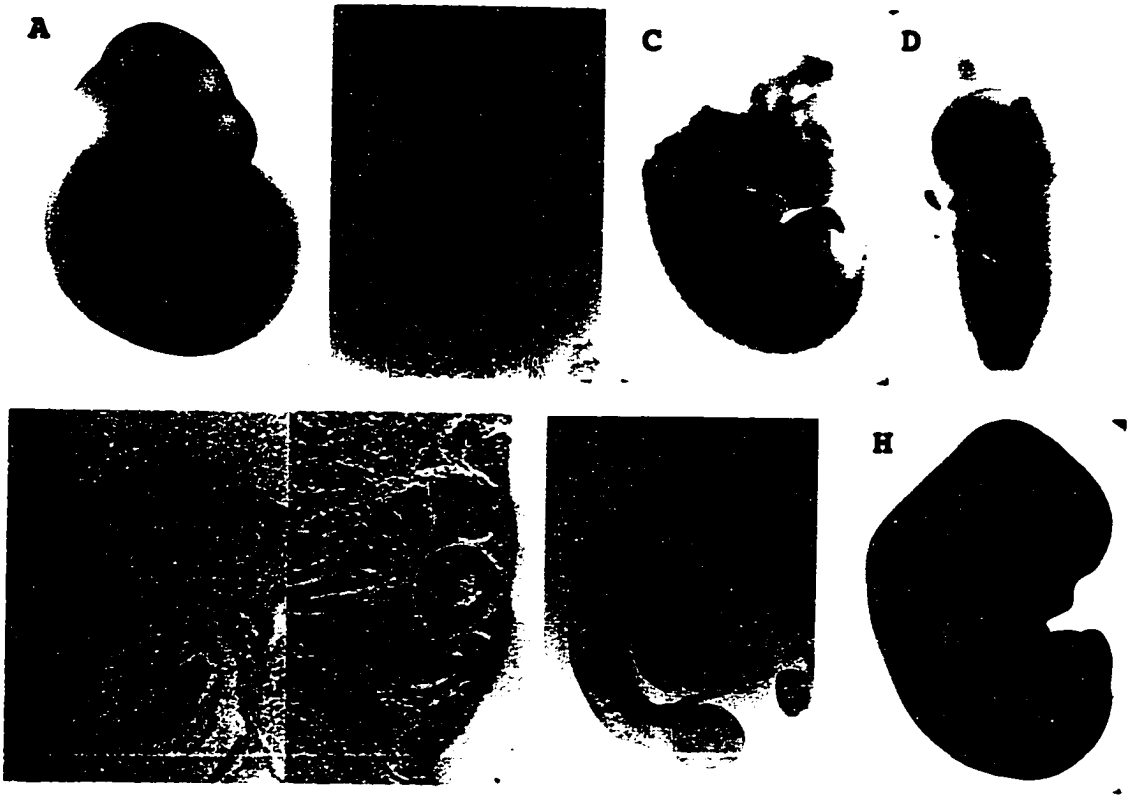

Figure 17

Figure 18. Expression pattern of *Hmx3.ires.lacZ* transgene. At early stage (E10.5), *Hmx3.ires.lacZ* is restricted to the dorsal portion of the neural retina in the eye (A, B and C). At later stage (E12.5), expression of the transgene extends to the neural tube and midbrain (D, E and F).

***Hmx3.ires.LacZ* transgene**

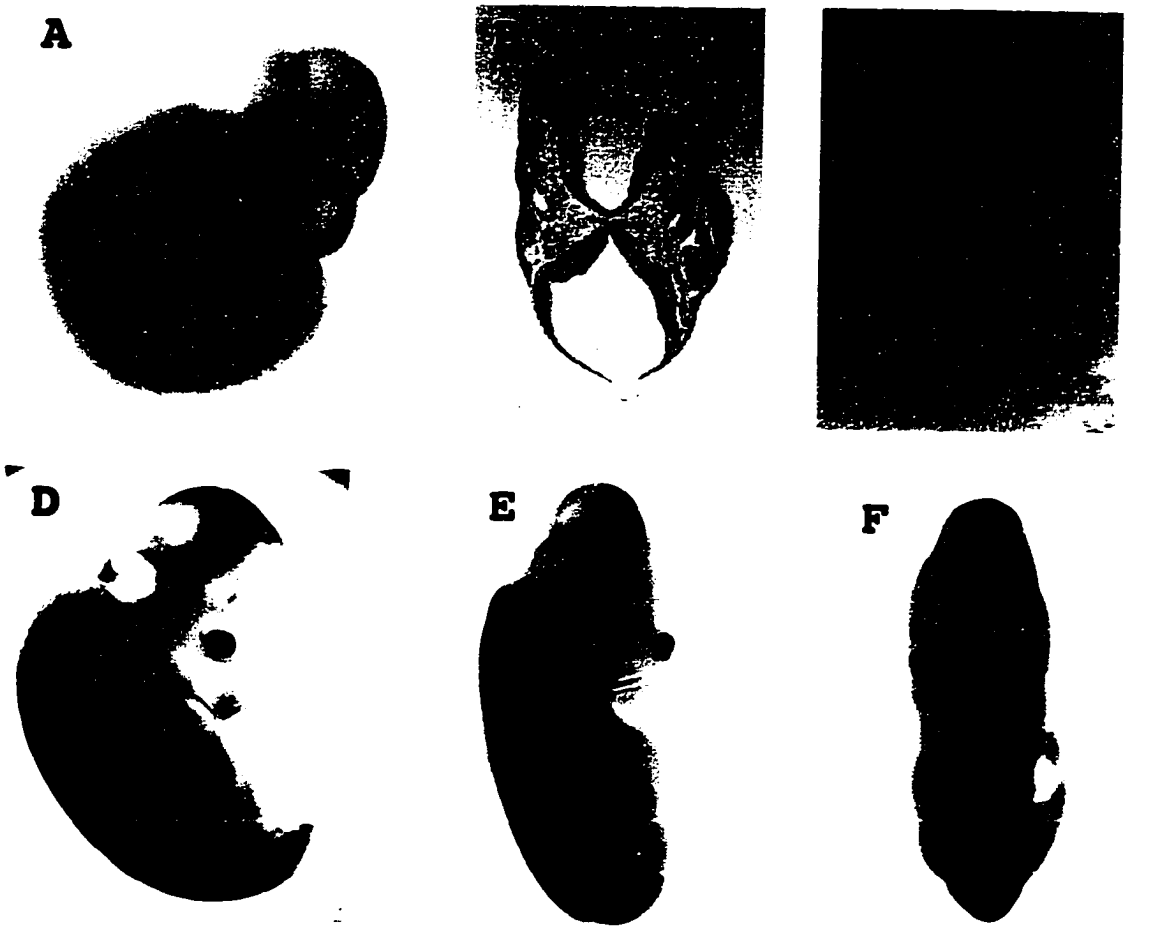

Figure 18

peripheral nerve systems, embryos from both lines showed similar patterns in the dorsal-lateral edge of neural tube, dorsal root ganglia and certain regions in the hindbrain and midbrain (Figure 18D-F).

These transgenic mouse assays demonstrate that regulatory elements located within the cloned genomic fragment can partially recapitulate the endogenous *Hmx* gene expression pattern in the CNS and PNS, as well as sensory in organs including the tongue, eye and nasal cavity. However, these two transgenes, each, failed to direct the reporter gene to be expressed in the developing inner ear. Two possibilities might account for this failure. One is that the regulatory element(s) responsible for inner ear development is not localized to the 31kb genomic fragment. The second possibility is that the regulatory element was split into two halves when the transgenes were made. Recovery of the inner ear-specific regulatory element(s) might require the elements in both transgenes to work synergistically, but not alternatively. In the future, we will try to link two constructs together to see whether the combination can restore the endogenous expression of *Hmx* genes in the developing inner ear.

The similar expression patterns of *Hmx2* and *Hmx3* and chromosomal co-localization of these two genes suggest that these two genes may share the same regulatory elements. Isolation of these regulatory elements may help us to outline the regulatory cascade involved in *Hmx* genes. Identification of regulatory elements in the isolated ~20kb *Hmx1* genomic fragment is still in progress.

5) Mice lacking *Hmx3* show hyperactivity, circling behavior, epilepsy, reduced viability and maternal infertility.

To fully understand the requirement of *Hmx3* gene in mouse development, targeted disruption of this gene was performed. Targeting construct was prepared by inserting the neomycin-resistance cassette (*neo*) or the *ires.lacZ* neomycin reporter and resistance (*ires.lacZ.neo*) (Li et al., 1997) cassette into the unique XhoI site located in the *Hmx3*

Figure 19. Targeting strategy for disrupting *Hmx3*. (A) *Hmx3* targeting construct, wildtype *Hmx3* locus, and disrupted allele. Homologous recombination of the targeting construct into the *Hmx3* locus results in the insertion of the *neo* gene into the *Hmx3* homeobox. This mutant allele will produce a nonfunctional truncated Hmx3 protein owing to the presence of translation stop codons at the 5' portion of the *neo* cassette. The two external probes for Southern blot analysis are indicated. The position of the probe used in the RNAse protection analysis (C) is shown in the figure. (B) Southern blot analysis of tailtip DNAs from wildtype, *Hmx3* heterozygote and *Hmx3* null offspring. BamHI digests show a 9.1 kb recombinant band detected by probe 1 and an 8.9 kb recombinant band by probe 2, in addition to the 17.8 kb wild-type band by both probes.(C) RNAse protection analysis of RNA from wildtype, *Hmx3* heterozygote and *Hmx3* null embryos at stage E11.5. The wildtype *Hmx3* transcripts protect a 472 bp fragment whereas the *Hmx3* mutant transcripts protect two fragments of 308bp and 164bp because of the insertion of the *neo* cassette into the XhoI site in the *Hmx3* homeobox. The mouse *β-actin* probe was used as an internal control.

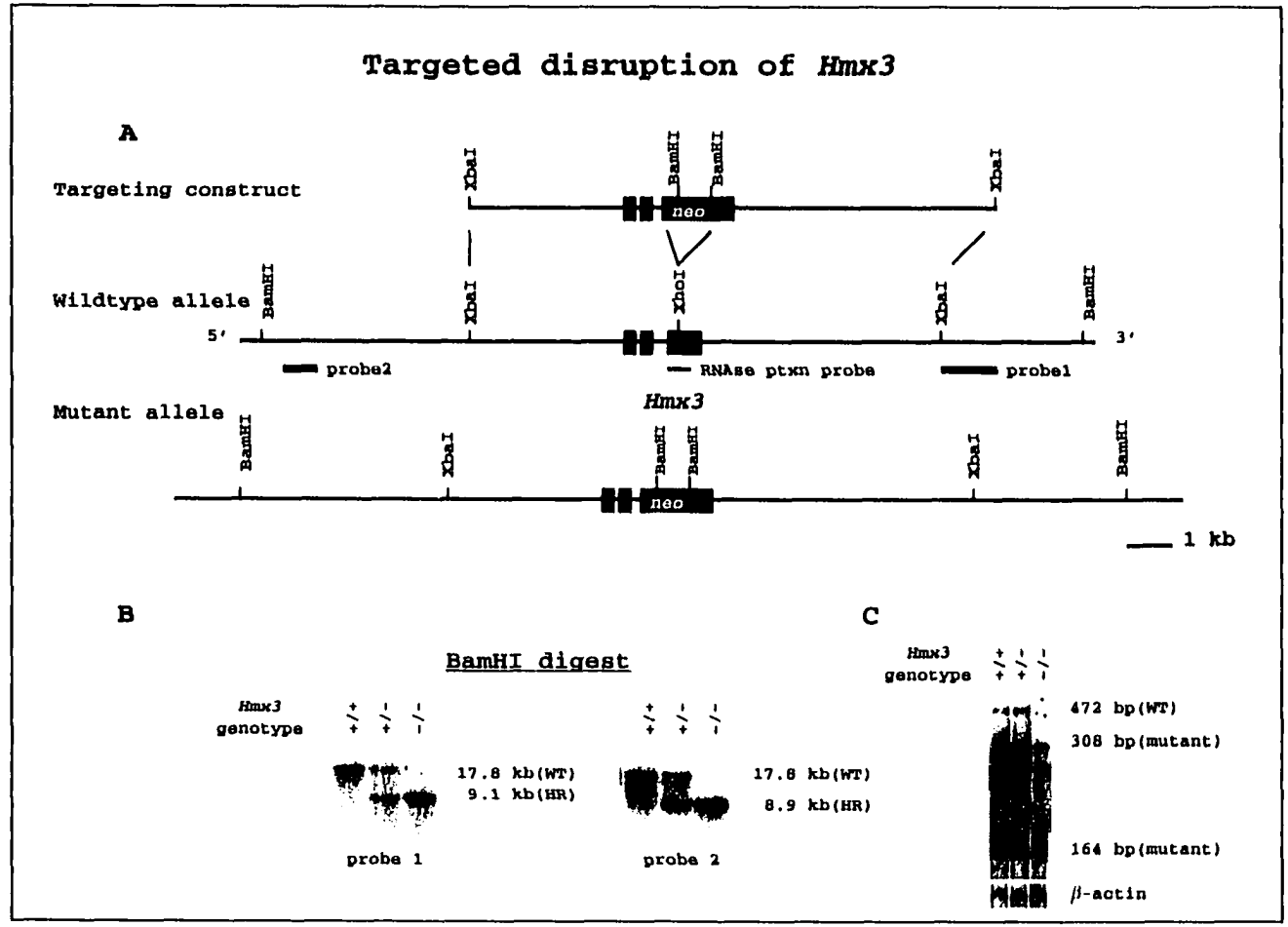

Figure 19

homeobox sequence (Figure 9A; Figure 19A). The insertion of *neo* or *ires.lacZ.neo* results in the truncation of the *Hmx3* protein in the N-terminal portion of the homeodomain (owing to stop codons present in the 5' portion of each cassette), thus generating a non-functional or null allele. Both constructs were electroporated into ES cells. G418-resistant clones that had undergone a homologous recombination were identified by Southern blotting. Among 50 G418-resistant clones, three positive clones for the $Hmx3^{neo}$ null allele were obtained. Five positive clones for the $Hmx3^{lacZ}$ null allele were obtained. Positive ES clones were microinjected into C57BL/6 blastocytsts. Transmitting chimeras were backcrossed to 129/Sv mice to put the *Hmx3* mutation on a congenic inbred background. Figure 19B shows the tail-tip Southern analysis of 3-week old wildtype, *Hmx3* heterozygote (+/-) and *Hmx3* homozygote (-/-) mice. In wildtype mice, both probe 1 and probe 2 were able to detect a 17.8 kb BamHI band. Insertion of *neo* cassette introduced two additional BamHI site in the *Hmx3* locus. In the *Hmx3* heterozygote mice, in addition to the wildtype band, probe 1 and probe 2 hybridized to 9.1 kb and 8.9 kb mutant bands, respectively. To further confirm that the *Hmx3* gene was functionally disrupted, a RNase protection assay was performed on embryo RNA using a probe spanning the site where the *neo* gene had been inserted (Figure 19A) Wildtype embryo RNA protected a fragment of 472 bp, whereas the mutant allele protected bands of 308 bp and 164 bp (Figure 19C). The mouse *β-actin* gene was used to control for the quality and quantity of RNA (Figure 19C). Results from both the DNA and RNA levels indicated that the targeting construct had been faithfully integrated into *Hmx3* locus by homologous recombination. There were no gross rearrangements, deletions, or secondary integration of the targeting construct. Mice carrying a null *Hmx3* gene have been generated successfully.

a) *Hmx3* null mice have diminished postnatal viability

Hmx3 heterozygotes were indistinguishable from wildtype mice. Mating between *Hmx3* heterozygotes resulted in viable *Hmx3* null animals. However, among 151 offspring

Table 3 Reduced postnatal viability of *Hmx3* null mice

A	P	+/- M	x	+/- F
	F1	+/+	+/-	-/-
3-week pups		39	86	26
	Ratio	1.0	2.2	**0.7**[a]

B	P	-/- M	x	+/- F
	F1	+/-		-/-
	E10.5	43		38
	E12.5	45		49
	E14.5	29		44
	E16.5-18.5	12		20
	Total	129		151
	Ratio	1.0		1.2[b]
3-week pups		219		141
	Ratio	1.0		**0.6**[c]

H_o: hypothesis.

a) H_o: the ratio of *Hmx3* wildtype, heterozygotes and homozygotes from the intermating of *Hmx3* heterozygote males and heterozygote females follows the expected 1:2:1 Mendelian distribution.
Chi-square = 5.1589; p-value = 0.0758

92% confidence level to reject above H_o

b) H_o: the ratio of *Hmx3* heterozygote and homozygote embryos from the intermating of *Hmx3* homozyote males and heterozygote females follows the expected 1:1 Mendelian distribution.

Chi-square = 1.7286; p-value = 0.1886

Ho can not be rejected at 90% confidence level.

c) H_o: the ratio of *Hmx3* heterozygote and homozygote pups from the intermating of *Hmx3* homozygote males and heterozygote females follows the expected 1:1 Mendelian distribution.

Chi-square = 16.9; p-value = 3.94×10^{-5}

H_o can be rejected at 99.9% confidence level.

---

analyzed at age of three weeks, only 70% of the expected 1:2:1 Mendelian ratio (+/+:+/-:-/-) of *Hmx3* null animals were obtained (Table 3A), suggesting a decreased viability of *Hmx3* null mice. A similar result was obtained from the intermating of *Hmx3* null males with *Hmx3* heterozygote females. Among 360 three week-old offspring tested, only ~60% of the expected *Hmx3* null mice presented at this age (Table 3B). Genotypes of 283 embryos from the intermating of *Hmx3* null males with *Hmx3* heterozygote females were examined from stages E10.5 to E18.5. Surprisingly, the expected Mendelian ratio (1:1) for heterozygotes and homozygotes was observed (Table 3B), suggesting that the decreased number of *Hmx3* null mice at three weeks of age was likely resulting from diminished postnatal viability or selective culling by the mothers. In many cases, we did find pup's remains eaten by the mothers left in the cages. We speculated that the mothers might be able to sense the defects associated with the *Hmx3* null genotype and selectively eliminate the mutants postnatally. Surviving *Hmx3* null pups appeared to be normal in size and appearance right after birth.

b) Circling behavior and inner ear defects in *Hmx3* null animals

By two weeks of age, 15% of the *Hmx3* null animals of a mixed genetic background (C57BL/6J x 129/Sv) and 91% of the *Hmx3* null mice of a congenic inbred (129/Sv) background exhibited an abnormal energetic circling behavior. The severity of the circling behavior varied between individuals, with the most severely affected mice circling at rates up to 176 revolutions per minute (rpm) for periods of several minutes, interspersed with non-circling periods of feeding, grooming, and sleep. In some cases, some circling mice also showed occasional head bobbing and a head tilt. The intermittent bi-directional circling behavior in the *Hmx3* null mice became the overt behavioral phenotype displayed throughout life. Hyperactivity and circling behaviors, commonly referred as a Shaker/Waltzer phenotype (Stein and Huber, 1960), are characteristic of mouse mutants with inner ear defects. The bi-directional circling behavior suggested that the inner ears of both sides were equally affected in the *Hmx3* null mice.

The expression of *Hmx3* in the vestibular portion of the developing inner ear suggested a possible connection with the circling behavior. No gross morphological abnormalities can be observed in either the formation of the vestibular labyrinth or the cochlear duct in the *Hmx3* null mice when compared to the wildtype or heterozygous mice (Figure 20). However, upon close examination of serial sectioned labyrinths from *Hmx3* null mice, several defects were observed in the vestibular sensory receptors. In both the wildtype and *Hmx3* heterozygous vestibular labyrinths, the utricle and saccule come into close apposition but always remain distinct endolymphatic chambers communicating only via the utriculosaccular valve (Figure 21A, C and E). In the vestibular labyrinths of the *Hmx3* null mice, the utricle and saccule do not remain separate because at the area of close apposition there is a fusion of the endolymphatic chambers of the utricle and saccule forming a common utriculosaccular space (Figure 21B, D and F). Fusion of the two

Figure 20. Macroscopic analysis of *Hmx3* null inner ear morphology. Macrophotographs of whole dissected bony labyrinths from adult wildtype (A) and *Hmx3* null circling (B) animals. No grossly morphological alteration can be observed in these bony labyrinths, indicating that the *Hmx3* null phenotype does not involve any severe dysmorphology of inner ear structures. Abbreviations: AC, anterior canal; CD, cochlear duct; HC, horizontal canal; OW, oval window; RW, round window; S, saccule; U, utricle.

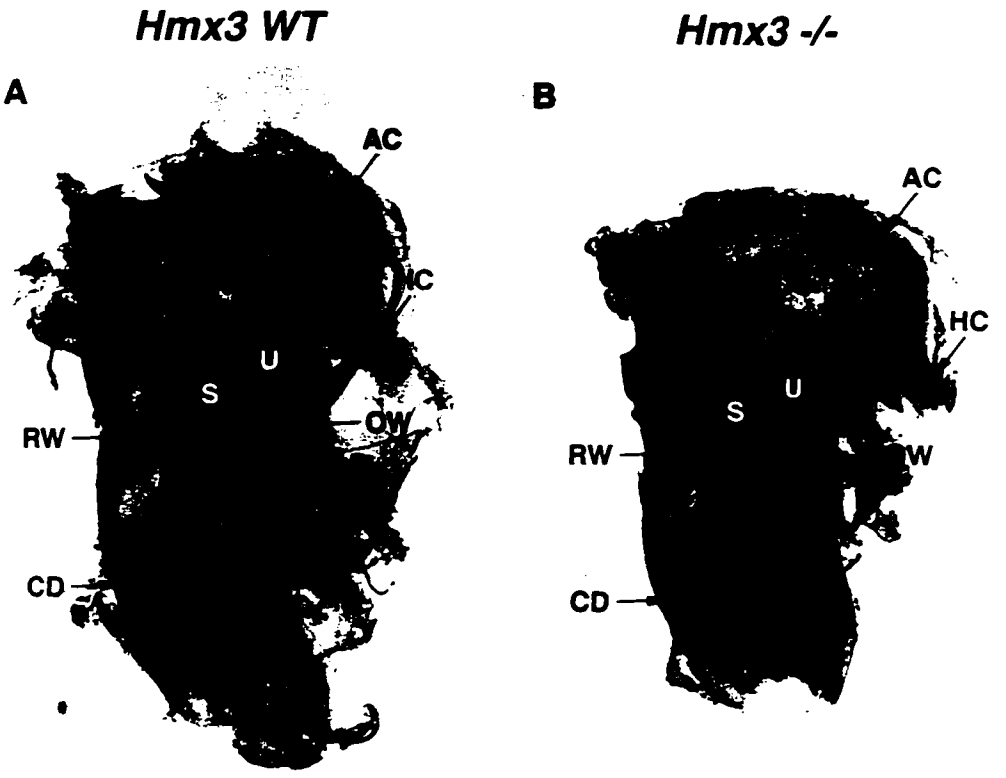

Figure 20

Figure 21. Histological analysis of inner ear defects in *Hmx3* null mice. Photomicrographs of toludine blue stained sections of adult temporal bones from wildtype (A, C, E, G and I) and *Hmx3* null circling (B, D, F, H and J) inner ears. The sections in A-F represent the area of close apposition of the utricle and saccule. In the wildtype inner ear, there is always a separation of the endolymphatic spaces and maculae of the sensory receptors (A, C and E). In contrast, serial sections show a fusion of these two separate sensory receptors into a common utriclosaccular chamber (U-S) with a contiguous endolymphatic space and a reduction in the size of the sensory cell area of the macula utriculus (B, D and F). Arrowheads in D mark the origin of the fusion. The crista (HC) of the horizontal semicircular duct is not present in the vestibular labyrinth of the *Hmx3* null animals (compare A, C with B, D). The absence of the horizontal crista is clearly shown at higher magnification in I and J. The crista of the anterior (AC) and posterior (data not shown) semicircular ducts were present and normal in the vestibular labyrinths of the *Hmx3* null mice. Abbreviations: AC, anterior crista; HC, horizontal crista; HD, horizontal semicircular duct; MS, macula sacculus; MU, macula utriculus; S, saccule; U, utricle; U-S, utriculosaccular space.

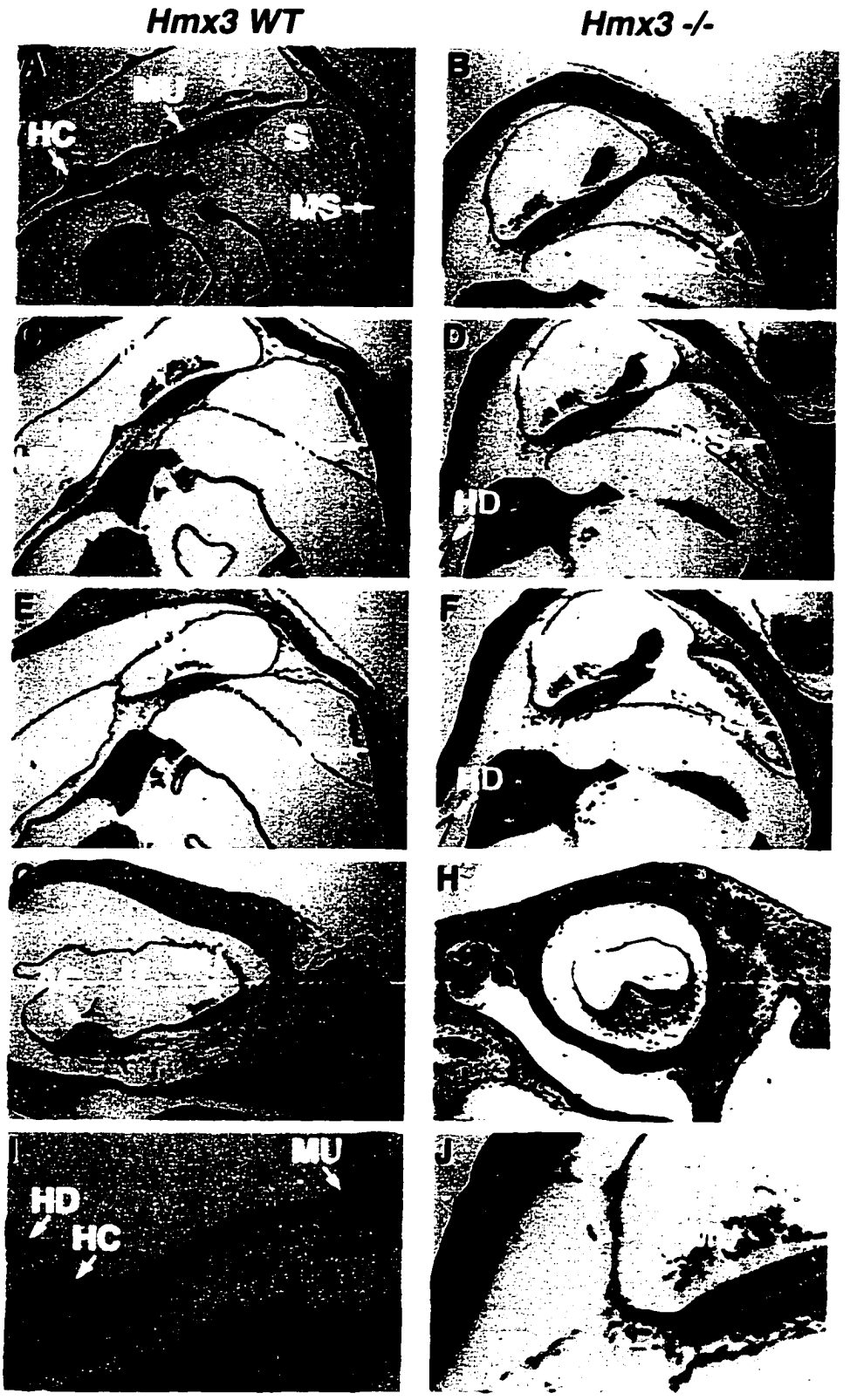

Figure 21

endolymphatic chambers into a common utriculosaccular space occurs on the underside of the utricular macula. This fusion results in the reduction in the area of the macula, the sensory organs of the utricle and saccule. The measurements of the sensory areas of the maculae of both the saccule and utricle of *Hmx3* wildtype and heterozygote vestibular labyrinths were essentially identical and therefore these measurements were analyzed as single unit and are presented in the histogram of Figure 22.

But in the *Hmx3* null vestibules, the measurements of the sensory epithelial areas of the utricles and saccules shows a highly significant loss of sensory cells from both the macula utriculus ($p< 1x\ 10^{-9}$) and the macula sacculus ($p<1\ x\ 10^{-3}$) when compared to those of the wildtype and *Hmx3* heterozygote vestibules. The *Hmx3* null utricles have lost 35% of their sensory epithelial area and their saccules have shown a 13% reduction in their sensory epithelial area (Figure 22). All three semicircular ducts were present and appeared normal in the *Hmx3* null inner ears, with the exception of the horizontal semicircular duct which lacked both a horizontal crista and the associated horizontal ampullary chamber (Figure 21B, J and Figure 23C). The anterior crista and the posterior crista were present and completely normal in the *Hmx3* null vestibular labyrinths (Figure 21G, H). Ultrastructural examination of the utricular sensory epithelium from wildtype, *Hmx3* heterozygote and *Hmx3* null mice did not show any differences in either the otoconia or the sensory hair bundles of the maculae (Figure 23A, B). The expression of *Hmx1*, *Hmx2* , *Hmx3* and zinc-finger transcription factor *GATA3* were examined in the inner ears of wildtype and *Hmx3* null embryos (Figure 24). *GATA3* was examined in addition to the *Hmx* genes, because it shows specific expression throughout the otic epithelium during development (George et al., 1994). Other molecular markers expressing the inner ear like *BMP4* and thyroid hormone α (*TRa*) were also examined (data not shown) on wildtype and *Hmx3* null background. Significantly, no discernible changes in the expression of any of these markers were observed in the *Hmx3* null embryos, suggesting that within the inner

Figure 22. Quantification of the loss of sensory epithelium in the saccule and utricle. Measurements of the sensory epithelial areas of the utricular and saccular maculae as determined by microscopic measurements of maculae from *Hmx3* wildtype (+/+ n=2), *Hmx3* heterozygote (+/- n=7) and *Hmx3* null (-/- n=9) inner ears. Since the area measurements of the maculae of the +/+ and +/- labyrinths were indistinguishable from one another, they were grouped as a single category. A comparison of the mean percent loss of sensory epithelial area of the *Hmx3* null to the *Hmx3* wildtype of the maculae of the utricle showed a highly significant ($p< 1x10^{-9}$) loss of 35% and for the saccule a highly significant ($p<1x10^{-3}$) loss of 13% of the sensory receptor area.

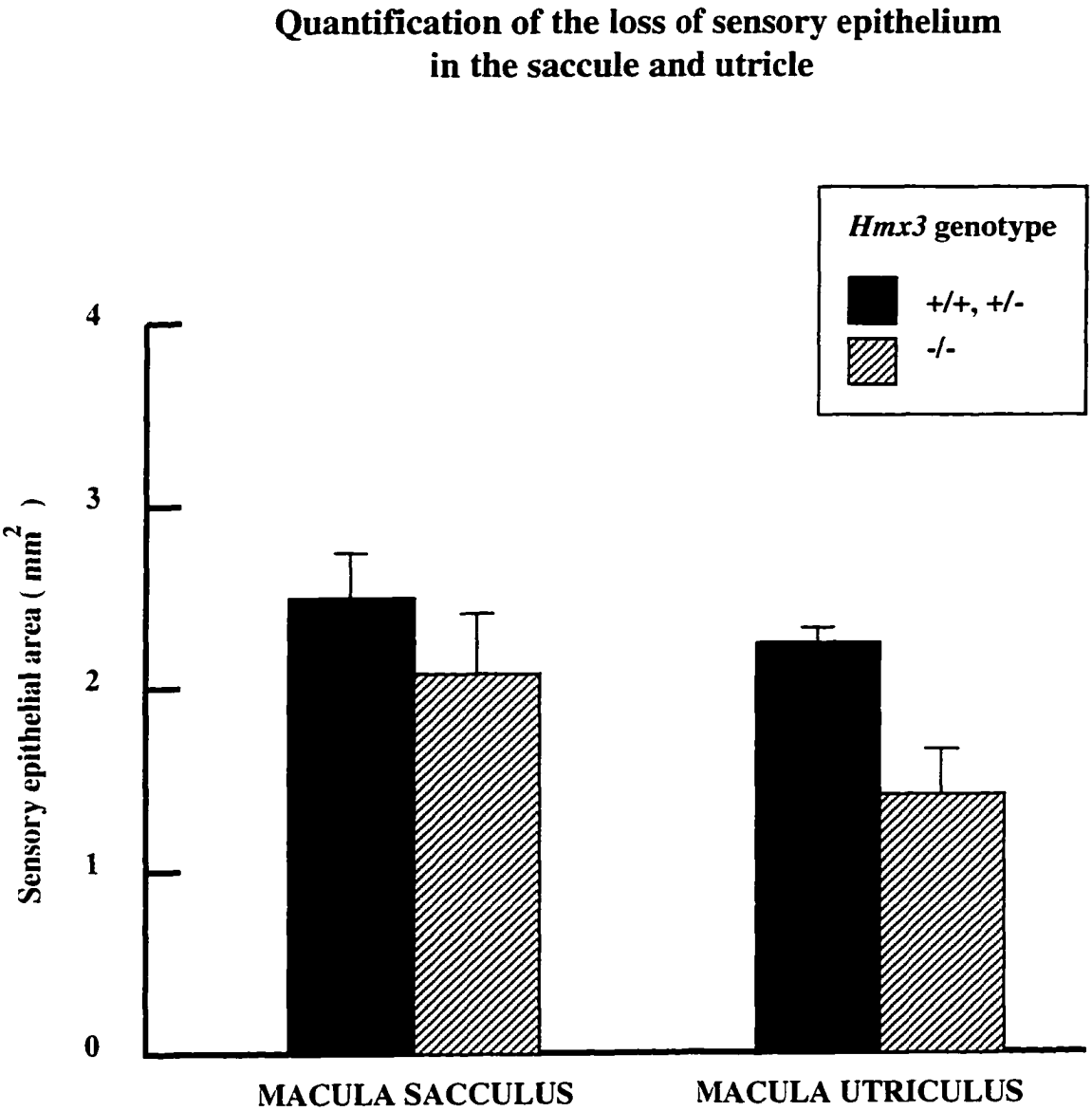

Figure 22

Figure 23. Ultrastructural analysis of the inner ears of *Hmx3* null animals. Scanning electron micrographs of the *Hmx3* null vestibule. (A) a low power view of the macula utriculus showing a normal arrangement of otoconia and stereociliary bundles from the vestibular hair cells. (B) a higher power view of the inset box region in (A) showing a normal configuration of these sensory structures in the *Hmx3* null labyrinth. (C) a low power micrograph of the bony tract of the horizontal semicircular duct that formed without a horizontal crista and ampullary chamber in the *Hmx3* null mouse. Abbreviations: HC, horizontal canal; SHB, sensory hair bundle; VN, vestibular nerve.

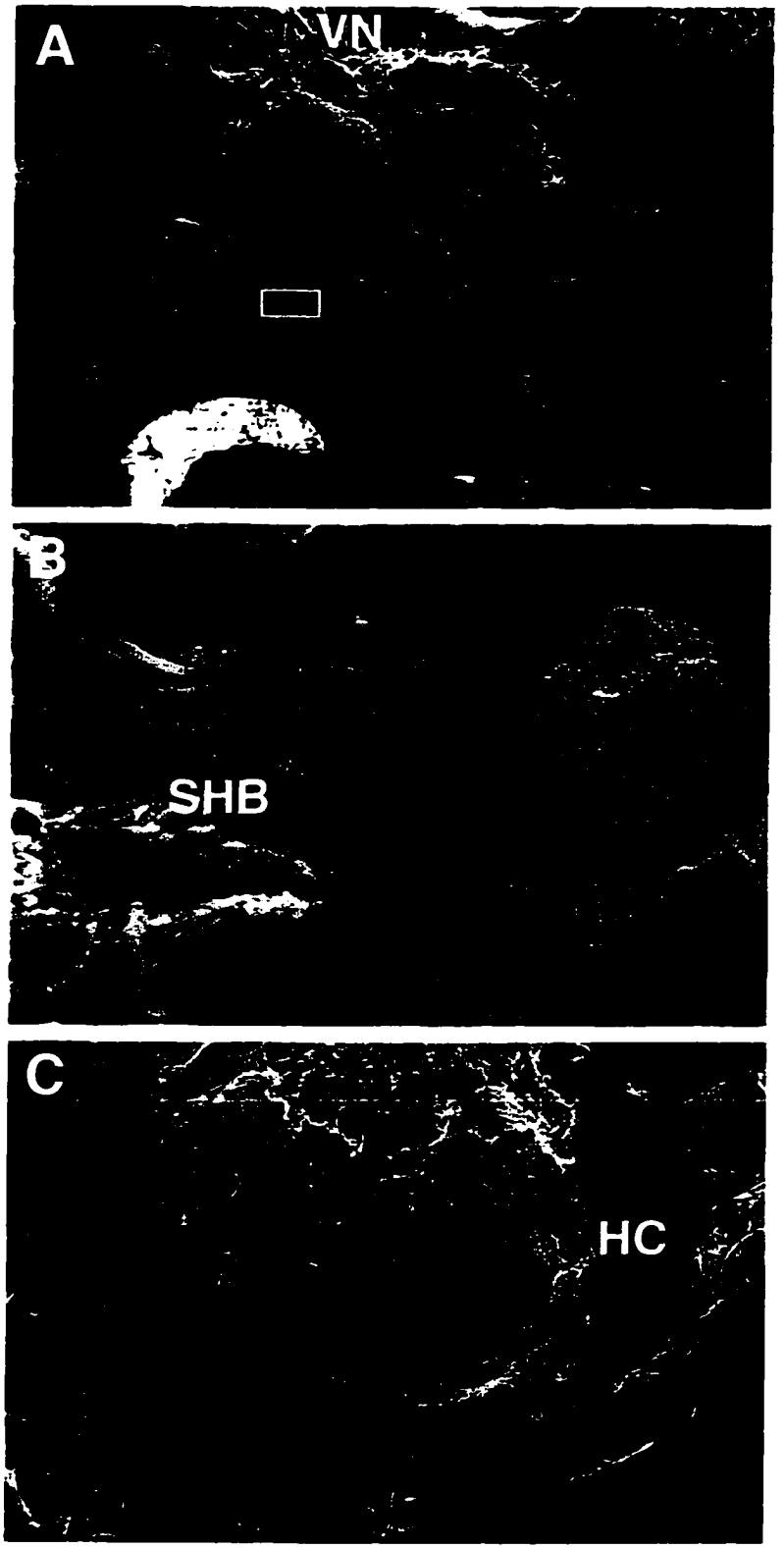

Figure 23

Figure 24. Expression of inner ear molecular markers in the wildtype and *Hmx3* null mice analyzed by RNA in situ hybridization on paraffin sections. Transverse sections through the heads of E14.5 embryos are presented. (A, B) lightfield and (C-J) darkfield. The RNA in situ probes used in the experiment are listed at the left. The *Hmx3* genotype of the embryos is shown at the top of each column. No significant differences were observed in RNA distribution in the inner ear between wildtype and *Hmx3* null embryos. Arrows (C, D, E, F, I and J) indicate expression in the semicircular ducts. Arrow head (in G and H) shows expression in cranial ganglia.

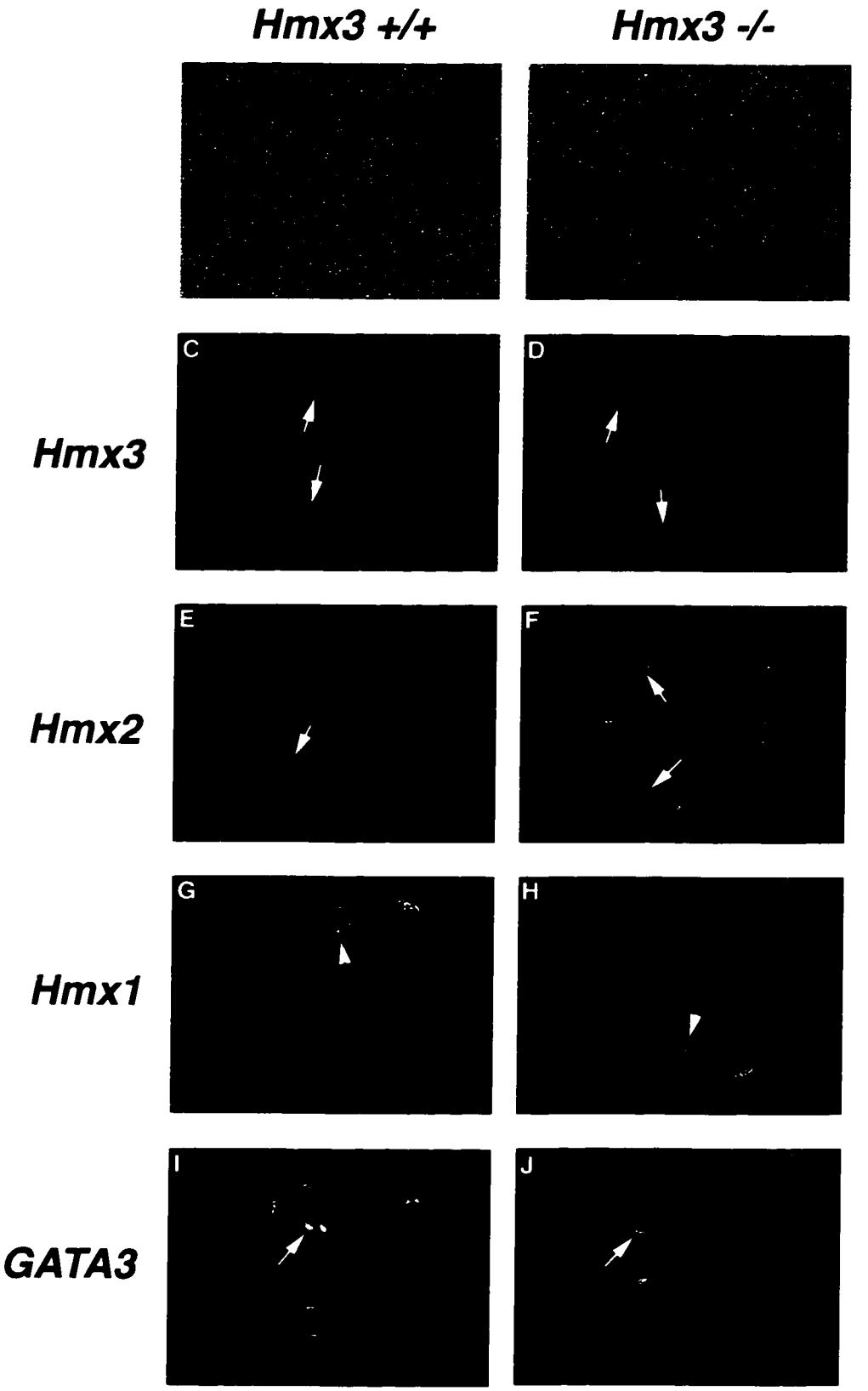

Figure 24

ear, neither the *Hmx* genes, nor *GATA3* fall under the direct or exclusive regulatory control of *Hmx3*. Interestingly, this is in contrast to what was observed for *Hmx* gene expression in the uterus, where significant differences were observed in the *Hmx3* null mice (described below).

c) Epilepsy in mice lacking the *Hmx3* gene.

Among approximately 75 *Hmx3* null mice monitored, 8 mice displayed spontaneous epileptic seizures, characterized by an arrest of normal behavior accompanied by teeth chattering, twitching, lurching and tail erection, followed by abruptly explosive clonic-tonic seizures. The earliest onset of epilepsy in *Hmx3* null mice happened at four weeks after birth. Most cases occurred in mice older than four months. Each occurrence lasted for about 1-3 minutes, then the mice recovered or developed additional seizures. Three mice died without any overt health problems. Judging the posture of the dead mice, it is possible that they died from epileptic complications. The pathological analysis of the epileptic mice is in progress. Epilepsy in *Hmx3* null mice may be related to its expression in the hypothalamus. *Hmx3* null mice is a new experimental model of epilepsy, making *Hmx3* gene a novel candidate of epileptogenic genes.

d) Overgrowth of teeth in *Hmx3* null mice.

About 15% of the *Hmx3* null mice show overgrowth of teeth. For rodents, they have to keep their teeth short by gnawing hard objects, because their teeth keep growing throughout their life. But a small portion of *Hmx3* null mice fail to do so. We have to clip their teeth every five days, otherwise they would die of starvation. Whether this phenotype is related to their abnormal behavior caused by defects in brain or structural abnormalities associated with its expression in the cleft between the first and second branchial arches remains to be investigated further.

e) Reduced fertility in *Hmx3* null females.

Table 4 Reduced post-implantation fertility of *Hmx3* null females

Hmx3 genotype	Sex	Mice tested	Individuals capable of successful pregnancy	Percentage of fertile individuals
+/-	F	27	24	89%
-/-	F	83	10	12%
+/-	M	11	11	100%
-/-	M	74	69	93%

Fertility of *Hmx3* null males was tested to be normal compared to that of wildtype males (Table 4). However, among 83 *Hmx3* null females tested in monitored matings with wildtype males, 88% were determined to be incapable of carrying out a normal pregnancy or producing litters following repeated independent vaginal pluggings. The remaining 12% of the *Hmx3* null females capable of carrying offspring could do so repeatedly, indicating that the penetrance of the infertility characteristic was stable within an individual animal (Table 4). Among nine successful pregnancies, only 4 pups were born per litter on average. Most *Hmx3* null mothers did not take care of the pups. The newborns were either eaten by the mothers or scattered around the cages.

To determine the time point of female infertility, *Hmx3* null females were mated with wildtype males and the plug date was monitored. On successive days following plugging, the *Hmx3* null females were sacrificed and the oviducts or uteri were removed and flushed

Table 5 Fertility of *Hmx3* females

Hmx3 Genotype M x F	Age Embryos	Embryos Recovered	Visible Implantation Sites	Embryos Transferred	Foster Mother	Pups Born
+/+ x -/-	E0.5	7	-			
+/+ x -/-	E0.5	10	-			
+/+ x -/-	E0.5	6	-	14	+/+	7
+/+ x -/-	E3.5	6	-			
+/+ x -/-	E3.5	4	-			
+/+ x -/-	E3.5	8	-			
+/+ x -/-	E3.5	8	-	22	+/+	13
+/+ x +/+	E3.5	4	-			
+/+ x +/+	E3.5	8	-			
+/+ x +/+	E3.5	2	-			
+/+ x +/+	E3.5	3	-	15	+/+	6
+/+ x +/+	E3.5	6	-			
+/+ x +/+	E3.5	8	-			
+/+ x +/+	E3.5	10	-			
+/+ x +/+	E3.5	9	-			
+/+ x +/+	E3.5	3	-			
+/+ x +/+	E3.5	8	-	44	-/-	0
+/+ x -/-	E5.5	1	0			
+/+ x -/-	E5.5	4	0			
+/+ x -/-	E5.5	0	0			
+/+ x -/-	E5.5	1	0			
-/- x +/+	E5.5	5	5			
-/- x +/+	E5.5	6	8			
-/- x +/+	E5.5	8	10			
-/- x +/+	E5.5	0	8			
+/+ x -/-	E9.5	0	0			
+/+ x -/-	E9.5	0	0			
+/+ x -/-	E9.5	8	10			
+/+ x -/-	E9.5	0	0			
+/+ x -/-	E9.5	0	0			
+/+ x -/-	E9.5	0	0			
+/+ x -/-	E9.5	10	10			
+/+ x -/-	E9.5	0	0			
+/+ x -/-	E11.5	0	0			
+/+ x -/-	E11.5	0	0			
+/+ x -/-	E11.5	0	0			
+/+ x -/-	E11.5	0	0			
+/+ x -/-	E11.5	0	0			
+/+ x -/-	E12.5	0	0			
+/+ x -/-	E12.5	0	0			
+/+ x -/-	E12.5	0	0			
+/+ x -/-	E12.5	0	0			
+/+ x -/-	E12.5	0	0			

with medium to recover embryos or unfertilized oocytes that might be present. Flushing of *Hmx3* null uteri at E0.5-E3.5 resulted in the recovery of developmentally normal embryos at the appropriate gestational stages and at normal numbers relative to wildtype animals (Table 5). When these recovered embryos were reimplanted into wildtype pseudopregnant mothers, they were able to undergo normal uterine implantation, embryonic development and birth, and were by all criteria indistinguishable from wildtype embryos. This indicated that normal ovulation and fertilization did take place in the *Hmx3* null females. *Hmx3* null females were capable of providing a suitable environment for preimplantation development of the embryos. In contrast, when wildtype preimplantation-stage embryos isolated from wildtype parents were implanted into pseudopregnant *Hmx3* null females, no pups could be obtained, indicating that the *Hmx3* null mothers failed to undergo a successful implantation and become pregnant (Table 5). Normal implantation occurs at E4.5 when the blastocysts hatched from the zona pellucida attach to the uterine wall. After implantation, the embryos will undergo decidualization and subsequent postimplantation development. At E5.5, decidual swellings or implantation should be visible in the normal pregnant uteri. However, when *Hmx3* null uteri naturally mated with wildtype males were examined at stages E4.5-E12.5, no visible implantation sites were observed in the majority of uteri (Table 5). Dissection of these embryos revealed no stromally implanted embryos. When flushed with medium at E5.5, embryos at around stage E4.5-E5.5 were recovered from *Hmx3* null uteri mated with wildtype males, indicating these embryos were still free in the uterus. In wildtype pregnant uteri, recovery of embryos by flushing can not happen at E5.5 because the embryos have already attached to the uterine wall and decidual swellings surrounding the implantation sites block any flow of medium through the uterine lumen. We did find normally developed embryos in two *Hmx3* null uteri at E9.5 stage (Table 5). This observation is consistent with the result that 12% of *Hmx3* null mice can successfully impregnate (Table 4) even though they produced less pups than did wildtype females.

Figure 25. Altered gene expression in the uteri of *Hmx3* null mice. RNA in situ hybridization was performed on the transverse sections of mouse uteri. The genotype of the female is shown at the top of each column, and whether the female was unpregnant or pregnant (4.5 days post coitus) is indicated directly above. The RNA in situ probe used is shown at the far left of each row. *Hmx2* and *Hmx3* are expressed in the stroma in wildtype unpregnant uteri (arrow) and *Hmx1-Hmx3* are all upregulated in the myometrial layer in wildtype pregnant uteri (arrows). However, in the *Hmx3* null uteri, transcripts of *Hmx1*, *Hmx2* and *Hmx3* are no longer detectable. *Wnt5A* is expressed in the endometrial epithelium and adjacent stroma in unpregnant wildtype females and upregulated in the endometrial epithelium and glands during pregnancy. In the *Hmx3* null females, *Wnt5A* fails to upregulate in the endometrial epithelium, but instead shows dramatic upregulation in the stroma. *Wnt7A* shows an upregulation in the *Hmx3* null unpregnant uteri (arrow) and fails to shift expression to the myometrium during pregnancy. Abbreviations: L, uterine luminal cavity; M, myometrium; S, uterine stroma (mesometrium).

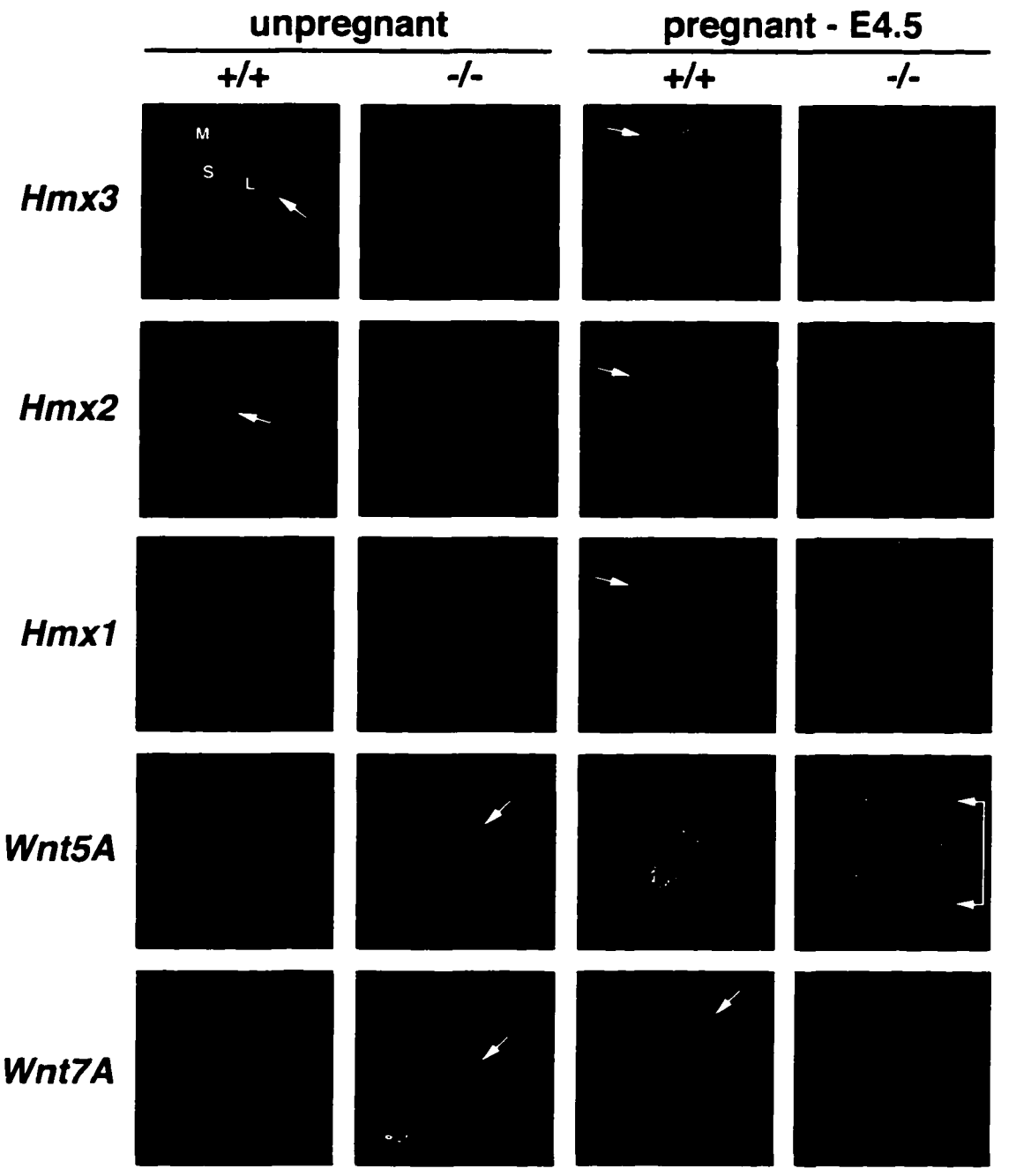

Figure 25

Taken together, these results suggested that failure to support a normal pregnancy by the *Hmx3* null females was likely occurring around the time of embryo implantation (the dashed line shown in Table 5).

f) Severe perturbation at the molecular level in the *Hmx3* null uteri.

Histological analysis of the *Hmx3* null uteri revealed no gross alterations of the luminal epithelium, stroma, or epithelial glands (Figure 26). *Hmx3* null uteri were closely examined at the molecular level. *Hmx3* is expressed in the uterus of both nonpregnant and pregnant females (Figure 25). In nonpregnant uteri, *Hmx3* transcripts can be observed in the uterine stroma with highest expression in cells closest to the epithelial layer of the endometrium with expression showing a mediolateral decrease with increasing distance from the uterine lumen. *Hmx3* gene expression changes during pregnancy, showing a dramatic increase in the myometrial layer, and a decrease to background levels in the uterine stroma. *Hmx1* and *Hmx2* are expressed in a manner nearly identical to *Hmx3*. However, *Hmx1* shows a relatively lower level of expression in the nonpregnant uterus compared to *Hmx2* and *Hmx3* (Figure 25). In the *Hmx3* null uteri, no signals of *Hmx1*, *Hmx2* and *Hmx3* could be detected above background levels. Down regulation of *Hmx3* gene expression in the *Hmx3* null uterus may be related to the instability of fused *Hmx3* RNA transcribed from the *Hmx3* null allele or the autoregulation of *Hmx3* itself or both. Decrease in expression of *Hmx1* and *Hmx2* in the *Hmx3* null uteri may be associated with the down-regulation of *Hmx3*, suggesting the involvement of all three *Hmx* genes in the same regulatory cascade in the uterus during pregnancy.

The myometrium is composed of two layers: an inner layer of circular smooth muscle; and an outer layer of longitudinal smooth muscle. A muscle-specific marker, *myosin* is specifically and equally expressed in both layers of the myometrum in the uterus (Miano et al., 1994). No change in myosin expression was observed in the *Hmx3* null uteri, in either

Figure 26. Histological and molecular analysis of uterine defects in *Hmx3* null animals. Transverse sections of uteri in dark field view are presented (top three rows). The genotype of the female is shown at the top of each column, and pregnancy status (nonpregnant or pregnant) is indicated directly above. The RNA in situ probe used is shown at the far left of each row. In the wildtype females, both *Wnt4* and LIF are strongly upregulated in E4.5 glandular epithelium (arrows). In *Hmx3* null females, no upregulation of either *Wnt4* or LIF is observed. The expression of myosin is unaffected in the *Hmx3* null females. Pictures in the bottom two rows (above, low power view; bottom, high power view) show the hematoxylin and eosin stained sections. *Hmx3* null females show an apparently normal uterine histology and the epithelial glands appear indistinguishable from wildtype.

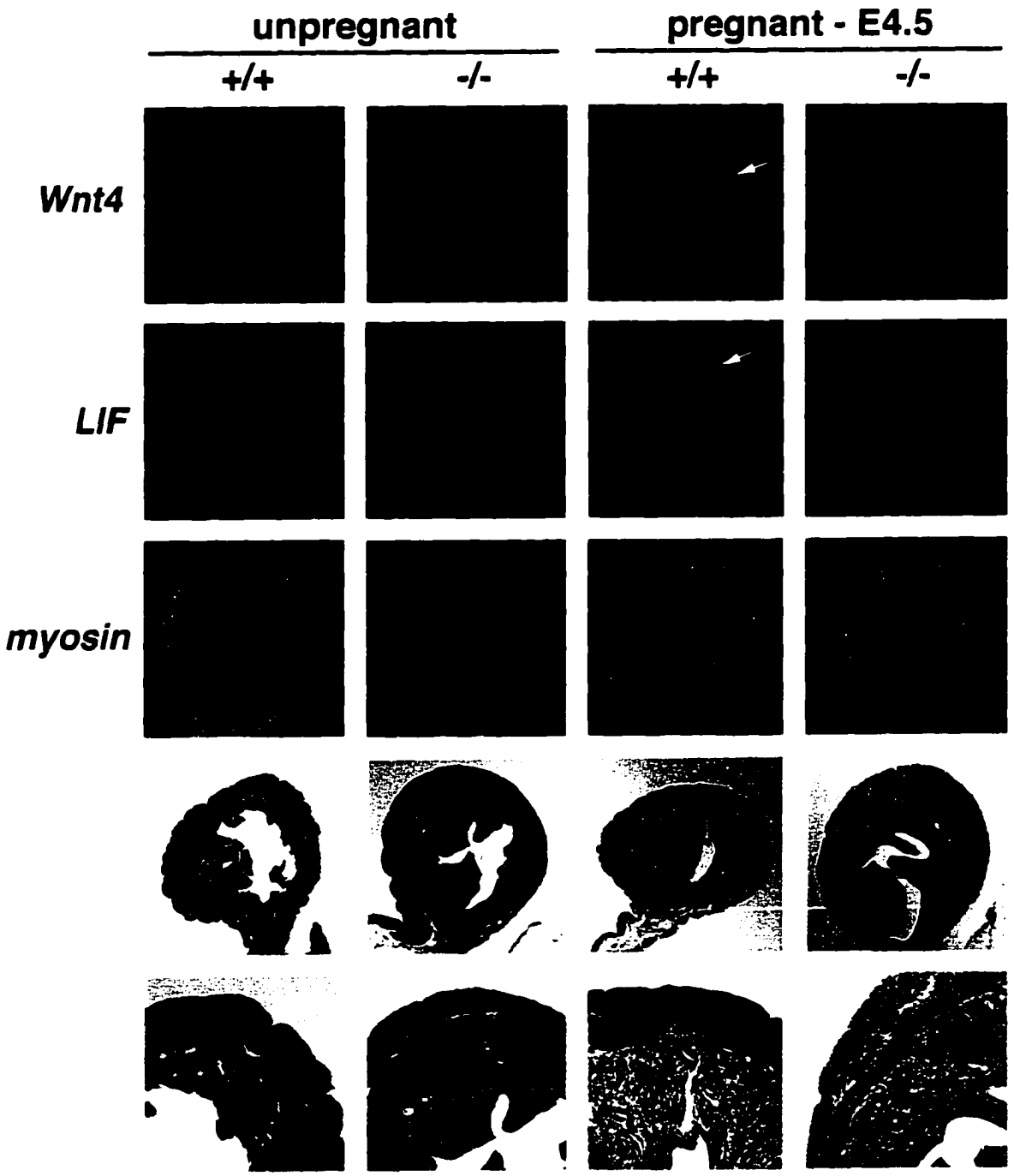

Figure 26

pregnant or unpregnant females (Figure 26). It indicated that there was no gross developmental alteration of the myometrial layer in the *Hmx3* null uterus.

Several uterine developmental markers deeply involved in female fertility were examined in wildtype and *Hmx3* null pregnant and nonpregnant uteri. The murine *Wnt* gene family which is homologous to *Drosophila wingless*, appears to be involved in cell-cell signaling (McMahon et al., 1992; Nusse and Varmus, 1992; Robertson et al., 1993). Three *Wnt* genes specifically expressed in the mouse uterus were examined. *Wnt5A* is a critical developmental control gene expressed in the uterus in a dynamic manner during pregnancy (Huguet et al., 1995; Kuhlman and Niswander, 1997; Pavlova et al., 1994). In wildtype nonpregnant females, *Wnt5A* is expressed in the uterine stroma and very weakly in the endometrial epithelium. However, in nonpregnant *Hmx3* null females, *Wnt5A* expression is dramatically altered, with stronger expression in the endometrial epithelium and normal levels in the stroma. In wildtype pregnant females, *Wnt5A* expression is strongly expressed in the glandular epithelium embedded in the stroma and in the endometrial epithelium. But, in the *Hmx3* null pregnant females, *Wnt5A* shows a dramatic overall increase in expression throughout the uterine stroma (bracketed, Figure 25). No elevated expression of *Wnt5A* within the endometrial epithelium was observed in the *Hmx3* null pregnant females.

In addition to its expression in the central nervous system, *Wnt7A* has previously been shown to be specifically expressed in the adult uterus (Ikegawa et al., 1996). In the wildtype nonpregnant uterus, *Wnt7A* is only expressed in the luminal epithelium and immediately adjacent stroma. In pregnant females, *Wnt7A* expression decreases in the luminal epithelium and specifically increases in the myometrium. In *Hmx3* null females, expression of *Wnt7A* in nonpregnant females shows significant upregulation in the luminal epithelium. However, in the pregnant *Hmx3* null females, its strong expression in the

luminal epithelium persisted. Neither decreases of *Wnt7A* expression in the luminal epithelium nor increases in the myometrial layer can be observed (Figure 25).

Wnt4 is expressed in the mesenchyme surrounding the luminal epithelium in nonpregnant wildtype females. During pregnancy, its expression shifts to the myometrium and the epithelial glands. In *Hmx3* null females, *Wnt4* expression is absent from the subluminal mesenchyme, but instead expressed specifically within the endometrial epithelium. In pregnant *Hmx3* null females, the expression of *Wnt4* is no longer detectable (Figure 26).

Requirement of leukemia inhibitory factor (LIF) in the uterus for proper embryo implantation has previously shown by targeted disruption of this gene (Stewart et al., 1992). LIF gene is expressed at low level in the nonpregnant uterus. At the time of embryo implantation, the glandular epithelium shows a burst of LIF expression (Bhatt et al., 1991; Shen and Leder, 1992). Absence of functional LIF product resulted in the failure of pregnancy at the implantation stage. In nonpregnant *Hmx3* null females, no significant changes can be detected in the expression of LIF. However, in the pregnant *Hmx3* null females, no detectable level of LIF can be observed anywhere in the uteri (Figure 26). Absence of the shift in LIF expression in *Hmx3* null uterus is sufficient to account for the infertility of *Hmx3* null females.

6) Generation of chimeric mice carrying disrupted *Hmx2* allele.

The ES cell lines R1 and D3 were electroporated with the targeting construct (Figure 27A). Southern blot analysis of 96 G418-resistant R1 clones and 96 D3 clones identified 1 correctly targeted clone from R1 cell lines and 4 from D3 cell lines (Figure 27B). When the ES cell DNA was digested with ClaI and NotI, probe 3 detected a 17.0 kb wildtype band and a 12.5 kb mutant band because of the introduction of another ClaI by the insertion of *ires.lacZ.neo* into the homeobox of *Hmx2* gene. Probe 4 hybridized with a 6.7 kb wildtype band and a 5.7 kb disrupted allele if the ES cell DNA was cut by XbaI. Two of the five

Figure 27. Targeting strategy for disrupting *Hmx2*. (A) Targeting construct, wildtype *Hmx2* locus and mutant allele are shown. Homologous recombination of the targeting construct into the *Hmx2* locus results in the insertion of *ires.lacZ.neo* cassette into the *Hmx2* homeobox. The mutant allele will produce a nonfunctional truncated Hmx2 protein and β-galactosidase. (B) Screening for correctly targeted ES clones. Insertion of *ires.lacZ.neo* cassette into the *Hmx2* homeobox introduces extra ClaI and XbaI sites into the *Hmx2* locus. The 5' external probe, probe 3, hybridized to a 17.0kb wildtype and a 12.5 kb mutant NotI-ClaI fragment. At the 3' end, external probe 4 detected a 6.7 wildtype fragment and a 5.7 mutant band when ES DNA was digested with XbaI.

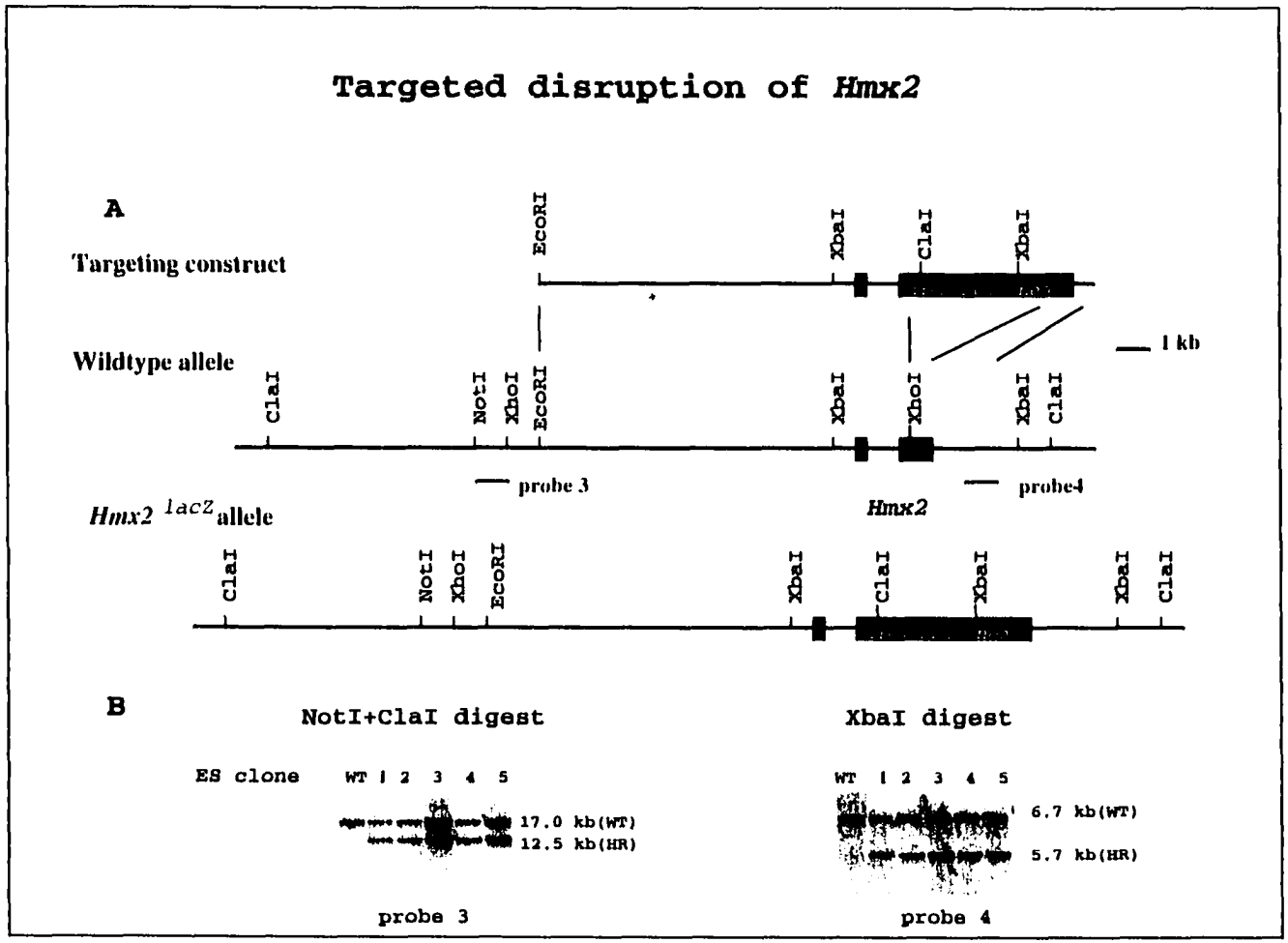

Figure 27

independent clones were microinjected into C57/BL6J blastocysts and chimeric mice were successfully obtained. Germline transmission of the mutant *Hmx2* allele is being examined.

The only R1 clone (clone 5 in Figure 27B) was also used to generate $Hmx2^{lacZ}$ heterozygote embryos by the tetraploid ↔ ES cell aggregation techniques (Nagy et al., 1990; Nagy and Rossant, 1993). Staining for β-galactosidase activity revealed that *Hmx2* is expressed in an identical temporal and spatial manner to *Hmx3* in the otic placode and the central nervous system (data not shown).

7) Mice lacking both *Hmx2* and *Hmx3* genes completely lose balance and die perinatally.

The striking similarity in their expression patterns and in the sequence of their homeodomain, as well as their close proximity on the chromosome, raise the possibility that *Hmx2* and *Hmx3* may share common regulatory elements and have overlapping functions. In the *Hmx3* null mice, lack of a phenotype in the anterior and posterior semicircular ducts might be interpreted by an overlap in function with *Hmx2*. The absence of overt defects in the nervous system in the *Hmx3* null mice may be related to the functional redundancy of *Hmx1* or *Hmx2* or both. To fully understand the function of the *Hmx* gene family, the double knockout of *Hmx2* and *Hmx3* was carried out.

The targeting strategy is shown in Figure 28A. Integration of the targeting construct into the *Hmx2* and *Hmx3* locus by homologous recombination resulted in the deletion of an 11.0 kb genomic fragment between the *Hmx2* and *Hmx3* homeoboxes, thereby creating a null allele. In the Southern blot analysis, probe 5 should probe a 17.5 kb wildtype EcoRI-band and a 21.0 kb mutant EcoRI-band (Figure 28B). The 3' external probe, probe 7 hybridized to a 6.8 kb wildtype band and a 5.7 kb mutant band when the genomic DNA was digested with XbaI (Figure 28B). The targeting construct was electroporated into ES cells (both R1 and D3 cell lines). Approximately 1000 G418-resistant clones were screened by Southern blot analysis. Three ES clones, one (clone 391) from D3 cell line and two

Figure 28. Targeting strategy for disrupting both *Hmx2* and *Hmx3*. (A) Targeting construct for double knockout, wildtype locus and disrupted allele. The homologous sequences are a 9.0 kb BamHI-XhoI genomic fragment 5' to the *Hmx3* homeobox and an 1.2 kb XhoI genomic fragment 3' to the *Hmx2* homeobox. Successful targeting results in the deletion of the 11.0 kb XhoI genomic fragment between *Hmx2* and *Hmx3* genes. (B) Southern blot analysis of tailtip DNAs from offspring carrying wildtype, heterozygous and null alleles for both genes. EcoRI digests show a 21.0 kb mutant band detected by probe 5 in addition to the 17.5 kb wildtype band. When digested with XbaI, tailtip DNAs show a 6.8 kb wildtype band and a 5.7 kb mutant band detected by probe 7. In the pups carrying null alleles for both genes, the 11.0 kb XhoI genomic fragment is absent when detected by probe 6.

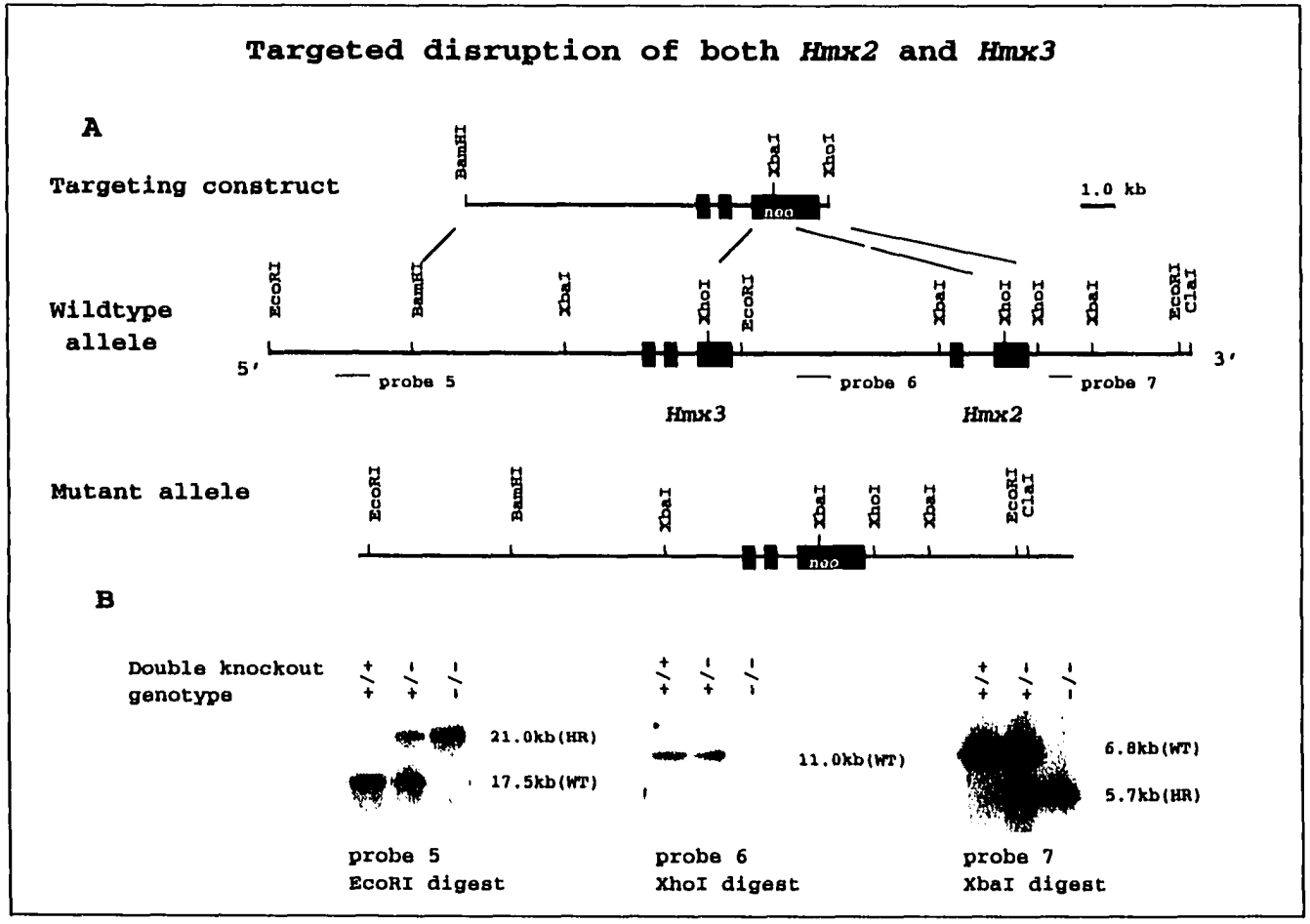

Figure 28

(clone 471 and 488) from R1 cell line, were tested to be correctly targeted clones. These three independent clones were microinjected into C57BL/6J blastocysts and chimeric mice were generated. Two clones, 391 and 471, gave rise to chimaeric mice capable of transmission of the targeted allele through the germ line.

The heterozygous progeny appeared to be indistinguishable from their wildtype littermates and intercrossed to produce homozygous pups. However, among 58 offspring obtained from matings between heterozygotes, 18 wildtype pups, 38 heterozygotes and only 2 homozygotes were present, indicating that most homozygotes died prenatally. These two homozygotes showed the same phenotypes. Right after birth, the homozygotes were indistinguishable from the others in size and appearance. But at day 4 after birth, severe delay in development was observed in the homozygotes. Behaviorally, the homozygotes lost balance completely and were not able to right themselves. Both pups died at day 9 after birth. At the time of death, their bodies were only half the size of their littermates. The cause of death is under investigation. Obviously, mice carrying disrupted *Hmx2* and *Hmx3* show a more severe phenotype than *Hmx3* null mice. Closer examination of the double knockout phenotype will give us more exciting results about the function of the *Hmx* genes and the functional relationship between *Hmx2* and *Hmx3*.

8) Refinement of the targeting strategy for *Hmx1* knock-out and generation of mice carrying null alleles for *Hmx1*, *Hmx2* and *Hmx3*.

The original targeting construct was make by our collaborator by replacing the XhoI fragment containing the *Hmx1* homeobox with PGK-neo. I modified this construct by replacing the *PGK-neo* with *ires.lacZ.neo* so that the expression pattern of *Hmx1* can be visualized by staining of the heterozygous embryos carrying the mutant allele for β-galactosidase activity (Figure 29). The construct was transfected into R1 ES cell line by electroporation. Three of 96 G418-resistant clones were correctly targeted, as verified by Southern blot analysis (data not shown).

Figure 29. Refinement of the targeting strategy for *Hmx1* disruption. The original targeting construct (made by Dr. Yoshiura) was modified by replacing the *PGK-neo* with *ires.lacZ.neo* cassette so that the endogenous *Hmx1* expression pattern can be monitored by β-galactosidase staining of the heterozygote embryos. Homologous recombination of the modified construct results in the deletion of a 500 bp XhoI fragment containing the entire homeobox, therefore generating a null mutation. In the mutant allele, the deleted XhoI fragment is replaced by a *ires.lacZ.neo* cassette. The position and size of the probes used for Southern blot analysis are indicated.

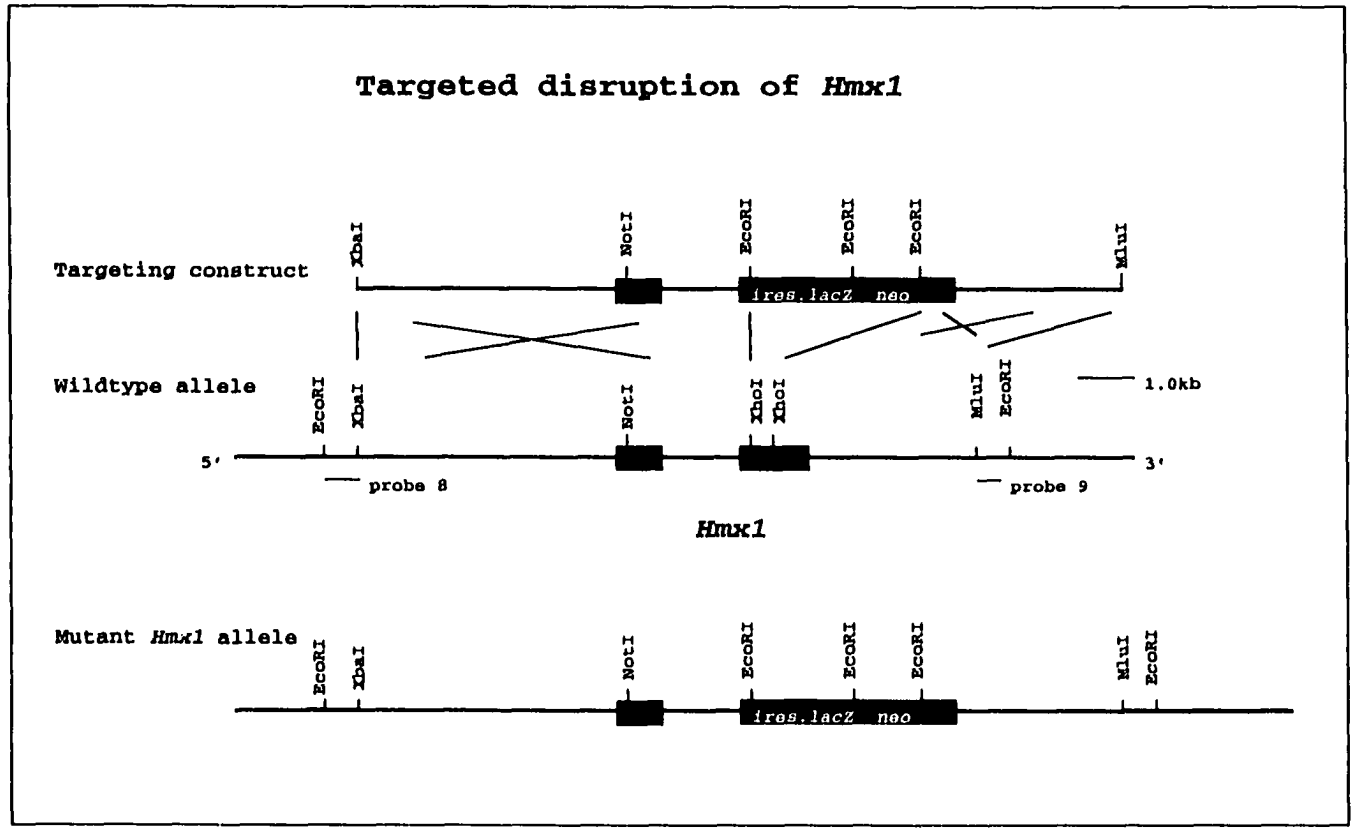

Figure 29

Microinjection of these clones and chimaeric mice generation will be performed in the near future.

Mice lacking both *Hmx1* and *Hmx2* can also be produced by mating *Hmx1* mutant mice (*Hmx1* +/- or *Hmx1* -/-, depends on their viability and fertility) with *Hmx2* mutant mice. Intermating of the resulting mice heterozygous for both genes will produce mice null for both *Hmx1* and *Hmx2*. Similarly, mice carrying null alleles for *Hmx1* and *Hmx3* can be produced.

All three *Hmx* genes are expressed in an overlapping manner in the central and peripheral nervous systems, which may represent the ancestral developmental function of this gene family. The absence of discernible defects in the nervous system in the *Hmx3* null mice may be related to the ancient function inherited by each members of the *Hmx* gene family. I would predict that disruption of all three *Hmx* genes will result in an overt phenotype in the nervous system. Triple knockout of all three *Hmx* genes can be achieved by mating *Hmx1* heterozygous mice (or *Hmx1* homozygotes, if they are viable and fertile) with mice heterozygous for both *Hmx2* and *Hmx3* genes. Intermating of the mice heterozygous for all three *Hmx* genes will produce mice or embryos homozygous for all three *Hmx* genes. Theoretically, one out of 16 mice or embryos obtained from the heterozygote intermatings will be homozygous for all three *Hmx* genes.

By analyzing the phenotype obtained from each single knockout, the double knockout of various combination of *Hmx* genes as well as the triple knockout of all three *Hmx* genes, the original and recently acquired functions of *Hmx* genes during evolution may be uncovered. The functional relationships among these three genes should thus become more clear.

Discussion

Hmx, a novel homeobox gene family of ancient origin

A growing number of *Hmx* genes have been cloned among different species from *Drosophila* to human. Widespread existence of *Hmx* genes in the animal kingdom indicates that this gene family is of ancient origin, which has been transmitted to higher creatures such as mouse and human by duplication and chromosomal translocation during evolution. High sequence similarity in their homeoboxes and expression patterns, as well as low level identity to other homeobox genes, suggests the strong conservation in their biological function during evolution. Cloning of *Drosophila Hmx* makes it clear that the *Hmx* genes belong to a distinct gene family originated from the same ancestor, and do not fit into any existing homeobox gene family (e.g. *Hox*, *Nkx*, *Dlx*). This distinct gene family has existed for at least 600 million years.

Like *Drosophila Hmx* gene which is expressed in the bilateral patches in the dorsal ectoderm of the head in regions which will give rise to brain neuroblasts, other vertebrate *Hmx* genes (e.g. mouse *Hmx1*, *Hmx2* and *Hmx3*) are also expressed in the central nervous system during embryogenesis. At adult stages, sea urchin *Hmx* is expressed in the intestine. Mouse *Hmx3* persists in its expression in the duodenum. It seems that the primary function of *Hmx* genes from various species is retained during evolution. The central nervous system and some internal organs may represent the primary regions where *Hmx* genes exert their function. On the other hand, during evolution, each *Hmx* gene also acquired distinct function as suggested by their unique expression pattern in certain regions, establishing their own identities. Unlike their similar expression in the CNS, *Hmx* genes have different expression profiles in the developing ear. *Hmx1* shows strong expression in the dorsolateral mesenchyme near the otic vesicles, whereas transcripts of *Hmx2* and *Hmx3* can only be detected in the vestibular portion of the developing inner ear at stage older than E10.5, indicating their unique roles in mouse ear development. Even

between *Hmx2* and *Hmx3*, differences in their spatial and temporal expression in the inner ear can be observed (data not shown). The multi-phasic expression pattern of the *Hmx* genes suggests that the regulation of gene expression is very complicated. The question of whether the transcripts of mouse *Hmx* genes (e.g., *Hmx3*) in adult structures like the duodenum and uterus are the same as those expressed at the embryonic stages remains to be investigated further.

Cloning of *Drosophila Hmx*, murine *Hmx2* and *Hmx3* genes make it easier for us to investigate the function of the *Hmx* genes. *Drosophila* and mouse are the two best experimental systems for investigating a gene's function in vivo. By chromosomal mapping of the *Drosophila Hmx* gene, we can find out if there is a pre-existing mutant which may provide informative clues as to the function of murine *Hmx* genes. Well-established transgenic techniques and germline manipulation in ES cells allow us to make mutations in *Hmx* genes in mice. *Loss-of-function* analyses, combined with *gain-of-function* studies, will eventually uncover the function of *Hmx* genes and may provide useful information on the etiology of some human diseases.

Hmx3, a candidate for an epileptogenic gene

It is interesting that the *Hmx1* gene maps to the proximal region of mouse Chromosome 5 since two other homeobox genes, such as *Bapx1* and *Sax2* also reside in this region (Tribioli et al., 1997; unpublished date.). It might be coincidental, but in *Drosophila*, the homologs of these genes (*bagpipe* and *S59*, respectively) are clustered on the same chromosome. If the *Drosophila Hmx* gene is also assigned to the same cluster, *Bapx1*, *Sax2* and *Hmx1* as well as other homeobox genes will comprise another homeobox gene cluster highly conserved during evolution in addition to the *Hox* gene clusters. If this is the case, it would be reasonable to predict that there might be a *tinman* homolog mapping to the proximal region of mouse Chromosome 5. *Hmx1* is linked to homeobox gene *Msx1*.

On Chromosome 7, *Hmx2* and *Hmx3* are also linked to another member of *Msx* family, *Msx3* (Wang et al., 1996).

Intriguingly, *Hmx2* and *Hmx3* map to the region syntenic to the 10q25-26 of human Chromosome 10 on which many epilepsy susceptibility loci have been mapped. Searching for epileptic genes has long been of interest for many investigators. In most cases, epilepsies represent a combination of disorders of neuronal hyperexcitability featuring recurrent, spontaneous episodes of abnormal synchronization in neural networks. These disorders can be inherited (genetic) or acquired (trauma, nongenetic) disturbances in neuronal bursting properties, connectivity and synaptic transmission (Noebels, 1996). In general, epilepsies are classified into "partial" or "generalized" based on origin. In partial epilepsy patients, seizures originate from a specific region in the cerebral cortex, whereas generalized epilepsies arise from the synchronized activation of the entire cortex. In the generalized epilepsies, the deeper, midline structures in the brain such as the thalamus play a critical role. Regarding causes, epilepsies can also be classified into "cryptogenic (lesion)" or "idiopathic". The idiopathic, generalized epilepsies are genetic in origin. Recent evidence strongly shows that genetic factors are also involved in partial epilepsies, even though partial epilepsies are associated with brain lesion or defects in brain development in most cases (Ryan, 1995; Ottman et al., 1995). Investigation of the cellular and molecular bases of epilepsies will benefit humans by broadening our knowledge about epileptogenesis, facilitating the diagnosis and treatment as well as providing for genetic counseling to prevent the epileptic genes from spreading in the population. The major challenges confronted by investigators are heterogeneous phenotypes, complex inheritance, inconsistent expressivity and a small sample size in humans. In epilepsy-prone families, the distribution of affected individuals does not follow the classic Mendelian patterns of inheritance and severity of the affected individuals within the family are variable. These suggest that multiple epileptic loci (including modifying genes) and environmental factors

are also involved. Recently, great progress has been achieved in epileptic locus mapping and gene cloning. The gene responsible for benign neonatal epilepsy (EBN1) maps to human Chromosome 20q (Leppert et al., 1989). A mutation in the gene for the a4 subunit of the nicotinic acetylcholine receptor results in spontaneous neonatal convulsions. Other epileptogenic loci for benign neonatal epilepsy (EBN2), Nocturnal frontal lobe epilepsy, Unverricht-Lundborg disease (EPM1), juvenile type Ceroid lipofuscinosis (CLN3) are assigned to human Chromosome 8q, 20q, 21q22.3 and 16p, respectively. Interestingly, human Chromosome 10q seems to be a very susceptible region since many syndromes associated with epilepsy are linked to this region. Guazzi syndrome has been localized to Chromosome 10. A patient carrying a chromosomal deletion of 10q26-qter manifests it as epilepsy and mental retardation (Smith et al., 1989). The work done by Ottman and colleagues showed the first evidence that partial epilepsy can also be genetic in origin. A novel, dominantly inherited partial epilepsy associated with auditory symptoms is assigned to genetic markers on Chromosome 10q (Ottman et al., 1995). In this work, *Hmx2* and *Hmx3* genes map to the region syntenic to human Chromosome 10q (actually, human *HMX2* maps to this region), and mice carrying a null *Hmx3* gene exhibit epileptic behaviors. These results make *Hmx3* gene a promising epileptic gene candidate. *Hmx3* knockout mice provide an invaluable, viable animal model for human epilepsy. Phenotypic analysis of *Hmx3* null mice will provide instructive information on epileptogenesis.

Animal models for epilepsy can overcome the obstacles encountered in humans. Both genetically simple (single locus involved, e.g. *stargazer*, *tottering* and *lethargic*) and complex (multiple loci involved, e.g., EL mice) models have been generated (Noebels et al., 1990; Noebels and Sidman 1979; Hosford et al., 1992; Frankel et al., 1994). Since epileptic seizures occur when neurons stimulate one another to become active excessively, much attention has been focused on searching for abnormalities in neurotransmitters and their synaptic receptors. The weaver mouse mutant is caused by a missense mutation of a

Gly to a Ser in a brain G protein-coupled inward rectifier K^+ channel (GIRK2). A nonfunctional K^+ channel fails to stop neurotransmitter releasing, resulting in the hyperexcitability of the neuronal network (Patil et al., 1995). Mice carrying a null gene for tissue nonspecific alkaline phosphatase fail to convert pyridoxal phosphate (plp) into nonphosphorylated vitamin B6, resulting in plp accumulation in the serum and significant reduction in the brain. Reduction of plp subsequently leads to the failure of glutamic acid decarboxylase to synthesize GABA, resulting in lethal tonic-clonic convulsions (Waymire et al., 1995). In normal mice, extracellular levels of the excitatory neurotransmitter glutamate is regulated by the activity of glutamate transporters which remove extra glutamate from the extracellular space. Targeted disruption of one of the transporters, GLT-1 results in the accumulation of glutamate in the brains. Phenotypically, the mice display lethal spontaneous seizures (Tanaka et al., 1997). Mutations in the mRNA of the GluRB receptor alter the Ca^{2+} permeability through AMPA channels on the postsynaptic membrane. Heterozygous mice that carry these mutations exhibit spontaneous recurrent limbic seizures (Brusa et al., 1995). Besides neurotransmitters and their receptors, increasing lines of evidence indicate that homeobox genes are also deeply involved in the epileptogenesis. Mice lacking *Otx1* exhibit epileptic behaviour and hyperactivity associated with inner ear defects (Acampora et al., 1996). Analysis of the *Otx1* mutant brains revealed the reduction in the cortex, increase in volume of the mesencephalon and generation of extra lobules in the cerebellum. The malformed *Otx1* null brain is responsible for the epileptic phenotype. In humans, *schizencephaly* has been linked to the mutations in the *EMX2* gene (Brunelli et al., 1996).

It is unlikely that the *Hmx3* gene is directly involved in the alteration of neurotransmitter release or their receptors' function in epileptogenesis, since *Hmx3* is only expressed in restricted regions in the brain at embryonic stages. Dysfunction of the *Hmx3* null brain possibly results from the malformed axonal growth, synaptogenesis, and glia cell

organization due to the developmental defects at embryonic stages. Close examination of the *Hmx3* null brain needs to be performed. Normally, epilepsy initiates in the cortex, then spread to the hippocampus from where it transmits to other brain regions. Altered gene expression in the hippocampus after the occurrence of epilepsy has been reported by many investigators (Gall et al., 1991). Differential expression of epilepsy-induced genes in the hippocampus gives us a good experimental system to screen for epileptic genes and may provide clues to gene therapy.

Hmx3, a gene required for regional-specification and cell-fate determination in the developing inner ear

The striking similarity in their expression pattern and close linkage on the same chromosome suggest that *Hmx2* and *Hmx3* may share some regulatory elements and have overlapping function. To avoid deleting any common regulatory elements, *neo* or *ires.lacZ.neo* cassette was inserted into the *Hmx3* homeobox in our targeting constructs. At the same time, the relatively weak *GT1.2* enhancer (Lufkin et al., 1991) was used to drive the *neo* gene in order to minimize the possibility that enhance/promoter affects the function of the adjacent gene(s), a problem that has been previously reported for the PGK and other promoters (Olson et al., 1996; Rijli et al., 1994). Successfully generated *Hmx3* null mice allow us to obtain in vivo evidence about the function of *Hmx3* during mouse development. *Hmx3* null mice can be easily identified in *Hmx3* null juveniles by their classic Shaker/Waltzer behavioral phenotype of hyperactivity and circling, indicative of vestibule dysfunction. Inner ear development is a complex process involving the competence of a region of surface ectoderm on the lateral hindbrain to invaginate and pinch off to create the otic vesicle. After delamination and coalescence of neuroblasts in the ventral part of the otic vesicle to form the VIIIth ganglion, the rest of the otic vesicle undergoes elongation and morphogenesis to form the three sensory systems of the inner

ear. The dorsal portion of the otic vesicle gives rise to the vestibular structures and the ventral portion develops into the cochlear labyrinth. The three sensory systems are comprised of six epithelia: (1) the three cristae, the sensory organs of the three semicircular canals, for sensing the angular acceleration. (2) the maculae, the sensory organs of the saccule and the utricle, for detecting linear acceleration (gravity). (3) organ of Corti in the cochlea for receiving sound pressure. Many gene products have been shown to be involved in the otogenesis of the inner ear. Inductive signals both from the underlying rhombomeres and from the otocyst itself are required for the formation and function of the inner ear. *Hoxa-1* null mice, in addition to the defects in the CNS, also exhibited severe morphogenetic malformation of the inner ear as showed by the absence of the cochlear labyrinth and the semicircular canals. Since *Hoxa-1* itself is not expressed in the otic vesicle, these defects in the inner ear might be caused by secondary effects due to the lack of inductive signal(s) from the adjacent rhombomeres. *kreisler* mutants (*kr*) result from the chromosomal inversion of the *krml* gene encoding a novel basic domain leucine zipper transcription factor. In wild type mice, *krml* can be only detected in the neural tube adjacent to the otic vesicle, but not in the otocyst at the beginning of otogenesis. In *kr* mutant mice, the malformed otic vesicle failed to form a recognizable vestibular structure and cochlea, resulting in deafness and typical Shaker/Waltzer phenotype. This result shows that signals from the underlying neural tube play critical roles in the inner ear development. In most cases, genes are essential for the development of the regions where they are expressed. *Otx1* null mutants, in addition to its defects in the brain, show the absence of the lateral semicircular duct, which is responsible for their high speed turning behavior. Strikingly similar to the *Otx1* null phenotypes, *Hmx3* null mice also exhibit a bi-directional circling behavior, indicating that both inner ears are affected. *Hmx3* mutant phenotypes do show incomplete penetrance on different genetic backgrounds and variable expressivity (severity of phenotype) even on the same genetic background. For example, on 129/Sv

genetic background. 91% *Hmx3* null mice display a high speed circling behaviour, compared to 16% on the mixed background. On the other hand, the noncircling *Hmx3* null mice do exhibit other defects, such as overgrowth of teeth which ca result in malnutrition. The variable severity of the phenotype may account for the reduced viability of *Hmx3* null neonates (Table 3). Those pups supposed to show much more severe phenotypes might die or have been selectively eliminated by the basic instinct of the mothers right after birth, since we did see remnants of pups left in the cages in many cases. The low penetrance of the phenotype in the CNS and no overt defects in the craniofacial region might be the result of extensive functional redundancy among *Hmx* genes. Expression of *Hmx3* in the dorsal portion of the otic placode suggests that it may play a role in the development of vestibular structures. In *Hmx3* null mice, no gross morphogenetic alteration can be observed either in the vestibular labyrinth or in the cochlear duct as showen in Figure 20. Upon closer examination, severe abnormalities in the vestibular sensory organs can be found in the *Hmx3* null mice. The fusion of the utricle and saccule into a common utriculosaccular space disrupts the normally restrictive communication between these two endolymphatic chambers. Moreover, the fusion subsequently results in the reduction of the area of the maculae of both the saccule and the utricle. Even though all the semicircular ducts were present in the *Hmx3 null* mice, the horizontal crista (sensory organ of the horizontal canal) and the associated ampullary chamber were missing in the horizontal semicircular duct. Missing the horizontal crista and the reduction of the maculae in both the saccule and the utricle are sufficient to cause the circling behaviour associated with the *Hmx3* knockout. Previous studies have shown that many defects can result in abnormalities in ear development. In the *Treacher-Collins* mutation, craniofacial malformation leads to the malformed external and middle ears, subsequently resulting in hearing impairment. Disruption of the POU-domain transcription factor *Brn3.1* leads to failure of hair cell survival both in the organ of Corti and in the vestibular labyrinth. As a result of defects in

hair cell survival, the vestibular ganglion undergoes neuronal degeneration. Consequently, *Brn-3.1* mice exhibit deficits in balance and coordination, hyperactivity as well as complete deafness (Erkman, et al. 1996). The *Isk* gene which encodes a cofactor of K^+ channel subunits is also required for the normal function of the inner ear. The *Isk* gene is not involved in the embryonic development of the inner ear. The maintenance of inner ear structure after birth requires the normal function of *Isk* . *Isk* null mice also show a Shaker/Waltzer phenotype. Histological analysis indicates that disruption of *Isk* gene results in the collapse of both *Reisner's* membrane in cochlea and vestibular wall in the vestibular labyrinth. At the same time, hair cell death in both the cochlea and vestibular labyrinth can be observed. Unlike the mutants described above, *Hmx3* null mice do not show overt defects in their hearing ability. Together with its expression pattern in the dorsal part of the otic vesicle, it seems that *Hmx3* specifically functions in the development of sensory epithelia in the vestibular labyrinth. Complete loss of crista in the horizontal duct and partial loss of sensory organs in the macule and saccule suggest a unique function in the regional specification and cell fate determination of vestibular sensory cells. Since no defects were found in the sensory hair bundles of the maculae, it suggests that *Hmx3* may exert its function prior to hair cell differentiation (~E13.5). At early embryonic stages, *Hmx3*, possibly working with other genes may define the regions to become competent to give rise to different sensory organs. Once the competent region is determined by *Hmx3*, hair cell development seems to be independent to *Hmx3*. In *Hmx3* null mice no region is capable of becoming horizontal crista-competent, resulting in the absence of this sensory organ. Whereas, the other regions are partially compensated for by the function of other gene(s). These regions are able to develop into maculae of both the saccule and utricle with partial loss of sensory cells. It is certain that the defects in the inner ear are associated with the loss of a functional *Hmx3* in the inner ear, but not with its loss in the neural tube since no obvious defects can be found there. Lack of a phenotype in the other two semicircular

canals might be interpreted as a functional compensation by *Hmx2* gene for the loss of *Hmx3* in these regions. It can be expected that the double knockout of *Hmx2* and *Hmx3* could show a much more severe phenotype than any single knockout. since their overlapping expression patterns suggest they may function redundantly or synergistically. Based on the *Hmx1* expression pattern. it is impossible that *Hmx1* has overlapping function with other *Hmx* genes in the inner ear development. Extensive overlapping expression patterns outside the inner ear make it difficult for us to investigate each gene's function. The triple knockout. and different combinations of the double knockouts as well as each single knockout will provide informative clues to the function of this gene family. The role of *Hmx3* in inner ear development and pregnancy may be a recently acquired developmental function as *Hmx* genes are present in many species (e.g., *Drosophila*) which have no anatomical equivalent to the organs affected in *Hmx3* null animals. On an evolutionary view, the mammalian inner ear and uterus represent two relatively newly evolved organs and the role of *Hmx3* in the development of these structures may represent a more recently acquired function relative to the original role of the ancestral *Hmx* gene. All three *Hmx* genes are expressed in an overlapping fashion in the central and peripheral nervous systems, which may represent the ancestral developmental role of this gene family. The absence of a discernible nervous system phenotype in the *Hmx3* null mice may be related to the ancient origin of the nervous system and the inherent functional overlap among gene family members, which is usually associated with genome evolution (Sidow, 1996).

Hmx3, a novel homeobox gene required for maternal fertility

Another important phenotype of *Hmx3* null mutants is the reduced fertility of the null females. Fertility of *Hmx3* null males is normal compared to the wild type and heterozygous males. But the null females show impaired reproduction irrespective of their

genetic background. Even the small portion (12%) of the null females that are capable of giving birth always deliver less pups (~ 4pups/litter) than do the normal mice. By examining the time point of fertility failure during pregnancy, it is clear that the ovulation in *Hmx3* null females is normal. They can produce normal oocytes that can be fertilized. As shown in Table 5, embryos flushed out from the *Hmx3* null uteri before implantation stage can develop to term when they were reimplanted into wild type pseudopregnant mothers. This indicates that before implantation the mother can provide the appropriate environment for embryos to develop autonomously and normally. But, at the implantation stage (~E4.5-5.5), embryos were still unattached to the null uteri and failed to initiate any decidualization reaction, indicating the failure of implantation. The implantation stage is critical in pregnancy as the majority of failed pregnancy occurs at this stage. Implantation of embryos into the uterine wall involves a series of molecular and cellular events. Proper implantation requires the uterus to become receptive to embryos. On E3.5, the uterus starts preparing for the implantation by inducing closure of the uterus which brings the trophectoderm and the luminal epithelium into close apposition. During this period, LIF produced by the glandular epithelium is upregulated with a peak at E4.5. Mice lacking LIF are infertile due to the failure of implantation (Stewart et. al., 1992). At the same time, the *Muc-1* gene product, a glycoprotein, starts degradation from the uterine wall so that the uterus becomes competent for the attachment of embryos (Surveryor et. al., 1995). Docking of embryos (blastocyst) to the uterus induces the production of a heparin-binding protein encoded by *HB-EGF* in the uterine epithelium surrounding the implantation sites. *HB-EGF* gene product is speculated to function as an adhesion molecule to anchor the embryos to the uterus. After the attachment of the embryo, the uterus shows increased vascular permeability around the implantation site. Subsequently, the uterus undergoes decidualization of the stromal cells (Dziadek et al., 1995). Finally, the implantation stage is finished by the contact of trophectoderm with the maternal decidua. In *Hoxa-10* knockout mice, female infertility

results from a combination of homeotic transformation of the proximal uterus into oviduct, decreased vascular permeability, as well as a deficiency in decidualization (Benson et al., 1996). But *Hoxa-10* null mice don't show alteration in LIF and *HB-EGF* expression. In contrast to *Hoxa-10* deficient mice, *Hoxa-11* null mice show defects in stromal, decidual and glandular cell development. The fewer uterine endometrial glands may account for the absence of LIF expression, subsequently leading to the infertility of *Hoxa-11* null females. Infertility of *Hmx3* null females provides another example of a homeobox gene involved in mammalian pregnancy. Expression of the *Hmx3* gene during pregnancy is a dynamic process in which a low level of expression in the stroma of nonpregnant uteri followed by a dramatic shift from stroma to the myometrial layer and a increase in its expression level after pregnancy. The significance of the shift of *Hmx3* expression from the stroma to the myometrium and the increase in expression levels is currently unknown. But this process is definitely required for the implantation. Even though no gross and histological abnormalities have been found so far, lack of functional *Hmx3* results in a deficiency in fertility. Close examination indicates that, at the molecular level, *Hmx3* null uteri have changed their identities. Morphologically normal endometrial glands fail to produce LIF, which is sufficient to cause infertility in female mice. The relationship between the shift of *Hmx3* from stroma to smooth muscle layers and the robust expression of LIF in implantation is very interesting. Why does a lack of functional *Hmx3* abolish LIF expression? It seems that *Hmx3* functions upstream of LIF. Their different expression domains suggest that their communication may be mediated by some diffusible factor(s). Alteration of cell identity in *Hmx3* null uteri can also be perceived by the expression patterns of other molecular markers. For example, in wild type nonpregnant females, *Wnt5A* is expressed in the uterine stroma and the endometrial epithelium. But in nonpregnant *Hmx3* null uteri, its expression in the endometrium is dramatically upregulated. Pregnancy induces the expression in the glandular epithelium and upregulates

the expression in the endometrial epithelium in wildtype mice. But in the *Hmx3* null pregnant uteri, almost all stromal cells become *Wnt5A*-positive in the absence of functional *Hmx3*. Together with the results from *Wnt7A* and *Wnt4* expression, we can conclude that the normal regulatory cascade in the uterus has been disturbed by loss of *Hmx3*. This regulatory pathway may involve different steroid hormone or cytokines. Even though *Hmx3* seems to play a less significant role in the morphogenesis of the female reproductive track, its function is absolutely required for normal biological function of the reproductive system. Alteration of expression of so many molecular markers in *Hmx3* null uteri suggests that many factors are involved directly or indirectly in the Hmx3-mediated signaling pathway. *Hmx1* and *Hmx2* are also expressed in uterus during pregnancy, but down-regulated in the *Hmx3* null uterus. It suggests a possible cross or autoregulatory role for the *Hmx* genes in the uterus. Cross-regulation and autoregulation of homeobox genes have been well characterized, particularly in the case of the *Hox* homeobox genes (reviewed in Lufkin, 1997).

Interestingly, although *Hmx1*, *Hmx2*, and *Hmx3* are no longer expressed in the *Hmx3* null myometrial layer, there are no obvious changes in the expression of the myometrial smooth muscle marker myosin, indicating that myosin is likely to fall into a regulatory cascade independent of the *Hmx* genes. Based on the results obtained from the transgenic studies, there is no obvious regulatory relationship among these three genes in the central nervous system (data not shown). And in the *Hmx3* knockout mice, there is no overt alteration in the expression of *Hmx1* and *Hmx2* in the inner ear. The regulatory hierarchy of *Hmx* genes in the female reproductive system may be conferred by specific cofactor(s) which can regulate *Hmx1* and *Hmx2* only in the presence of *Hmx3* product.

Involvement of *Hmx3* gene in other sensory organs' development has not been investigated. It is highly possible that *Hmx3* null mice also have defects in their vision and olfaction, since *Hmx3* is expressed in the optic stalk and olfactory epithelium.

Prospects

Hmx2 and *Hmx3* double knockout mice show more severe phenotypes than the *Hmx3* single knockout. The majority of the homozygotes died prenatally. Few surviving pups showed complete loss of balance and died before day 9 after birth. Analyzing the time point at which the double knockout mice die and the pathology are in progress. Comparison of the phenotypes of double knockout mice with those of either single knockout will provide instructive insights into the functional relationship between *Hmx2* and *Hmx3* gene. It will become clear then, in what regions and at what time point, *Hmx2* and *Hmx3* genes function redundantly or synergistically. Moreover, the triple knockout and different combinations of double knockout among the *Hmx* genes will eventually uncover the function of *Hmx* gene family.

The spatial and temporal expression patterns of the *Hmx* genes suggest that regulatory pathways involving *Hmx* genes is quite complex. Dissecting out the regulatory elements of each *Hmx* gene can help us to find out the upstream regulators of *Hmx* genes. Using transgenic analysis, the minimal elements responsible for tissue-specific expression of *Hmx* genes can be obtained. Isolation of the cis-acting elements of *Hmx* genes will make it possible to identify the trans-acting factors by screening an expression cDNA library using radioactive labeled cis-acting elements. Two hybrid system allows us to screen for the cofactors of *Hmx* gene products. Isolation of these cofactors will help us to interpret why the cross and auto-regulation among *Hmx* genes exits in the uterus, but not in the inner ear. Targeted disruption of the *Hmx* genes results in the failure of their DNA binding ability. It

is certain that expression of the genes regulated by *Hmx* gene products will be altered in mice carrying null *Hmx* alleles. mRNA extracted from the affected tissues, like wildtype and null uteri can be used for searching for *Hmx* downstream genes. mRNA differential display technique and subtractive hybridization can be employed.

In summary, *Hmx3* plays an important role in mouse vestibular sensory organ integrity as well as mammalian fertility. *Hmx3* null mice are a novel viable animal model for epilepsy. To fully understand the function of the *Hmx* genes, in addition to disruption of these genes, overexpression and misexpression of these genes can also provide us with useful information. In the near future, the overall picture of the function of this gene family will be delineated.

References:

Acampora, D., Mazan, S., Lallemand, Y., Avantaggiato, V., Maury, M., Simeone, A., and Brulet, P. (1995). Forebrain and midbrain regions are deleted in *Otx2-/-* mutants due to a defective anterior neuroectoderm specification during gastrulation. *Dev Suppl* 121, 3279-90.

Acampora, D., Mazan, S., Avantaggiato, V., Barone, P., Tuorto, F., Lallemand, Y., Brulet, P., and Simeone, A. (1996). Epilepsy and brain abnormalities in mice lacking the *Otx1* gene. *Nat Genet* 14, 218-22.

Alonso, S., Minty, A., Bourlet, Y., and Buckingham, M. (1986). Comparison of three actin-coding sequences in the mouse; evolutionary relationships between the actin genes of warm-blooded vertebrates. *J. Mol. Evol.* 23 (1), 11-22.

Ang, S. L., Jin, O., Rhinn, M., Daigle, N., Stevenson, L., and Rossant, J. (1996). A targeted mouse *Otx2* mutation leads to severe defects in gastrulation and formation of axial mesoderm and to deletion of rostral brain. *Dev Suppl* 122, 243-52.

Ausubel, F. M., Brent, R., E., K. R., and Moore, D. D. (1994). Current Protocols in Molecular Biology, 1st Edition, Volume 7.01-7.2.20: A joint venture between Greene Publishing Associates, Inc. and John Wiley &Sons, Inc.).

Becerra, S. P., Rose, J. A., Hardy, M., Baroudy, B. M., Anderson, C. W. (1985): Direct mapping of adeno-associated virus capsid proteins B and C: a possible ACG initiation codon. *Proc Natl Acad Sci USA* 82: 7919-23.

Benson, G. V., Lim, H., Paria, B. C., Satokata, I., Dey, S. K., and Maas, R. L. (1996). Mechanisms of reduced fertility in *Hoxa-10* mutant mice: uterine homeosis and loss of maternal *Hoxa-10* expression. Development 122, 2687-96.

Bhatt, H., Brunet, L. J., and Stewart, C. L. (1991). Uterine expression of leukemia inhibitory factor coincides with the onset of blastocyst implantation. *Proc Natl Acad Sci USA* 88, 11408-12.

Bober, E., Baum, C., Braun, T., and Arnold, H. H. (1994). A novel *NK*-related mouse homeobox gene: expression in central and peripheral nervous structures during embryonic development. *Dev Biol* 162, 288-303.

Bradley, D. J., Towle, H. C., and Young, W. S. R. (1994). Alpha and beta thyroid hormone receptor (TR) gene expression during auditory neurogenesis: evidence for TR isoform-specific transcriptional regulation in vivo. *Proc Natl Acad Sci USA* 91, 439-43.

Brunelli, S., Faiella, A., Capra, V., Nigro, V., Simeone, A., Cama, A., and Boncinelli, E. (1996). Germline mutations in the homeobox gene *EMX2* in patients with severe schizencephaly. *Nat Genet* 12, 94-6.

Carpenter, E. M., Goddard, J. M., Chisaka, O., Manley, N. R., and Capecchi, M. R. (1993). Loss of *Hox-A1* (*Hox-1.6*) function results in the reorganization of the murine hindbrain. *Development* 118, 1063-75.

Cavener, D. R., and Ray, S. C. (1991). Eukaryotic start and stop translation sites. *Nucleic Acids Res* 19, 3185-92.

Chakraborty, I., Das, S. K., and Dey, S. K. (1995). Differential expression of vascular endothelial growth factor and its receptor mRNAs in the mouse uterus around the time of implantation. *J Endocrinol* 147, 339-52.

Chen, X. and Lufkin, T. (1997). Linkage mapping of *Sax2* to mouse Chromosome 5. *Mamm Genome* 8: 697-8

Chisaka, O., Musci, T. S., and Capecchi, M. R. (1992). Developmental defects of the ear, cranial nerves and hindbrain resulting from targeted disruption of the mouse homeobox gene Hox-1.6 [see comments]. *Nature* 355, 516-20.

Chomczynski, P., and Sacchi, N. (1987). Single-step method of RNA isolation by acid guanidinium thiocyanate- phenol-chloroform extraction. *Anal Biochem* 162, 156-9.

Cordes, S. P., and Barsh, G. S. (1994). The mouse segmentation gene kr encodes a novel basic domain-leucine zipper transcription factor. *Cell* 79, 1025-34.

Corey, D. P., and Breakefield, X. O. (1994). Transcription factors in inner ear development. *Proc. Natl. Acad. Sci. USA* 91, 433-436.

Corwin, J. T., Warchol, M. E., and Kelley, M. W. (1993). Hair cell development. *Curr Opin Neurobiol* 3, 32-7.

Cross, J. C., Werb, Z., and Fisher, S. J. (1994). Implantation and the placenta: key pieces of the development puzzle. *Science* 266, 1508-18.

Danielson, P. E., Watson, J. B., Gerendasy, D. D., Erlander, M. G., Lovenberg, T. W., de Lecea, L., Sutcliffe, J. G., and Frankel, W. N. (1994). Chromosomal mapping of mouse genes expressed selectively within the central nervous system. *Genomics* 19, 454-61.

Davis, A. P., and Capecchi, M. R. (1994). Axial homeosis and appendicular skeleton defects in mice with a targeted disruption of hoxd-11. *Development* 120, 2187-98.

Deitcher, D. L., Fekete, D. M., and Cepko, C. L. (1994). Asymmetric expression of a novel homeobox gene in vertebrate sensory organs. *J Neurosci* 14, 486-98.

Deol, M. S. (1964). The abnormalities of the inner ear in kreisler mice. *J. Embryol. Exp. Morphol.* 12, 475-490.

Dixon, J., S.J., E., J., G. A., Dixon, M. J., Loftus, S. K., Bonner, C. A., Koprivnikar, K., and Wasmuth, J. J. (1996). Positional cloning of a gene involved in the pathogenesis of Treacher Collins syndrome. *Nature Genet* 12, 130-136.

Dixon, J., Edwards, S. J., Anderson, I., Brass, A., Scambler, P. J., and Dixon, M. J. (1997). Identification of the complete coding sequence and genomic organization of the Treacher Collins syndrome gene. *Genome Res* 7, 223-34.

Dziadek, M., Darling, P., Zhang, R. Z., Pan, T. C., Tillet, E., Timpl, R., and Chu, M. L. (1995). Expression of collagen alpha 1(VI), alpha 2(VI), and alpha 3(VI) chains in the pregnant mouse uterus. *Biol Reprod* 52, 885-94.

Ekker, M., Akimenko, M. A., Bremiller, R., and Westerfield, M. (1992). Regional expression of three homeobox transcripts in the inner ear of zebrafish embryos. *Neuron* 9, 27-35.

Epstein, D. J., Vekemans, M., and Gros, P. (1991). *Splotch (Sp2H)*, a mutation affecting development of the mouse neural tube, shows a deletion within the paired homeodomain of Pax-3. *Cell* 67, 767-74.

Epstein, D. J., Vogan, K. J., Trasler, D. G., and Gros, P. (1993). A mutation within intron 3 of the *Pax-3* gene produces aberrantly spliced mRNA transcripts in the *splotch (Sp)* mouse mutant. *Proc Natl Acad Sci U S A* 90, 532-6.

Erkman, L., McEvilly, R. J., Luo, L., Ryan, A. K., Hooshmand, F., O'Connell, S. M., Keithley, E. M., Rapaport, D. H., Ryan, A. F., and Rosenfeld, M. G. (1996). Role of transcription factors Brn-3.1 and Brn-3.2 in auditory and visual system development. *Nature* 381, 603-6.

Ernfors, P., Van De Water, T., Loring, J., and Jaenisch, R. (1995). Complementary roles of BDNF and NT-3 in vestibular and auditory development [published erratum appears in Neuron 1995 Sep;15(3):739]. *Neuron* 14, 1153-64.

Evans, S. M., Yan, W., Murillo, M. P., Ponce, J., and Papalopulu, N. (1995). *tinman*, a Drosophila homeobox gene required for heart and visceral mesoderm specification, may be represented by a family of genes in vertebrates: *XNkx-2.3*, a second vertebrate homologue of tinman. *Development* 121, 3889-99.

Fekete, D. M. (1996). Cell fate specification in the inner ear. *Current Opinion in Neurobiology* 6, 533-541.

Foerst-Potts, L., and Sadler, T. W. (1997). Disruption of *Msx-1* and *Msx-2* reveals roles for these genes in craniofacial, eye, and axial development. *Dev Dyn* 209, 70-84.

Forrest, D., Erway, L. C., Ng, L., Altschuler, R., and Curran, T. (1996). Thyroid hormone receptor beta is essential for development of auditory function. *Nat Genet* 13, 354-7.

Frankel, W. N., Taylor, B. A., Noebels, J. L., and Lutz, C. M. (1994). Genetic epilepsy model derived from common inbred mouse strains. *Genetics* 138, 481-9.

Frasch, M., Chen, X., and Lufkin, T. (1995). Evolutionary-conserved enhancers direct region-specific expression of the murine *Hoxa-1* and *Hoxa-2* loci in both mice and Drosophila. *Development* 121, 957-74.

Fritzsch, B., Silos-Santiago, I., Bianchi, L. M., and Farinas, I. (1997). The role of neurotrophic factors in regulating the development of inner ear innervation. *Trends Neurosci* 20, 159-164.

Gall, C., Lauterborn, J., Bundman, M., Murray, K., and Isackson, P. (1991). Seizures and the regulation of neurotrophic factor and neuropeptide gene expression in brain. *Epilepsy Res* Suppl 4, 225-45.

Gaunt, S. J., Blum, M., De Robertis, E. M. (1993). Expression of the mouse *goosecoid* gene during mid-embryogenesis may mark mesenchymal cell lineages in the developing head, limbs and body wall. *Development* 117: 769-78.

Gavin, B. J., McMahon, J. A., and McMahon, A. P. (1990). Expression of multiple novel Wnt-1/int-1 -related genes during fetal and adult mouse development. *Genes* Dev 4: 2319-32.

Gendron, R. L., Paradis, H., Hsieh-Li, H. M., Lee, D. W., Potter, S. S., and Markoff, E. (1997). Abnormal uterine stromal and glandular function associated with maternal reproductive defects in *Hoxa-11* null mice. *Biol Reprod* 56, 1097-105.

George, K. M., Leonard, M. W., Roth, M. E., Lieuw, K. H., Kioussis, D., Grosveld, F., and Engel, J. D. (1994). Embryonic expression and cloning of the murine GATA-3 gene. *Development* 120, 2673-86.

Gilbert, S. F. (1994). Developmental Biology, 4th Edition. Sunderland, Massachusetts: Sinauer Associated, Inc. Publisher.

Gossler, A., Doetschman, T., Korn, R., Serfling, E., and Kemler, R. (1986). Transgenesis by means of blastocyst-derived embryonic stem cells lines. *Proc Natl Acad Sci USA* 83:9065-9069

Goulding, M. D., Chalepakis, G., Deutsch, U., Erselius, J. R., and Gruss, P. (1991). *Pax-3*, a novel murine DNA binding protein expressed during early neurogenesis. *Embo J* 10, 1135-47.

Goulding, M. D., Sterrer, S., Fleming, J., Bailling, R., Nadeau, J., Moore, K. J., Brown, S. D., Steel, K. P., and Gruss, P. (1993). Analysis of the *Pax-3* gne in the mouse mutant *splotch*. *Genomics* 17:355-63.

Granata, T., Farina, L., Faiella, A., Cardini, R., D'Incerti, L., Boncinelli, E., and Battaglia, G. (1997). Familial schizencephaly associated with EMX2 mutation. *Neurology* 48, 1403-6.

Hann, S. R., King, M. W., Bentley, D. L., Anderson, C. W., and Eisenman, R. N. (1988). A non-AUG translational initiation in *c-myc* exon 1 generates an N- terminally distinct protein whose synthesis is disrupted in Burkitt's lymphomas. *Cell* 52:185-95.

Henrique, D., Adam, J., Myat, A., Chitnis, A., Lewis, J., and Ish-Horowicz, D. (1995). Expression of a *Delta* homologue in prospective neurons in the chick [see comments]. *Nature* 375, 787-90.

Hill, R. E., Favor, J., Hogan, B. L., Ton, C. C., Saunders, G. F., Hanson, I. M., Prosser, J., Jordan, T., Hastie, N. D., and van

Heyningen, V. (1991). Mouse small eye results from mutations in a paired-like homeobox- containing gene. *Nature* 354, 522-5.

Hoffman, D., Liu, Y., Sangiorgi, F., Kundu, R., Sininger, Y., Linthicum, F., Conne-Wesson, B., and Maxson, R., (1995). Ectopic expression of Msx2 in transgenic mice results in deafness, vestibular dysfunction and late degeneration of the organ of Corti. Mol. *Biol.Hear Deafness Symp.*, Bethesda.

Huguet, E. L., Smith, K., Bicknell, R., and Harris, A. L. (1995). Regulation of *Wnt5a* mRNA expression in human mammary epithelial cells by cell shape, confluence, and hepatocyte growth factor. *J Biol Chem* 270, 12851-6.

Hunt, N. H., Lim, L. K., Eichner, R. D., Buffinton, G. D., and Weidemann, M. J. (1984). Activation of cyclic AMP-dependent protein kinase in macrophages. *Biochem Biophys Res Commun* 119, 1082-8.

Hunt, J. S., Manning, L. S., Mitchell, D., Selanders, J. R., and Wood, G. W. (1985). Localization and characterization of macrophages in murine uterus. *J Leukoc Biol* 38, 255-65.

Ieshima, A., Koeda, T., and Inagaki, M. (1986). Peculiar face, deafness, cleft palate, male pseudohermaphroditism, and growth and psychomotor retardation: a new autosomal recessive syndrome? *Clin Genet* 30, 136-41.

Jabs, E. W., Muller, U., Li, X., Ma, L., Luo, W., Haworth, I. S., Klisak, I., Sparkes, R., Warman, M. L., Mulliken, J. B., (1993). A mutation in the homeodomain of the human *MSX2* gene in a family affected with autosomal dominant craniosynostosis. *Cell* 75, 443-50.

Jang, S. K., Krausslich, H. G., Nicklin, M. J., Duke, G. M., Palmenberg, A. C., and Wimmer, E. (1988). A segment of the 5' nontranslated region of encephalomyocarditis virus RNA directs internal entry of ribosomes during in vitro translation. *J Virol* 62, 2636-43.

Jang, S. K., Davies, M. V., Kaufman, R. J., and Wimmer, E. (1989). Initiation of protein synthesis by internal entry of ribosomes into the 5' nontranslated region of encephalomyocarditis virus RNA in vivo. *J Virol* 63, 1651-60.

Jang, S. K., Pestova, T. V., Hellen, C. U., Witherell, G. W., and Wimmer, E. (1990). Cap-independent translation of picornavirus RNAs: structure and function of the internal ribosomal entry site. *Enzyme* 44, 292-309.

Jordan, T., Hanson, I., Zaletayev, D., Hodgson, S., Prosser, J., Seawright, A., Hastie, N., and van Heyningen, V. (1992). The human *PAX6* gene is mutated in two patients with aniridia. *Nat Genet* 1, 328-32.

Kappen, C., Schughart, K., and Ruddle, F. H. (1993). Early evolutionary origin of major homeodomain sequence classes. *Genomics* 18, 54-70.

Khan, A. S., Taylor, B. R., and Ringer, D. P. (1994). A Rapid Method for Preparation of Lambda Double-stranded DNA. *BioTechniques* 15, 149-150.

Kikuchi, K., Hilding, D. A. (1967). The spiral vessel and stria vascularis in *shaker-1* mice. Electron microscopic and histochemical observations *Acta Otolaryngol (stockh)* 63: 395-410

Kissinger, C. R., Liu, B. S., Martin-Blanco, E., Kornberg, T. B., and Pabo, C. O. (1990). Crystal structure of an engrailed homeodomain-DNA complex at 2.8 A resolution: a framework for understanding homeodomain-DNA interactions. *Cell* 63, 579-90.

Ko, L. J., Yamamoto, M., Leonard, M. W., George, K. M., Ting, P., and Engel, J. D. (1991). Murine and human T-lymphocyte GATA-3 factors mediate transcription through a cis-regulatory element within the human T-cell receptor delta gene enhancer. *Mol Cell Biol* 11, 2778-84.

Kozak, M. (1987). At least six nucleotides preceding the AUG initiator codon enhance translation in mammalian cells. *J Mol Biol* 196, 947-50.

Krumlauf, R. (1993). *Hox* genes and pattern formation in the branchial region of the vertebrate head. *Trends Genet* 9, 106-12.

Kuhlman, J., and Niswander, L. (1997). Limb deformity proteins: role in mesodermal induction of the epical ectodermal ridge. *Development* 124, 133-139.

Leppert, M., Anderson, V. E., Quattlebaum, T., Stauffer, D., O'Connell, P., Nakamura, Y., Lalouel, J. M., and White, R. (1989). Benign familial neonatal convulsions linked to genetic markers on chromosome 20. *Nature* 337, 647-8.

Li, C. W., Van De Water, T. R., and Ruben, R. J. (1976). In vitro study of fate mapping of the mouse otocyst. *Trans Am Acad Ophthalmol Otolaryngol* 82, 273-80.

Li, C. W., Van De Water, T. R., and Ruben, R. J. (1978). The fate mapping of the eleventh and twelfth day mouse otocyst: an in vitro study of the sites of origin of the embryonic inner ear sensory structures. *J Morphol* 157, 249-67.

Li, X., Wang, W., and Lufkin, T. (1997). Sensitive dicistronic markers for the simultaneous analysis of multiple transgene expression in transgenic mice. *BioTechniques*. In press.

Lints, T., Parsons, L., Hartley, L., Lyons, I., and Harvey, R. (1993). Nkx-2.5: a novel murine homeobox gene expressed in early heart progenitor cells and their myogenic descendants. *Dev Suppl* 119, 419-31.

Liu, I. S., Chen, J. D., Ploder, L., Vidgen, D., van der Kooy, D., Kalnins, V. I., and McInnes, R. R. (1994). Developmental expression of a novel murine homeobox gene (Chx10): evidence for roles in determination of the neuroretina and inner nuclear layer. *Neuron* 13, 377-93.

Lufkin, T., Dierich, A., LeMeur, M., Mark, M., and Chambon, P. (1991). Disruption of the Hox-1.6 homeobox gene results in defects in a region corresponding to its rostral domain of expression. *Cell* 66, 1105-19.

Lufkin, T., Mark, M., Hart, C. P., Dolle, P., LeMeur, M., and Chambon, P. (1992). Homeotic transformation of the occipital bones of the skull by ectopic expression of a homeobox gene. *Nature* 359, 835-41.

Lufkin, T., Lohnes, D., Mark, M., Dierich, A., Gorry, P., Gaub, M. P., LeMeur, M., and Chambon, P. (1993). High postnatal lethality and testis degeneration in retinoic acid receptor alpha mutant mice. *Proc Natl Acad Sci U S A* 90, 7225-9.

Lufkin, T. (1996). Transcriptional control of Hox genes in the vertebrate nervous system. *Curr Opin Genet Dev 6*, 575-80.

Lumsden, A., Sprawson, N., and Graham, A. (1991). Segmental origin and migration of neural crest cells in the hindbrain region of the chick embryo. *Development* 113, 1281-91.

Martinez, P., and Davidson, E. H. (1997). *SpHmx*, a sea urchin homeobox gene expressed in embryonic pigment cells. *Dev Biol* 181, 213-22.

Matsuo, I., Kuratani, S., Kimura, C., Takeda, N., and Aizawa, S. (1995). Mouse *Otx2* functions in the formation and patterning of rostral head. *Genes Dev* 9, 2646-58.

McGinnis, W., and Krumlauf, R. (1992). Homeobox genes and axial patterning. *Cell* 68, 283-302.

McKay, I. J., Muchamore, I., Krumlauf, R., Maden, M., Lumsden, A., and Lewis, J. (1994). The kreisler mouse: a hindbrain segmentation mutant that lacks two rhombomeres. *Development* 120, 2199-211.

McKenzie, A., Ferguson, M. W. J., Sharpe, P. T., (1992). Expression patterns of the homeobox gene, Hox-8 in the mouse embryo suggest a role in specifying tooth initiation and shape. *Development* 115, 403-420.

McMahon, A. P., Gavin, B. J., Parr, B., Bradley, A., and McMahon, J. A. (1992). The Wnt family of cell signalling molecules in postimplantation development of the mouse. In *Postimplantation development in the mouse* (ed. D. J. Chadwick and J. Marsh), pp. 199-212. John Wiley & Sons, Chichester.

Mehdi, H., Ono, E., and Gupta, K. C. (1990) Initiation of translation at CUG, GUG, and ACG codons in mammalian cells. *Gene* 91: 173-8

Miano, J. M., Cserjesi, P., Ligon, K. L., Periasamy, M., and Olson, E. N. (1994). Smooth muscle myosin heavy chain exclusively marks the smooth muscle lineage during mouse embryogenesis. *Circ Res* 75, 803-12.

Monaghan, A. P., Davidson, D. R., Sime, C., Graham, E., Baldock, R., Bhattacharya, S. S., and Hill, R. E. (1991). The Msh-like homeobox genes define domains in the developing vertebrate eye. *Development* 112, 1053-61.

Monkley, S. J., Delaney, S. J., Pennisi, D. J., Christiansen, J. H., and Wainwright, B. J. (1996). Targeted disruption of the Wnt2 gene results in placentation defects. *Development* 122, 3343-53.

Nagy, A., Gocza, E., Diaz, E. M., Prideaux, V. R., Ivanyi, E., Markkula, M., and Rossant, J. (1990). Embryonic stem cells alone are able to support fetal development in the mouse. *Development* 110, 815-21.

Nagy, A., and Rossant, J. (1993). Gene Targeting: a practical approach. (A. Joyner, ed.) Oxford: Oxford University.

Noebels, J. L. (1996). Targeting epilepsy genes. *Neuron* 16, 241-4.

Nornes, H. O., Dressler, G. R., Knapik, E. W., Deutsch, U., and Gruss, P. (1990). Spatially and temporally restricted expression of Pax2 during murine neurogenesis. *Development* 109, 797-809.

Nusse, R., and Varmus, H. E. (1992). *Wnt* genes. *Cell* 69, 1073-87.

Oliver, G., Mailhos, A., Wehr, R., Copeland, N. G., Jenkins, N. A., and Gruss, P. (1995). *Six3*, a murine homologue of the sine oculis gene, demarcates the most anterior border of the developing neural plate and is expressed during eye development. *Development* 121, 4045-55.

Oliver, G., Wehr, R., Jenkins, N. A., Copeland, N. G., Cheyette, B. N., Hartenstein, V., Zipursky, S. L., and Gruss, P. (1995). Homeobox genes and connective tissue patterning. *Development* 121, 693-705.

Oliver, G., Loosli, F., Koster, R., Wittbrodt, J., and Gruss, P. (1996). Ectopic lens induction in fish in response to the murine homeobox gene *Six3*. *Mech Dev* 60, 233-9.

Olson, E. N., Arnold, H. H., Rigby, P. W., and Wold, B. J. (1996). Know your neighbors: three phenotypes in null mutants of the myogenic bHLH gene MRF4. *Cell* 85, 1-4.

Ottman, R., Risch, N., Hauser, W. A., Pedley, T. A., Lee, J. H., Barker-Cummings, C., Lustenberger, A., Nagle, K. J., Lee, K. S., Scheuer, M. L., Neystat, M., Susser, M. and Wilhelmsen, K. C. (1995). Localization of a gene for partial epilepsy to chromosome 10q [see comments]. *Nat Genet* 10, 56-60.

Pavlova, A., Boutin, E., Cunha, G., and Sassoon, D. (1994). *Msx1* (*Hox-7.1*) in the adult mouse uterus: cellular interactions underlying regulation of expression. *Development* 120, 335-45.

Pellegrini, M., Mansouri, A., Simeone, A., Boncinelli, E., and Gruss, P. (1996). Dentate gyrus formation requires *Emx2*. *Development* 122, 3893-8.

Pollard, J. W., Hunt, J. S., Wiktor-Jedrzejczak, W., and Stanley, E. R. (1991). A pregnancy defect in the osteopetrotic (op/op) mouse demonstrates the requirement for CSF-1 in female fertility. *Dev Biol* 148, 273-83.

Preston, R. A., Post, J. C., Keats, B. J., Aston, C. E., Ferrell, R. E., Priest, J., Nouri, N., Losken, H. W., Morris, C. A., Hurtt, M. R., and et al. (1994). A gene for Crouzon craniofacial dysostosis maps to the long arm of chromosome 10. *Nat Genet* 7, 149-53.

Price, M., Lemaistre, M., Pischetola, M., Di Lauro, R., and Duboule, D. (1991). A mouse gene related to Distal-less shows a restricted expression in the developing forebrain. *Nature* 351, 748-51.

Price, M. (1993). Members of the *Dlx*- and *Nkx2*-gene families are regionally expressed in the developing forebrain. *J Neurobiol* 24, 1385-99.

Qiu, M., Bulfone, A., Martinez, S., Meneses, J. J., Shimamura, K., Pedersen, R. A., and Rubenstein, J. L. (1995). Null mutation of *Dlx-2* results in abnormal morphogenesis of proximal first and second branchial arch derivatives and abnormal differentiation in the forebrain. *Genes Dev* 9, 2523-38.

Qiu, M., Bulfone, A., Ghattas, I., Meneses, J. J., Christensen, L., Sharpe, P. T., Presley, R., Pedersen, R. A., and Rubenstein, J. L. (1997). Role of the Dlx homeobox genes in proximodistal patterning of the branchial arches: mutations of *Dlx-1*, *Dlx-2*, and *Dlx-1* and *-2* alter morphogenesis of proximal skeletal and soft tissue structures derived from the first and second arches. *Dev Biol* 185, 165-84.

Raab, G., Kover, K., Paria, B. C., Dey, S. K., Ezzell, R. M., and Klagsbrun, M. (1996). Mouse preimplantation blastocysts adhere to cells expressing the transmembrane form of heparin-binding EGF-like growth factor. *Development* 122, 637-45.

Redmond, R. M., Graham, C. A., Kelly, E. D., Coleman, M., and Nevin, N. C. (1992). Prenatal exclusion of Norrie's disease. *Br J Ophthalmol* 76, 491-3.

Rijli, F. M., Dolle, P., Fraulob, V., LeMeur, M., and Chambon, P. (1994). Insertion of a targeting construct in a *Hoxd-10* allele can influence the control of *Hoxd-9* expression. *Dev Dyn* 201, 366-77.

Rinkwitz-Brandt, S., Justus, M., Oldenettel, I., Arnold, H. H., and Bober, E. (1995). Distinct temporal expression of mouse *Nkx-5.1* and *Nkx-5.2* homeobox genes during brain and ear development. *Mech Dev* 52, 371-81.

Rinkwitz-Brandt, S., Arnold, H. H., and Bober, E. (1996). Regionalized expression of *Nkx5-1*, *Nkx5-2*, *Pax2* and sek genes during mouse inner ear development. *Hear Res* 99, 129-38.

Rivolta, M. N. (1997). Transcription Factors in the Ear: Molecular Switches for Developement and Differentiation. *Audiology & Neuro-Otology* 2, 36-49.

Robertson, E. J., Maxfield, F. R., and Vogel, H. J. (1993). Cell-Cell Signaling in Veterbrate Development .San Diego: Academic Press, Inc.

Robinson, G. W., and Mahon, K. A. (1994). Differential and overlopping expression domains of *Dlx-2* and *Dlx-3* suggest distinct roles for *Distal-less* homeobox genes in craniofacial development. *Mech. Dev.*, 199-215.

Rowe, L. B., Nadeau, J. H., Turner, R., Frankel, W. N., Letts, V. A., Eppig, J. T., Ko, M. S., Thurston, S. J., and Birkenmeier, E. H. (1994). Maps from two interspecific backcross DNA panels available as a community genetic mapping resource [published erratum appears in Mamm Genome 1994 Jul;5(7):463]. *Mamm Genome* 5, 253-74.

Rutland, P., Pulleyn, L. J., Reardon, W., Baraitser, M., Hayward, R., Jones, B., Malcolm, S., Winter, R. M., Oldridge, M., Slaney, S. F., and et al. (1995). Identical mutations in the FGFR2 gene cause both Pfeiffer and Crouzon syndrome phenotype. *Nat Genet* 9, 173-6.

Ryan, S. G. (1995). Partial epilepsy: chinks in the armour. *Nature Genet* 10, 4-6.

Ryan, A. F. (1997). Transcription factors and the control of inner ear development. *Semi Cell Dev Bio* 8, 249-256.

Sambrook, J., Fritsch, E. F., and Maniatis, P. (1989). Molecular Clonging: A Laboratory Manual, 2nd Edition (Cold Spring Harbor, New York: Cold Spring Harbor Laboratory).

Sanes, J. R., Rubenstein, J. L., and Nicolas, J. F., (1986). Use of a recombinant retrovirus to study post-implantation cell lineage in mouse embryos. *Embo J* 5, 3133-42.

Sanger, F., Nicklen, S., and Coulson, A. R. (1977). DNA sequencing with chain-terminating inhibitors. *Proc Natl Acad Sci U S A* 74, 5463-7.

Sanyanusin, P., Schimmenti, L. A., McNoe, T. A., Ward, T. A., Pierpont, M. E., Sullivan, M. J., Dobyns, W. B., and Eccles, M. R. (1996). Mutation of the gene in a family with optic nerve colobomas, renal anomolies and vesicoureteral reflux. *Nat Genet* 13, 129.

Satokata, I., and Maas, R. (1994). Msx1 deficient mice exhibit cleft palate and abnormalities of craniofacial and tooth development [see comments]. *Nat Genet* 6, 348-56.

Satokata, I., Benson, G., and Maas, R. (1995). Sexually dimorphic sterility phenotypes in Hoxa10-deficient mice. *Nature* 374, 460-3.

Schultz, G. A., and Heyner, S. (1993). Growth factors in preimplantation mammalian embryos. *Oxf Rev Reprod Biol* 15, 43-81.

Schwarzer, C., and Sperk, G. (1995). Hippocampal granule cells express glutamic acid decarboxylase-67 after limbic seizures in the rat. *Neuroscience* 69, 705-9.

Shen, W. F., Rozenfeld, S., Lawrence, H. J., and Largman, C. (1997). The Abd-B-like Hox homeodomain proteins can be subdivided by the ability to form complexes with Pbx1a on a novel DNA target. *J Biol Chem* 272, 8198-206.

Sidow, A. (1996). Gen(om)e duplications in the evolution of early vertebrates. *Curr Opin Genet Dev* 6, 715-22.

Simeone, A., Acampora, D., Gulisano, M., Stornaiuolo, A., and Boncinelli, E. (1992). Nested expression domains of four homeobox genes in developing rostral brain [see comments]. *Nature* 358, 687-90.

Simon, A. M., Goodenough, D. A., Li, E., and Paul, D. L. (1997). Female infertility in mice lacking connexin 37. *Nature* 385, 525-9.

Small, K. M., and Potter, S. S. (1993). Homeotic transformations and limb defects in Hox A11 mutant mice. *Genes Dev* 7, 2318-28.

Smith, A., W.A., E., and H., W. (1989). Post-mortem studies on two patients with 1-2 band cytogenetic deletions:10q26---qter and r(9)(p24q34). *Ann. Genet.* 32, 220-224.

Stadler, H. S., Padanilam, B. J., Buetow, K., Murray, J. C., and Solursh, M. (1992). Identification and genetic mapping of a homeobox gene to the 4p16.1 region of human chromosome 4. Proc Natl Acad Sci U S A 89, 11579-83.

Stadler, H. S., and Solursh, M. (1994). Characterization of the homeobox-containing gene *GH6* identifies novel regions of homeobox gene expression in the developing chick embryo. *Dev Biol* 161, 251-62.

Stadler, H. S., Murray, J. C., Leysens, N. J., Goodfellow, P. J., and Solursh, M. (1995). Phylogenetic conservation and physical mapping of members of the H6 homeobox gene family. *Mamm Genome* 6, 383-8.

Stahl, J., Gearing, D. P., Willson, T. A., Brown, M. A., King, J. A., and Gough, N. M. (1990). Structural organization of the genes for murine and human leukemia inhibitory factor. Evolutionary conservation of coding and non-coding regions. *J Biol Chem* 265, 8833-41.

Steel, K. P., and Brown, S. D. M. (1996). Genetics of deafness. *Curr Opin Neurobio* 6, 520-525.

Stein, K. F., and Huber, S. A. (1960). Morphology and behavior of waltzer-type mice. *J Morphology* 106, 197-203.

Stewart, C. L. (1994) Leukaemia inhibitory factor and the regulation of pre-implantation development of the mammalian embryo. *Mol Reprod Dev* 39: 233-8

Stewart, C. L., Kaspar, P., Brunet, L. J., Bhatt, H., Gadi, I., Kontgen, F., and Abbondanzo, S. J. (1992). Blastocyst implantation depends on maternal expression of leukaemia inhibitory factor [see comments]. *Nature* 359, 76-9.

Surveyor, G. A., Gendler, S. J., Pemberton, L., Das, S. K., Chakraborty, I., Julian, J., Pimental, R. A., Wegner, C. C., Dey, S. K., and Carson, D. D. (1995). Expression and steroid hormonal control of Muc-1 in the mouse uterus. *Endocrinology* 136, 3639-47.

Sutherland, L. B., Amendt, B. A. and Russo, A. F. (1997). The Hmx and Nkx homeodomain families share a unique DNA binding specificity. *J Biol Chem* (in press)

Takeda, K., Sakurai, A., DeGroot, L. J., and Refetoff, S. (1992). Recessive inheritance of thyroid hormone resistance caused by complete deletion of the protein-coding region of the thyroid hormone receptor- beta gene. *J Clin Endocrinol Metab* 74, 49-55.

Tanaka, K., Watase, K., Manabe, T., Yamada, K., Watanabe, M., Takahashi, K., Iwama, H., Nishikawa, T., Ichihara, N., Kikuchi, T., Okuyama, S., Kawashima, N., Hori, S., Takimoto, M., and Wada, K. (1997). Epilepsy and exacerbation of brain injury in mice lacking the glutamate transporter GLT-1. *Science* 276, 1699-702.

Tecott, L. H., Sun, L. M., Akana, S. F., Strack, A. M., Lowenstein, D. H., Dallman, M. F., and Julius, D. (1995). Eating disorder and epilepsy in mice lacking 5-HT2c serotonin receptors [see comments]. *Nature* 374, 542-6.

Tribioli, C., Frasch, M., and Lufkin, T. (1997). Bapx1: an evolutionary conserved homologue of the Drosophila bagpipe homeobox gene is expressed in splanchnic mesoderm and the embryonic skeleton. *Mech Dev* 65, 145-62.

van Dijk, M. A., Peltenburg, L. T. C., Murre, C. (1995). *Hox* gene products modulate the DNA binding activity of *Pbx1* and *Pbx2*. *Mech Dev* 52, 99-108.

Vastardis, H., Karimbux, N., Guthua, S. W., Seidman, J. G., and Seidman, C. E. (1996). A human *MSX1* homeodomain missense mutation causes selective tooth agenesis [see comments]. *Nat Genet* 13: 417-21.

Vetter, D. E., Mann, J. R., Wangemann, P., Liu, J., McLaughlin, K. J., Lesage, F., Marcus, D. C., Lazdunski, M., Heinemann, S. F., and Barhanin, J. (1996). Inner ear defects induced by null mutation of the isk gene. *Neuron* 17, 1251-64.

Walther, C., Guenet, J. L., Simon, D., Deutsch, U., Jostes, B., Goulding, M. D., Plachov, D., Balling, R., and Gruss, P. (1991). *Pax*: a murine multigene family of paired box-containing genes. *Genomics* 11, 424-34.

Walther, C., and Gruss, P. (1991). *Pax-6*, a murine paired box gene, is expressed in the developing CNS. *Development* 113, 1435-49.

Wang, G. V. L., Dolecki, G. J., Carlos, R., and Humphreys, T. (1990). Characterization and Expression of Two Sea Urchin Homeobox Gene Sequences. *Devl. Biol.* 11, 77-87.

Wang, W., Chen, X., Xu, H., and Lufkin, T. (1996). *Msx3*: a novel murine homologue of the Drosophila msh homeobox gene restricted to the dorsal embryonic central nervous system. *Mech Dev* 58, 203-15.

Waymire, K., JD, M., JM, J., TR, G., SP, C., and MacGregor, G. R. (1995). Mice lacking tissue non-specific alkaline phosphatase die from seizures due to defective metabolism of vitamin B-6. *Nat Genet* 11:45-51.

Weil, D., Blanchard, S., Kaplan, J., Guilford, P., Gibson, F., Walsh, J., Mburu, P., Varela, A., Levilliers, J., Weston, M. D., and et al. (1995). Defective myosin VIIA gene responsible for Usher syndrome type 1B. *Nature* 374, 60-1.

Wieschaus, E., Perrimon, N., and Finkelstein, R. (1992). *orthodenticle* activity is required for the development of medial structures in the larval and adult epidermis of Drosophila. *Development* 115, 801-11.

Winograd, J., Reilly, M. P., Roe, R., Lutz, J., Laughner, E., Xu, X., Hu, L., Asakura, T., vander Kolk, C., Strandberg, J. D., and Semenza, G. L. (1997). Perinatal lethality and multiple craniofacial malformations in *MSX2* transgenic mice. *Hum Mol Genet* 6, 369-79.

Yoshiura, K., Leysens, N. J., Reiter, R., and Murray, J. C. (1997). Cloning, characterization, and gene mapping of mouse *Hmx1*, a new homeobox gene. *Mechanism of Development*. in press.

IMAGE EVALUATION TEST TARGET (QA-3)

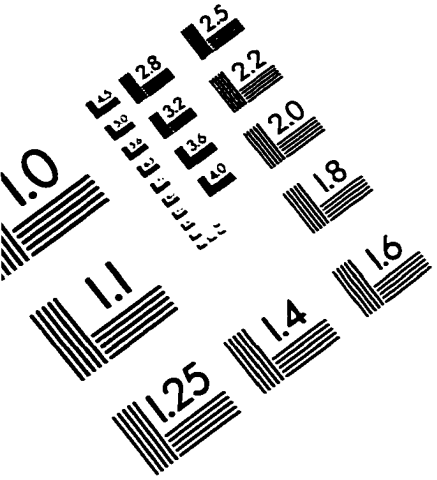

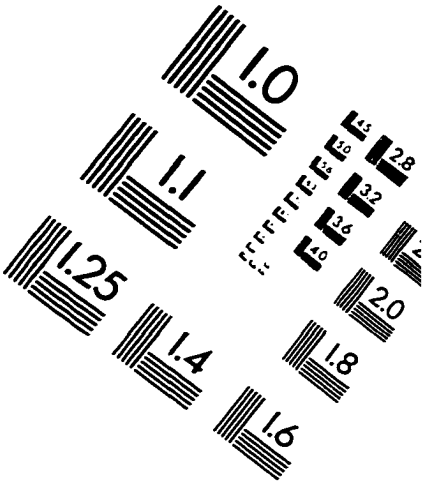

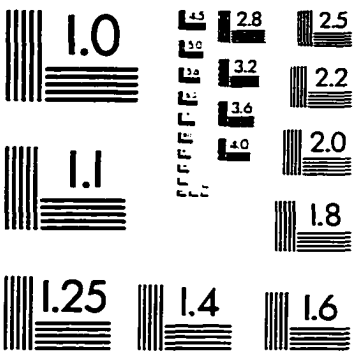

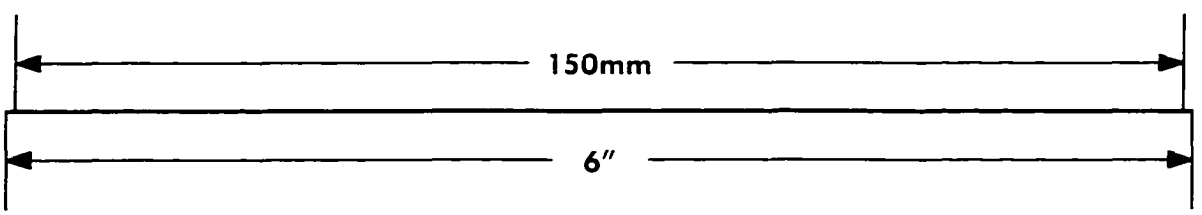

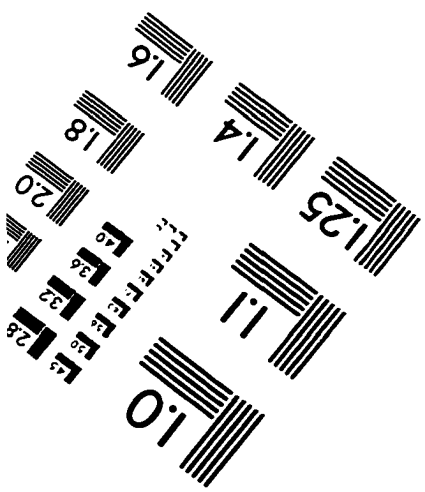

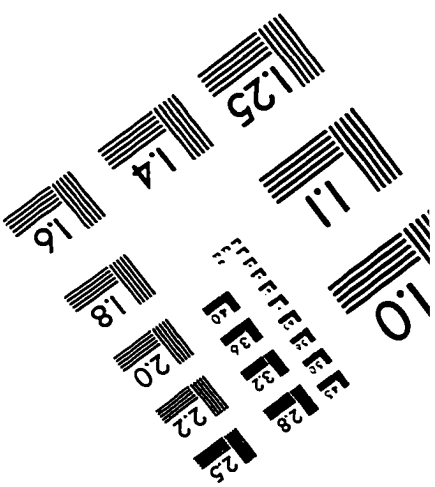

APPLIED IMAGE, Inc
1653 East Main Street
Rochester, NY 14609 USA
Phone: 716/482-0300
Fax: 716/288-5989